Mining University of Leoben / Montanuniversität Leoben

Department of Petroleum Engineering

Casing wear analysis

An analysis of the parameters causing casing wear in Troll field and possible solutions

---

Author:
Petra M. Seitinger

University of Leoben supervisor:

Prof. Dr. mont. Gerhard Thonhauser, Head of department of Petroleum Engineering

Statoil supervisor:

Harry Procope

Statoil co-supervisor:

Rikke Øhrenschlæger-Pedersen

Affidavit

I hereby declare in the lieu of oath that I wrote this thesis and performed the associated research myself, using only literature stated in this volume.

Eidesstattliche Erklärung

Ich erkläre and Eides statt, dass ich diese Arbeit selbstständig verfasst, andere als die hier angegebenen Quellen und Hilfsmittel nicht benutzt und mich auch sonst keiner unerlaubten Hilfsmittel bedient habe.

Ort, Datum Petra M. Seitinger

Acknowledgement

This thesis is carried out at the Mining University of Leoben, Department of Petroleum Engineering for Statoil Troll drilling group.

I wish to thank Professor Dr. mont. Gerhard Thonhauser for great guidance and co-operation throughout the developing and outlining of the thesis. Appreciation is also shown with regards to technical insight and advice on the subject of the thesis.

Thank you to Harry Procope for his general expertise on drilling engineering and excellent guidance. In addition, he has been of great support discussing the outline and the development-path for the thesis.

A very special thank you goes to Terje Skram for his support in all aspects of development of this thesis and for the many motivating words.

I would also like to thank Bjørn Olav Dahle for sharing his expertise on completions and corrosion issues and Geir Johnsen for his support in the analysis approach.

Leoben, Austria

June 2010

_____

Petra M. Seitinger

Table of content

1 Abstract

”Push the limit” – a catchwords to describe today’s and tomorrow’s drilling industry. The need to reach deeper, more remote and complex reservoirs with super extended reach, multi laterals and designer wells has driven operators to change traditional drilling programs. Also the requirements on the drill string and the casing had to be adapted: Internal wear of the casing during drilling is an increasing concern nowadays.

The tensioned or compressed drill string is the main cause of casing wear, as it is pulled firmly against the casing while rotating to drive the bit.

Often the wear penetration into the casing is acceptable, but in some fields, such as the Troll field on the Norwegian continental shelf, excessive casing wear is reported. The reduced pressure integrity of the casing represents a safety hazard; completion problems and additional costs for repairing or replacing worn casing arise.

The work presented here is split in two parts. The first part covers general information on casing wear. The second part will be a field analysis to identify parameters affecting excessive casing wear in Troll field.

As an introduction to the first part some information on the Troll field and the drilling strategy shall be given before basic wear mechanisms shall be presented. Models to describe and predict casing wear shall be outlined. Furthermore, it shall be discussed how operational parameters, drilling mud composition, drill string and tool joint design and formation parameters affect casing wear. Next, logging tools and mathematical models to calculate worn casing burst and collapse rating shall be presented. The last chapter of the first part will deal with general and Troll specific CO_2 corrosion facts.

In the second part some general information on Troll wells shall be given and problems occurring due to excessive casing wear shall be outlined. The analysis approach shall be presented, listing all the assumptions made for the field analysis. Available data for the field study shall be presented before identifying parameters affecting casing wear on Troll and presenting the results of sensitivity analysis on side force. Finally, the results of the casing wear analysis shall be presented and reasons for occurring deviation discussed. In the last chapter possible solutions to avoid excessive casing wear on Troll shall be given taking into consideration the operators planned drilling activities.

2 Introduction

2.1 The Troll field

The Troll field lies in the northern part of the North Sea, around 65 kilometres west of Kollsnes, near Bergen (Fig. 1).

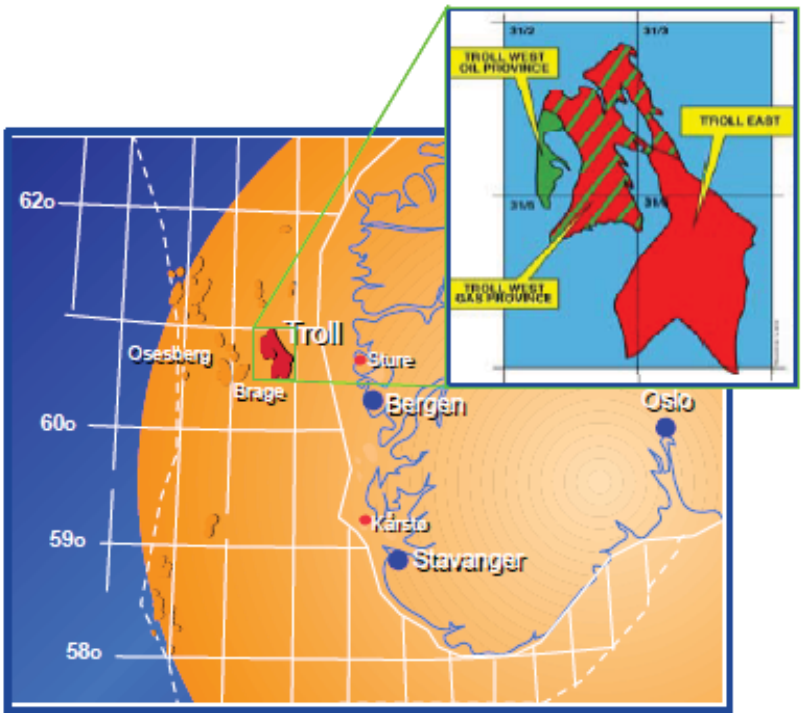

Fig. 1 The Troll field is located in the North Sea near the west coast of Norway. The field is divided into three provinces: TWOP, TWGP and Troll East

The field comprises the main Troll East and Troll West structures in blocks 31/2, 31/3, 31/5 and 31/6.

Containing about 40 percent of total gas reserves on the Norwegian continental shelf (NCS), it represents the very cornerstone of Norway's offshore gas production.

Troll is also one of the largest oil fields on the Norwegian continental shelf. In 2002 the oil production was more than 400,000 barrels per day.

Statoil operates the Troll A, B and C platforms and the landfall pipelines, while Gassco is operator for the gas processing plant at Kollsnes on behalf of Gassled.

The enormous gas reservoirs lying 1,400 metres below sea level are expected to produce for at least another 70 years.[1]

Troll is divided by two major north-south trending faults, which separate the field into three provinces, named Troll West Oil Province (TWOP), Troll West Gas Province (TWGP) and Troll East.

2.1.1 Troll gas production

Troll Gas comprises the Troll A platform, the Kollsnes gas processing plant west of Bergen and the pipelines between the platform and the land plant.

Fig. 2 Troll A platform

Troll A is the tallest structure ever moved by humans over the surface of the Earth. Its concrete support section has been built for a producing life of 70 years (Fig. 2). [1]

2.1.2 Troll oil production

Troll B, a floating process and accommodation platform with concrete hull, and Troll C, a floating process and accommodation platform with a steel hull, produce from thin oil-bearing layers in the Troll West reservoir.

The thin oil layer is between 22 and 26 meters in the Troll West oil province and 11 and 13 meters in the Troll West gas province.

In order to maintain the reservoir pressure and recover oil from the thin layer, it has been necessary to develop advanced drilling and production technology. Considerable amount of oil production would be lost, if gas was produced together with the oil. To avoid early gas coning the wells must be geosteered precisely about half a meter above the oil water contact (OWC).

All of the more than 110 planned wells in Troll Oil are horizontal wells. This entails drilling in two phases: First, down to the reservoir (0.5 m above OWC), which lies at 1,600 meters beneath the sea bottom and then to more than 3,000 meters in a horizontal direction through the reservoir. [1]

2.1.3 Reservoir framework

The Troll field is located within three large tilted fault blocks at the Edge of the Horda Platform (Fig. 3).

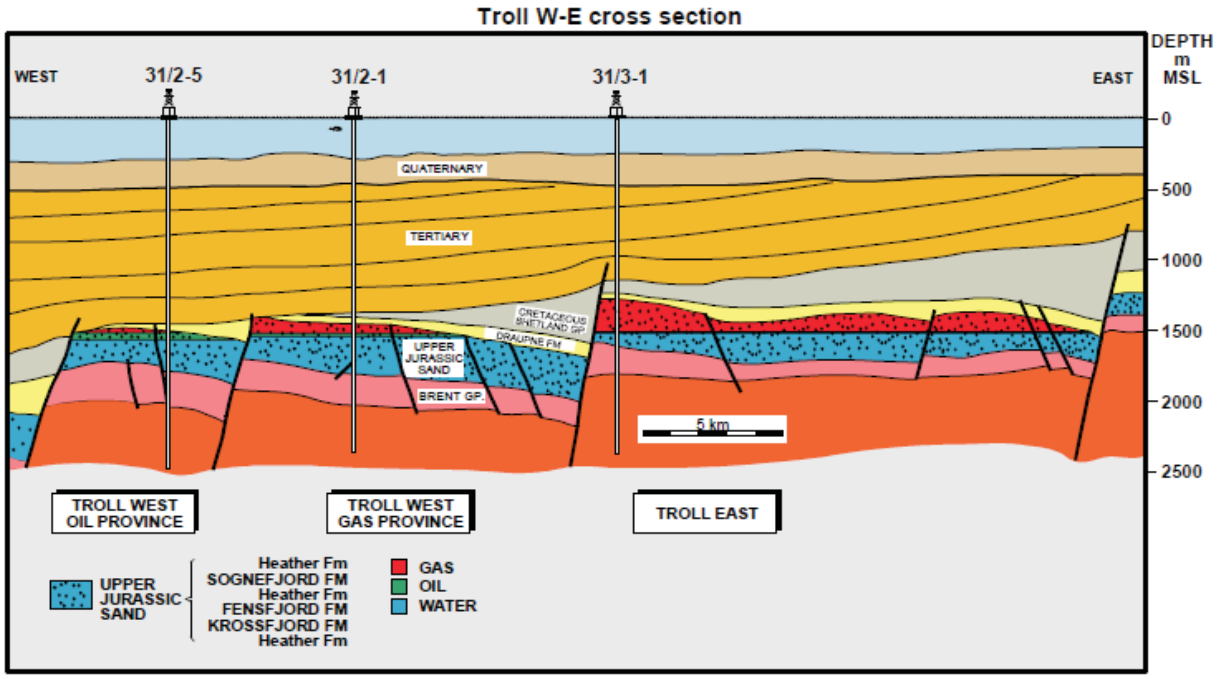

Fig. 3 East/West cross-section through the Troll field [2]

The Jurassic age (Oxfordian) Sognefjord Formation got its name from the largest fjord in Norway, the Sognefjord. It developed in the middle to late stages of the Upper Jurassic rift event and is interpreted to represent an extensive coastal spit system with sedimentary input from the northwest and a tidal backbasin in the east [2].

It consists of looses sands subdivided into clean «c» and micaceous «m» units, and locally hard calcareous cemented zones derived from shell material within the sands. Theses zones are believed to occur as discrete nodules, grading through to continuous beds. The photograph of the Bridport Sands on the Dorset Coast (UK Great Britain) shown in Fig. 4 provides a good impression of the structure of the calcites in Troll reservoir.

Fig. 4 Calcite stringers and nodules observed in the Bridport Sands [3]

The Sognefjord Formation has a gradational lower boundary, due to the interdigitation of sandstones with the siltstones which form the upper part of the Heather Formation. The top of the formation is marked by the distinct lithological break into clay stones or shales, which in the wells are the overlying Draupne Formation[4].

Reservoir sections are drilled horizontally in 8-1/2" hole. The reservoir oil zone is typically between 12m and 14m thick. Varying in thickness from a few centimetres to approximately 25m, the calcareous cemented zones constitute between 3% and 10 % of the entire section length. The sections must be drilled in a very tight horizontal plane, some 1m above the oil-water contact. Most steering is done in the azimuth to stay within the desired reservoir sand body.

In the Troll C formation, the calcitic zones often initiate drill string vibrations resulting in down-hole tool failures and premature bit damage.

3 General wear theory

The mechanical interaction between two contacting surfaces leads to a progressive loss of substance, namely *wear*. Mostly the two surfaces are subjected to load and in relative motion to one another.

Depending on different environmental factors characteristic wear mechanisms take place, initiated by local mechanical failure of the highly stressed surface.

There exist several types of wear; probably the three most important under these are *adhesive, abrasive* and *fatigue* wear. In each of this wear processes the stress transfer takes place via a solid-solid interface, whereas in *fluid wear* (e.g. cavitation and fluid erosion) stress is transferred by a fluid with high impact velocity.

Chemical wear should not be placed in an isolated category, as it is a minor or major factor contributing to all forms of wear[5].

3.1 Abrasive wear

Abrasive wear is the loss of material caused by the passage of hard particles over a surface[6]. The mechanisms behind abrasive wear were long thought to be one or two relative simple ones; now it is realized that many different processes are involved in abrasive wear and yet they are not fully understood.

Forms of abrasive wear are cutting, fracture, fatigue and grain pull out wear.

3.1.1 Mechanisms of abrasive wear

Originally abrasive wear by hard asperities was thought to be quite similar to cutting by a series of machine tool, but there are many more mechanisms involved.

3.1.1.1 Cutting

Cutting very much resembles the classic model where a sharp grit or hard asperities cuts into the softer surface.

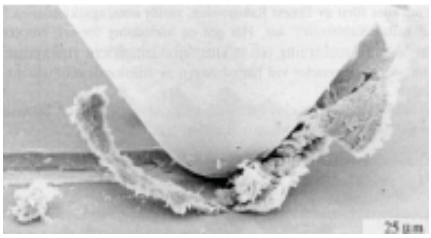

Fig. 5 Micro-cutting on a microscope view[6]

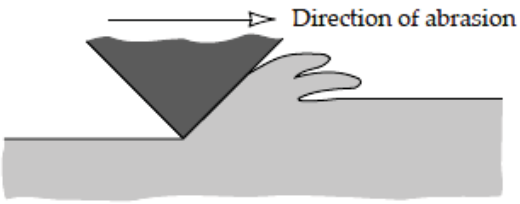

Fig. 6 Cutting[6]

With the development of Scanning Electron Microscopes (SEM) a more complex view on cutting is possible. Closer investigation revealed that basically two mechanisms are involved: *Micro-cutting,* a cutting mechanism and *ploughing*, a wedge build-up mechanism with flake like debris.

The geometry of the grit affects the mechanism of abrasive wear. A rounded, unfractured grit causes less abrasive wear than one with fractured surface and sharp micro-cutting edges. Grits originating from freshly fractured material are more efficient than worn off ones.

Beneath the surface of the abraded material, plastic deformation occurs, which can lead to strain hardening. This as a consequence usually results in a reduction of abrasive wear.

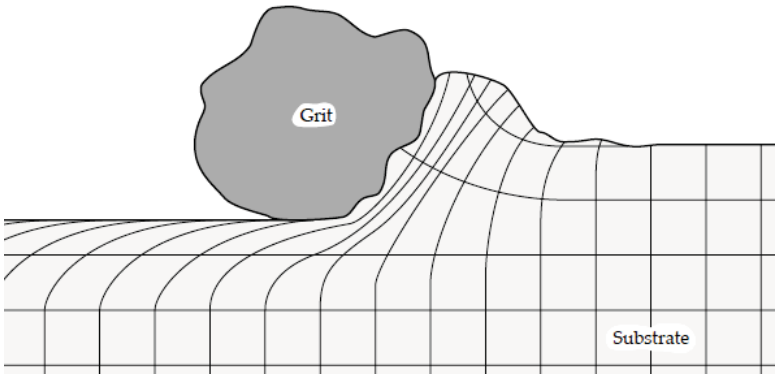

Fig. 7 Plastic deformation during passage of a grit[6]

In an actual wear situation, where only ploughing and/or micro-cutting occurs, also called *pure abrasion*, the wear is considerably less severe than cutting in the presence of fatigue.

Micro-cutting occurs for instance if tungsten carbide hardbanded tool joints are scratching on the casing. The higher the lateral forces and the drill string revolutions, the more wear is observed.

Ploughing occurs if the hardness of the two surfaces differs by more than a factor of 0.2. If the penetration depth of the harder material into the softer one is shallow, elastic deformation may occur and the relatively softer material will go back into its initial state. No wear groove is formed. If penetration depth is deep, wear flakes may form. Ploughing occurs mainly during tripping operations and not during drilling when the string is rotating.

3.1.1.2 Fracture

If the abraded material is brittle, such as ceramic, fracture formation on the worn surface may occur. Wear debris is then formed by crack convergence (Fig. 8).

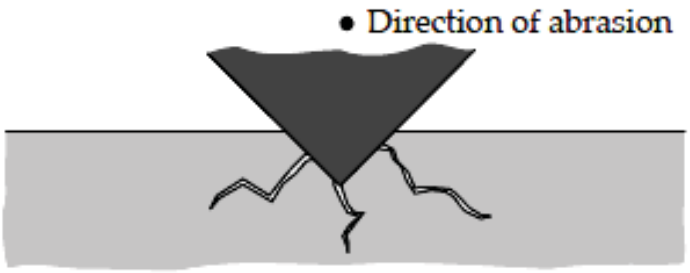

Fig. 8 Fracture and crack convergence[6]

Constant grit impact on the surface can lead to a crack accumulation where all of the sudden large quantities of material are released.

High loads acting on each grit encourage brittle fracturing. Thus, especially hardened materials are prone to fracturing, as hardening reduces toughness. This explains why hardened material can wear off rapidly, after the wear mechanism changed from a cutting-dominated to a fracture dominated.

Percussion drilling of hard rock is based on the idea of fracture wear. In casing wear this wear mechanism may not be observed frequently.

3.1.1.3 Fatigue

When a ductile material is abraded by a blunt grit, the worn surface is repeatedly deformed.

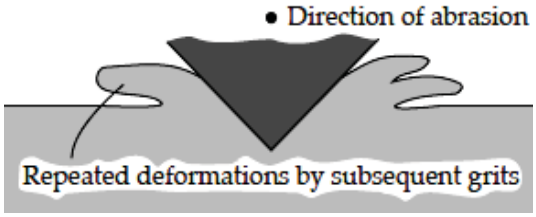

Fig. 9 Fatigue by repeated ploughing[6]

The induced strain caused by deformation of the surface area can cause metal fatigue.

The material is likely to be displaced sideways from the centre of an abrasion groove (Fig. 9).

Fatigue in combination with micro-cutting is a very effective wear mechanism and is exemplified once more by the action of the rotating tooljoint on the casing wall.

3.1.1.4 Grain pull-out

This mechanism is not likely to be observed in metals, but it applies to ceramics where the boundary between grains is relatively weak. The entire grain can be lost at once as wear debris (Fig. 10).

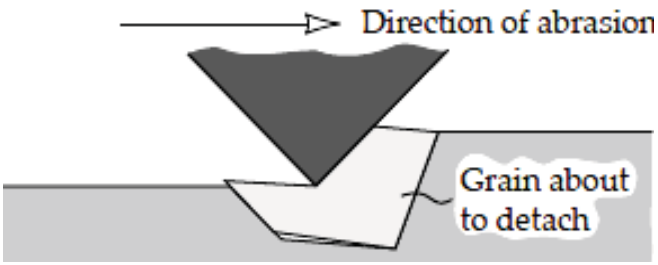

Fig. 10 Grain pull out[6]

This wear mechanism can become extremely rapid when inter-grain bond forces are weak and grain size is large.

3.1.2 Modes of abrasive wear

3.1.2.1 Two body abrasive wear

Two body abrasive wear is wear between two solid surfaces, where the abrasive surface is of equal or greater hardness compared to the abraded surface.

An example of two body abrasive wear is the action of sand paper on a surface.

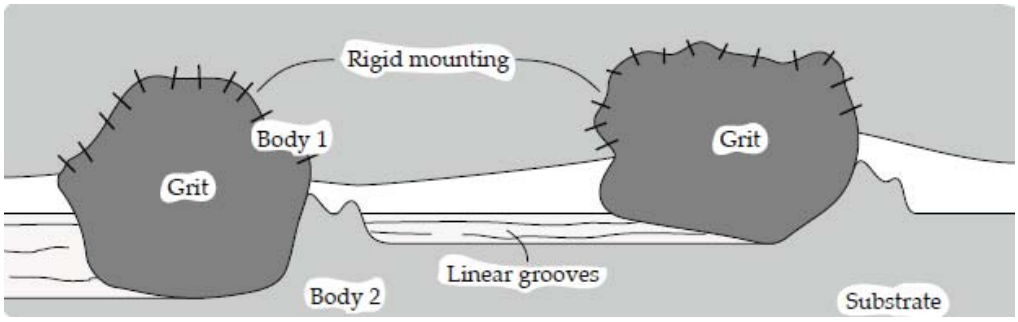

Fig. 11 Two body mode[6]

Two-body abrasive wear shows up as a steady wear pattern, such as continuous wear scratches, if the surface roughness of the abrasive element is harder than the surface it wears on.

3.1.2.2 Three body abrasive wear

In three body abrasive wear (Fig. 12) the grits are not held rigidly in place, but can roll and slide over the surface.

The observed wear pattern displays a random topography suggesting gradual removal of surface layers by the successive contact of grits. [7]

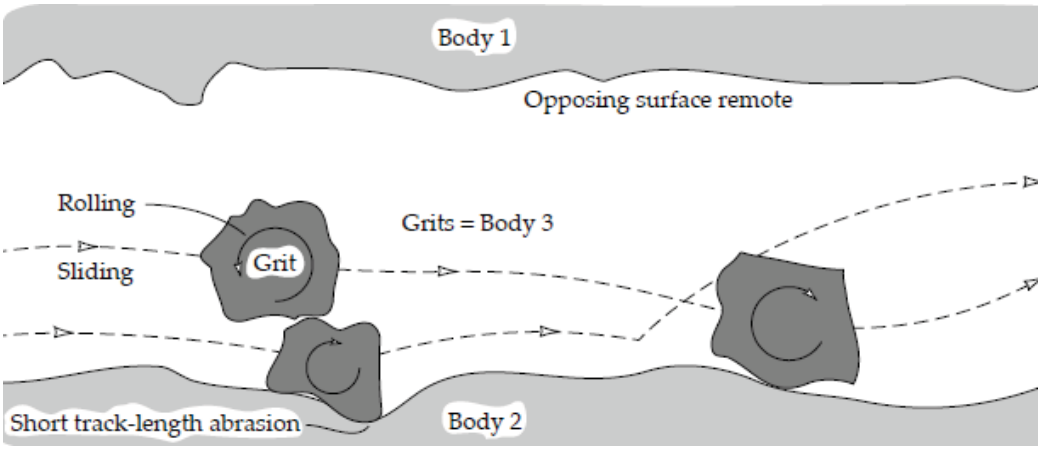

Fig. 12 Three body wear[6]

3.1.2.3 Two body versus three body abrasive wear

Two body abrasive wear is considered to be three time more harmful than three body wear. This can be reasoned by the fact that three body wear has to compete with other mechanisms of wear such as adhesive wear. [6,8]

Two body wear follows the cutting wear mechanism, whereas very little is known about the mechanisms in three body wear.

3.1.3 Effect of temperature on abrasive wear[6]

The effect of elevated ambient temperature on wear resistance cannot be compared to the effect of temperature increase in the worn material due to high grit speed.

The first one results in a uniform temperature increase in the whole wear body. At a temperature of approximately 0.8 times the melting temperature of the metal, the hardness of the metal becomes negligible.

Temperature increase in the worn material due to high grit speed will reduce the hardness of the worn surface, as plastic deformation occurs. The grit temperature contrarily remains relatively cool due to the transient nature of abrasion and effectively maintains its hardness. Thus at high grit speeds soft materials tend to wear hard materials significantly.

High ambient temperatures can additionally promote oxidative-abrasive wear. Oxidation rates at elevated temperatures are much more rapid and the resulting wear rates increase dramatically.

3.1.4 Abrasive wear resistance and means to reduce wear

Knowing the mechanisms that control abrasive wear, one can easily and successfully reduce wear rate [6,8].

3.1.4.1 Hardness

A generally accepted fact and proved also by experiments: harder materials wear slower than softer materials. Fig. 13 illustrates how wear resistance increases for pure metals post heat treatment. The relative wear resistance is defined as the reciprocal of the wear rate of the test material divided by the reciprocal of the wear resistance of a reference metal.

There seems to be no fundamental distinction between alloyed hardened metals and pure annealed metals. [6]

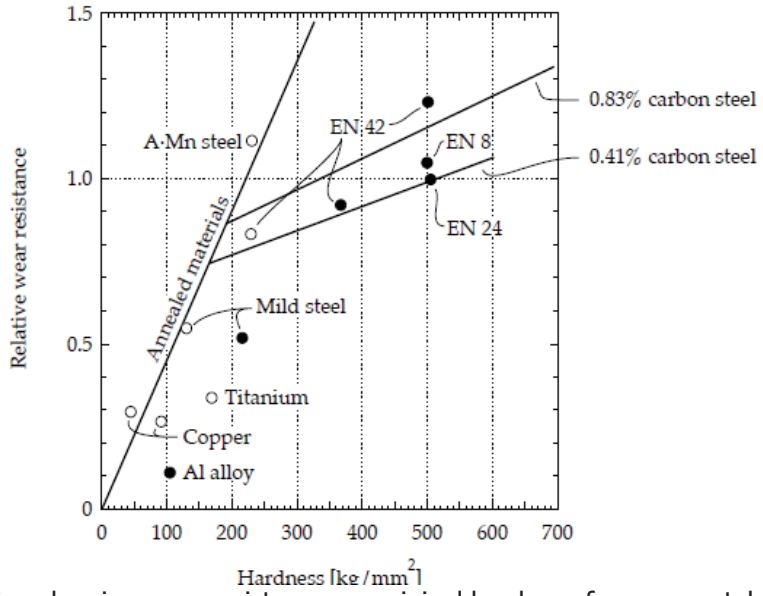

Fig. 13 Relative abrasive wear resistance vs. original hardness for pure metals and alloys [6]

As a measure to reduce wear the hardness of the softer metal should be greater than 0.8 the hardness of the abrasive.

3.1.4.1.a Abrasive wear resistance of steels

For steels this general statement is not always true.

The wear resistance of steel needs to be examined separately as it depends on more factors than just hardness. It can be enhanced by proper selection of the metallurgical phases.

If the abrasive is soft (<1,000 VHN[i]) a steel hardness that is greater than 0.8 the hardness of the abrasive is sufficient: e.g. quenched martensite with app. 800 VHN. Soft abrasives are relatively seldom found.

[i] Vickers hardness

Most abrasives are hard (>1,000 VHN). In this case a careful steel selection is important, as wear resistance is no longer only determined by hardness, but also by toughness and ductility. The proportion of austenite, baenite, pearlite, martensite, ferrite and cementite influences wear resistance.

Laboratory tests and field observations show that martensitic steels are more prone to abrasive wear than austenitic steels, which are relatively softer. Austenite has greater toughness and ductility and thus is more resistant to rapid forms of wear, such as micro cutting and fracture.

Hyper-eutectoid steels with lamellar cementite (iron carbide, 900-1,000 VHN) inclusions are found to be more wear resistant compared to martensite. The lamellar carbide inclusions hinder the abrasive to penetrate into the steel matrix. Spherical inclusions improve wear resistance to a lower extent.

3.1.4.1.b Abrasive wear resistance of stainless steels

Alloying of steels with elements such as chromium, manganese and nickel can also be useful means to reduce wear. Useful alloying elements are especially chromium and molybdenum since their carbides are extremely hard. The wear resistance of carbide free to carbide containing steel can differ by a factor of four, but to avoid brittleness the carbide content should not exceed 30%.

Soft alloying elements are not suitable to avoid abrasive wear. Most stainless steels have relatively low hardness and therefore poor resistance to wear unless a surface modification treatment can be applied.

AISI 420 stainless steel (properties in App. 16.2) has a martensitic microstructure with embedded carbides. It is extensively used in the oil industry as casing and tubing steel owing to its reasonable corrosion resistance. The major alloying addition in martensitic stainless steels is chromium in the range of 11 to 17%. The carbon levels can vary from 0.10 to 0.65% in these alloys. The high carbon enables the material to be hardened by heating to a high temperature, followed by rapid cooling (quenching). The martensitic grades are usually sold in the soft state. For further diversification of its applications, the relatively poor hardness and hence wear resistance of AISI 420 needs to be improved. However, the maximum obtainable hardness for AISI 420 after treatment cannot exceed 23 HRc. In drilling industry AISI 420 is synonymous to 13Cr steel or simple chrome steel.

3.1.4.2 Hardness contrast

Wear resistance increases with decreasing hardness contrast between the materials [6]. The hardness difference should ideally be less than 10%.

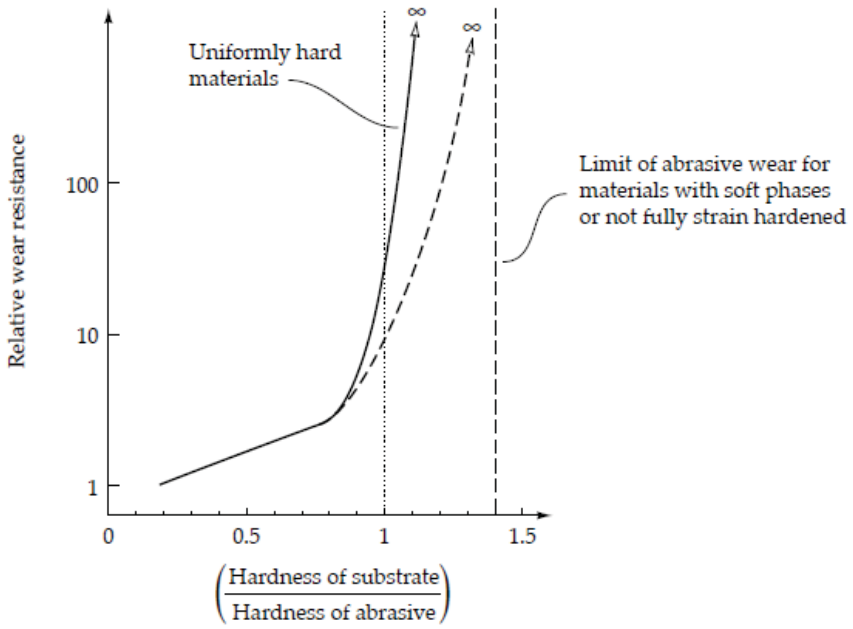

Fig. 14 Relative abrasive wear resistance versus hardness ratio of worn to abrasive material [6]

3.1.4.3 Reducing the surface roughness

Roughness is often closely related to the friction and wear properties of a surface. A surface with a large roughness value will usually have high friction and wear fast. Smoothening of the harder surface can reduce the wear rate.

However, decreasing the roughness of a surface will increase exponentially its manufacturing costs. This often results in a trade-off between the manufacturing cost of a component and its performance in application.

3.2 Adhesive wear

Per definition, *adhesion* is the tendency of certain dissimilar molecules to cling together due to attractive forces. When brought into close contact all materials have the tendency to mutually adhere to each other. This is the basic cause of adhesive wear.

Although atmospheric contaminants and lubricants provide effective means of preventing adhesive wear, they can never entirely eliminate it.

Adhesion results in high coefficients of friction and serious damage to the contacting surfaces. In extreme cases friction can be so high that the sliding motion between the surfaces is interrupted [6].

3.2.1 Principle of adhesion

All metals, apart from noble metals such as gold and platinum, are covered by a thin layer of oxide film when present in unreacted form in an oxidizing environment. Their reactivity is determined by their position in the electrochemical series.

As the layer can be only a fey nanometres thick it is usually invisible, but it hinders the true contact between two metals and thus severe adhesive wear, unless deliberately removed.

One way to reduce the contamination between two metals is to heat them up.

Experiments have shown that in case of strong adhesion, the weaker metal transfers material to the stronger one. [6] This can be explained by electron transfer between the contacting surfaces which allows a strong adhesive bond to be formed between two identical or different metallic elements. Adhesive bonds can be formed if the distance between two surfaces does not exceed about 1 nm.

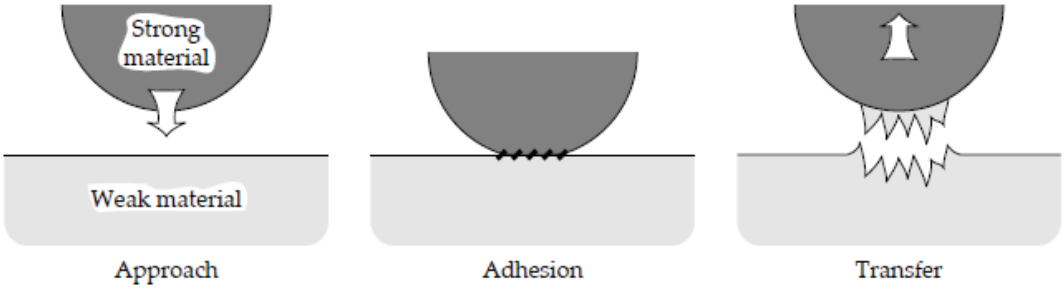

Fig. 15 Process of metal transfer due to adhesion[6]

The adhesive force can be measured and is greater for a combination of two very similar metals, i.e. iron and iron than between two dissimilar metals.

It has been found experimentally that metals with hexagonal close packed structure show much less adhesion than other crystal structures. High hardness, large elastic modules and surface energy of the metal also suppress adhesion. [6]

3.2.2 Adhesion wear

Strong adhesion between two surfaces generates friction due to fracture of adhesive bonds and can remove asperities from the softer surface to form wear particles or transfer layers.

3.2.2.1 Dry friction due to adhesion

The coefficient of friction μ is a proportionality factor between the effective shear stress of the junction τ between two materials and the plastic flow stress or yield pressure γ of the softer material.

$$\mu_{abhesion} = \frac{\tau}{\gamma} \qquad \text{[Eq. 1]}$$

The coefficient of adhesion in air is in the range of about 1, whereas for ductile solids in the range of 0.2. This can be reasoned by the fact that work hardening during plastic deformation increases the plastic flow stress.

As the highest adhesion is between identical metals, corresponding coefficients of friction are higher for those. Dissimilar metals have lower coefficients of friction. Heterogeneous materials (e.g. steel, cast iron) have lower coefficients of friction due to the non-metallic components in their microstructure.

It should be noted that the largest contributor to friction is still thought to be due to deformation of asperities rather than separation of adhesive bonds. [6] Frictional forces due to adhesion are especially high if no form of lubrication is present, which is seldom found in practical examples.

The total friction may also be written as [5]:

Total friction = Friction due to ploughing + Friction due to adhesion

3.2.2.2 Seizure and galling wear

Adhesion wear is often found in threads and sliding contacts, such as bearings, gears and chains, where it can be the cause of rapid and catastrophic failures. The rotation of the drill string in the casing can lead to severe galling wear as well.

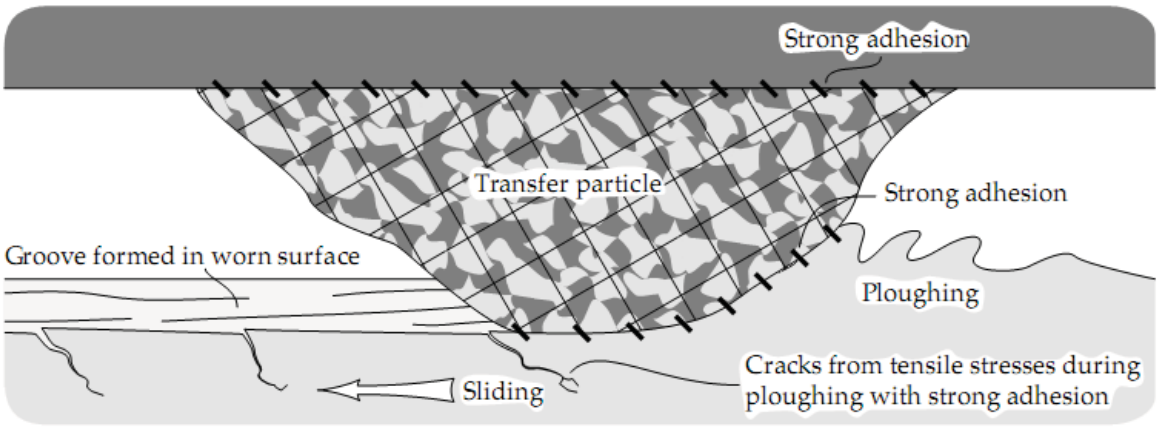

Fig. 16 Groove formation due to work-hardened transfer particle

Between localized contact points on the tool and work material surface cold welding occurs in the presence of stresses. Micro welds can break up during movement of tool and work material. If breakage takes place in the tool surface, small fragments will be torn out (Fig. 17). This leads to a gradual loss of material. Metal at the sheared junctions becomes work hardened and transferred material can behave like a cutting tool or break loose and act like abrasive particles and produce severe grooves in the surface (Fig. 16). The mechanism of groove formation involves ploughing of the softer substrate material by work-hardened transfer particles. As mentioned earlier ploughing is an inefficient form of cutting, which can lead to crack formation on the worn surface as a result of high tensile stresses.

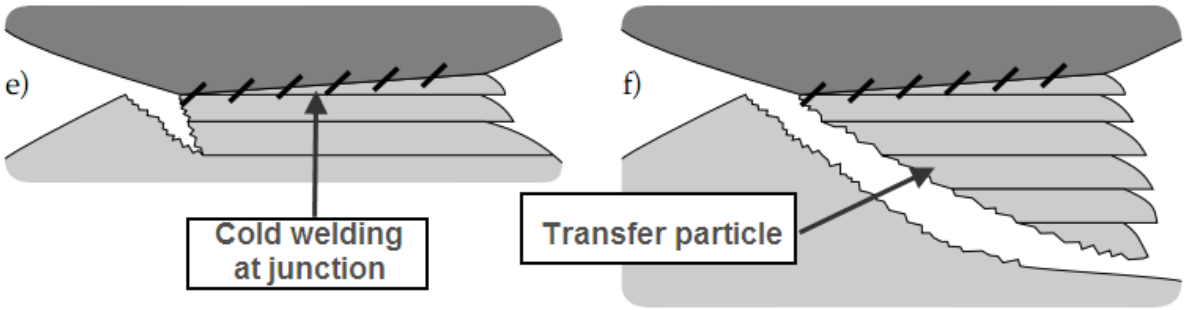

Fig. 17 Transfer particle formation after cold welding: Shear occurs along a different plane than that defined by localized welding [6]

Since the strength of the welded junction is often higher than that of the softer metal the shear occurs along a plane which is different from that defined by the localized welding (Fig. 17).

In case micro welds do not break in the tool surface, repeated tearing will form micro cracks. Those cracks will grow together over time and after reaching a critical size, larger pieces of the edge will start to break out.

Experiments conducted on model asperities revealed that the contacting asperities of brittle materials tend to break away cleanly with little deformation and produce fewer wear particles compared to ductile materials.

The particle of metal detached from one of the asperities remains attached to the other surface. Depending on conditions it may subsequently be removed by further asperity contact to form a true wear particle or it will remain on the surface to form a 'transfer film'.

The formation of transfer films can dramatically increase wear rate.

A transfer film is a series of metal particles detached to asperities of another metal. It will remain attached to its original surface until by further asperity contact worn off to form wear particles (Fig. 18). [6]

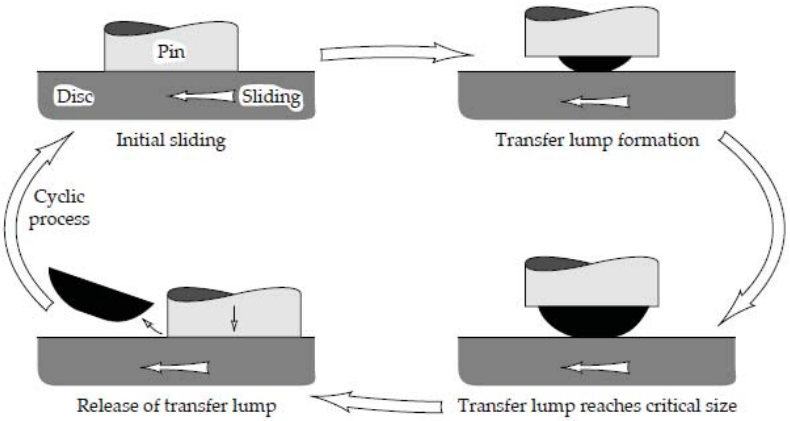

Fig. 18 Formation and removal of a transfer particle[6]

Fig. 18 illustrates how a transfer particle can lift the pin away from the surface to cause a negative wear rate. This is frequently observed in casing wear tests. However, negative wear rates are sooner or later compensated by particle removal and turn into positive wear rates.

3.2.3 Steel properties to reduce adhesive wear

Adhesive force is greater for a combination of two very similar metals, i.e. iron and iron than between two dissimilar metals. This is reasoned by stronger junctions due to heavy work-hardening during shear and large fragments may be torn out of both surfaces. For this reason it is generally a bad idea to slide similar metals against each other. If they are similar hard materials which do not work-harden further during sliding and limited ductility should be chosen. A better alternative are also materials of inhomogeneous structure such as cast iron.

To reduce adhesive wear, the following steel properties should be considered:

- Low coefficient of friction: Surface roughness should be as low as possible. The grinding and polishing should be preferably with the direction of tooling movement.
- High yield strength: Improves resistance to breakage of micro welds and formation of micro cracks.
- Hard carbides in the matrix: Micro welds cannot form between the carbides and the work material. Small carbide size and even distribution are important to ensure high ductility.
- High ductility: The ability of a metal to deform on a microscopic scale rather than forming cracks improves the resistance to micro weld breakage or chipping. Cold work grades with low ductility have a low adhesive wear resistance because of their large and non-uniform carbide distribution. The smaller size and uniform distribution of the carbides in the matrix of powder-metallurgical steels produce increased

ductility compared to conventionally produced steels with similar carbide volume and hardness.

3.2.3.1 Adhesive wear resistance of stainless steels

13Cr stainless steel material has high sensibility of galling. This is often observed during make up connection and special procedure has to be applied. Thread compound is used as a lubrication system and the connection speed should be limited to 5 RPM during making and 2 RPM during breaking connection [9].

Test results (App. 16.1) from stainless-steel couples indicate the relatively poor galling resistance of austenitic grades and martensitic grades. Good to excellent galling resistance was demonstrated by Armco's *Nitronic 32* and *60 alloys* (the latter were developed specifically for antigalling service) and Carpenters *Gall-Tough* alloy.

Designers typically get around galling by using cast alloys or by applying a cobalt facing to stainless parts. Either way, the fixes can be expensive and may pose new problems that accompany the hard-facing process. These include maintaining uniform facing thickness and ensuring proper adhesion between facing and substrate.

Studies on elemental effects of silicon, manganese, and nickel on galling resistance of nitrogen-strengthened, austenitic stainless steels show that silicon is a catalyst for galling resistance, while nickel and manganese are not.

The silicon levels in gall-resistant stainless alloy are between 3 and 4%. Silicon levels must remain lower than 5% to maintain the proper metallurgical structure. In addition, too much silicon decreases nitrogen solubility. To maintain strength, higher amounts of costly nickel would need to be added.

Results show the galling threshold for gall-resistant stainless is over 15 times higher than that of conventional stainless steels.

Both Armco gall-resistant alloys beat Types 304 and 430 alloys in strength and hardness. The new alloys also show a uniquely high ultimate tensile strength, possibly due to martensite formation during tensile testing. Ductility is excellent. These findings indicate that gall-resistant alloys can economically bridge the gap between corrosion, galling, and metal-to-metal wear resistance.

3.2.4 Methods to control adhesive wear

As discussed, high friction with possibility of seizure and the formation of transfer particles can result from adhesive wear.

Fortunately, it is relatively easy to reduce or even eliminate adhesive wear by establishing a contaminant layer between the two surfaces or adding a lubricant. [6]

3.2.4.1 Lubricants

The surfaces between two metals should be contaminated by a thin layer of lubricant that acts to suppress adhesive wear.

Galling can occur only after breakdown of lubricity. Initially, sliding surfaces are separated by an adsorbed film. The film can provide lubricity until it is destroyed by heat generation or simply displaced by high localized stresses. However, the very properties that make a substance or material a good lubricator also hinder them to adhere to the surface they intend to lubricate.

Suggested lubricants should contain substantial amounts of molybdenum disulfide, graphite, mica or talc.

An effective anti-galling film must adhere to the surface and additionally not participate chemically or galvanically in reactions.

Mud additives that in casing wear tests have shown to decrease adhesive wear will be discussed in Chapter 5.5.

3.2.4.2 Contaminant layer

After breakdown of a lubricating film, surface oxidation can still lower adhesion to acceptable levels. The thin contaminant layer is formed almost instantaneously in air, but not in inert gases. If the protective film is removed, it reforms in a few microseconds.

The presence of a thick oil film should be avoided as it can lead to oxygen starvation.

Bulk material impurities can form a contaminant layer, though a less effective one. The high temperatures resulting from friction and wear promote the migration of material impurities to the surface, where they can locally concentrate. This explains why alloys and composite materials are usually superior to pure metals in terms of adhesive wear resistance.

3.2.4.3 Proper material selection

A careful material choice is crucial to reduce adhesive wear.

As outlined earlier, adhesion is strongest between identical metals and no adhesion is observed in the noble metals. The high cost of noble materials, drastically limits their use for application.

Hardbanding manufacturers do not recommend to use chromium based hardbanding in chrome casings as this might lead to severe adhesive wear.[10]

Choosing dissimilar metals or metals with some impurities can reduce wear caused by adhesion.

4 Prediction of casing wear

Due to the constant impact of the rotating tooljoint on the casing or riser, a crescent shaped wear groove (key seat) is worn into the casing after some time. The lateral impact load is higher if additionally tensional load from the drill string below is present.

Mathematical models describing the casing wear process in terms of hole geometry, casing/tooljoint material, mud composition and drilling trajectory have been developed by R.W. Hall et alii. The "casing wear model" [11] (1994) and the more recently published "contact pressure threshold model" [12] (2005) are the two most relevant.

To implement such models into a computer programme required experimental results. Standardized tests to establish a benchmark for comparison of casing wear were conducted and the results expressed as a general *wear factor*. The wear factor describes the wear potential of a hardbanding material or a non-hardbanded tooljoint in the casing and can be compared to the unknown friction factor in torque calculations.

The industry leading casing wear simulation software based on the "casing wear model" is CWEAR by Petris (former Maurer Engineering). It uses the experimental wear factor to predict the percentage of expected casing wear.

4.1 Casing wear model

The fundamental assumption of the casing wear model by R.W. Hall et alii[11] model is that the volume worn away from the casing or riser wall is proportional to the frictional work done on the inner wall by the rotating tooljoint.

This can be expressed mathematically:

$$V = \frac{\mu \cdot \phi \cdot SD}{\varepsilon} \qquad SD = \pi \cdot ODtj \cdot N \cdot 60 \cdot t \cdot f \qquad f = \frac{L_{tj}}{L_{dp}}$$

V…Volume worn away from casing inner wall [in^3/ft]
μ…Friction factor
Φ…Lateral load [lb/ft]
ε…specific energy [lb in/in^3]
SD…sliding distance [in]
OD_{tj}…tool joint OD [ft]
N…Rotary speed [RPM]
t…Rotating time [hr]
f…time fraction the tooljoint contacts the casing
L_{dp}…Length of one joint of drill pipe [in]
L_{tj}…Length of tooljoint [in]

[Eq. 2, Eq. 3, Eq. 4]

Or in words: Volume removed per foot = frictional work done per foot / specific energy.

- The *specific energy* ε is the energy required to remove one cubic inch of material from one foot the inner casing/riser wall.
- The *sliding distance SD* is the distance travelled by a point on the periphery of the tool joint as it contacts the inner casing / riser wall.

This worn casing volume equation can be rewritten to define the wear factor as wear factor = friction factor / specific energy:

$$WF = \frac{\mu}{\varepsilon} \qquad V = WF \cdot \phi \cdot \pi \cdot ODtj \cdot N \cdot 60 \cdot t \cdot f$$

[Eq. 5, Eq. 6]

The volume removed per foot, normal force per foot and sliding distance can be determined in laboratory tests. This allows computation of the wear factor.

Geometry of the crescent wear groove is a function of casing and tool joint OD and depth of penetration into the casing wall. The volume of the worn crescent increases nonlinearly with wear depth because the wear groove becomes wider as wear depth increases (Fig. 19).

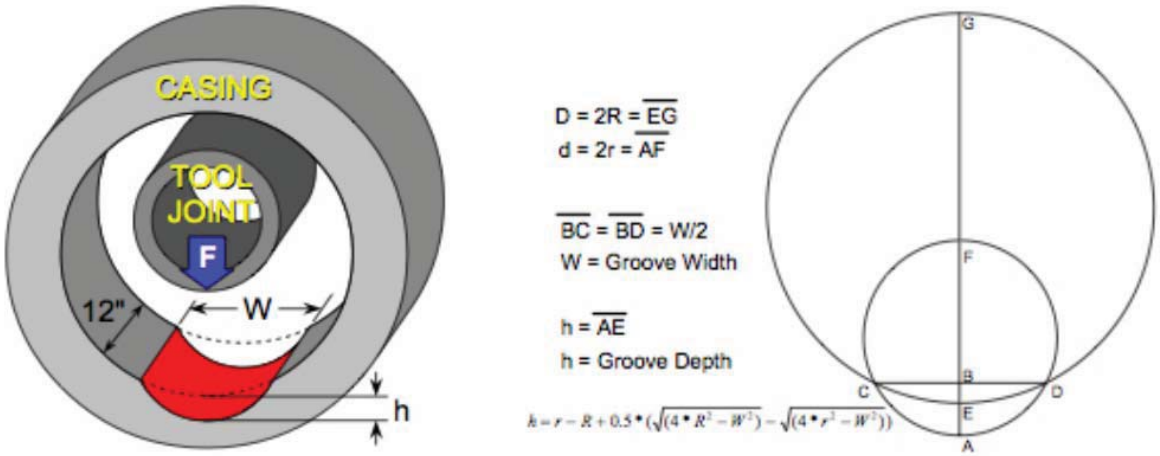

Fig. 19 Wear groove depth and width relationship

An example wear depth/wear volume relationship is shown for a 6 ½ inch tool joint rotating in 9 inch casing. The 0.47-in. thick casing is completely worn through when the groove wear volume reaches 22.13 in³/ft.

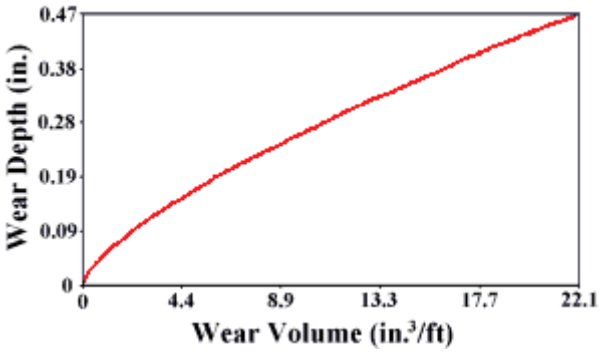

Fig. 20 Wear volume - wear depth relationship

4.2 Contact pressure threshold concept

Before Hall came up with the contact pressure threshold (CPT) concept, the effect of contact pressure was studied by Williamson in 1981[13].

To test for the existence of a pressure / wear-rate relationship, he ran several experiments. The results show a good correlation between wear rate and contact pressure.

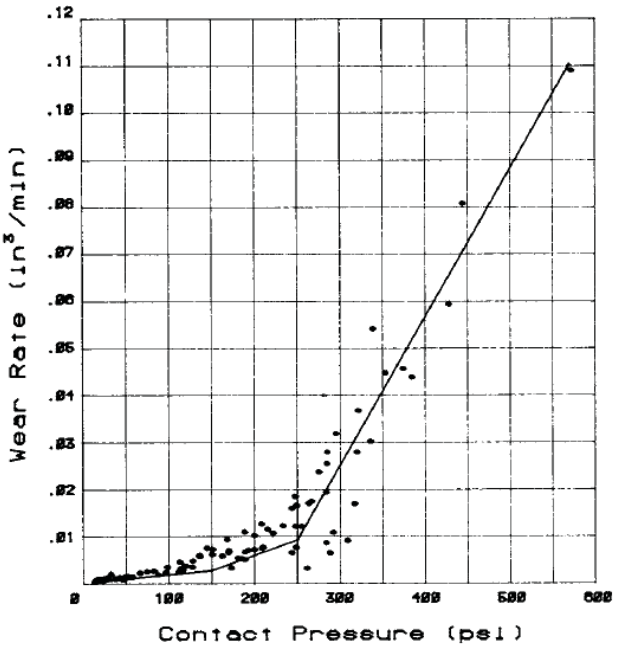

Fig. 21 Casing wear rate vs. contact pressure in a laboratory test mud[13]

In Fig. 21 two clear break points can be made out at 150 and 250 psi (1.0 and 1.7 MPa), which define a transition zone of changing wear mechanism. At low pressures (<150 psi) abrasive wear dominates. It is caused by sand ploughing into metals as a result of high contact stress between the sharp sand grains and the casing. If the sand is rounded or the contact pressures are very low, the sand cannot penetrate into the casing. This in terms suggests that a critical pressure for the onset of abrasive wear exists, which Williams found in low pressure experiments.

At higher pressures (>250 psi) adhesive wear is the primary mechanism, where the two rubbing surfaces try to weld themselves together.

The most important thing Williamson observed during his experiments is a high initial increase in wear groove depth, where contact pressure is high. The wear rate is flattening out the lower the contact pressure becomes at later conditions.

4.2.1 Contact pressure threshold model[12]

R.W. Hall developed a more precise mathematical model based on contact pressure and experimental results of more than 475 casing/riser wear tests, the largest casing wear dataset known.

The corresponding equations are all empirical and obtained by curve fitting based on the best correlation between the so called work function Ψ and the wear volume per foot.

$$V = WF \cdot \Psi = A \cdot \left(1 - e^{\left(-b \cdot \Psi^{C}\right)}\right) \qquad \text{[Eq. 7]}$$

Now the relationship between casing wear volume and work function is no longer described by a single proportionality constant, the wear factor, but by a set of three parameters.

The function can represent a wide variety of different shapes, but they all have in common that as the work function increases, the wear volume approaches a limiting values. This limiting value is equal to the constant A.

The model can predict this limiting wear volume and thus the maximum wear groove depth for a given lateral load. This can be achieved by determination of the contact pressure threshold (CPT), which is the value of contact pressure, where the *conventional wear factor* and a newly defined *differential wear factor* converge at the abscissa. How to do this is well documented in the paper on contact pressure threshold by R.W. Hall[12]. The higher the CPT value for a material, the shallower the predicted wear groove.

Equally to the wear factor, the CPT value can only be obtained experimentally through material testing.

4.2.2 Significance of the CPT model

It is important to emphasize the striking difference between wear factor and CPT for a given drilling environment: The wear factor provides a means of indicating the wear rate at certain conditions, whereas the contact pressure threshold provides an indication of the ultimate wear groove depth at the same conditions. If the predicted wear factor is high, operating companies often found decision making on further drill string rotation difficult. With increasing drilling time, they assumed that the wear groove will steadily grow. If the predicted CPT value for the same environment would also be high, then operating companies would no longer need to bother about drill string revolutions, as for high CPT values only a shallow wear groove is expected.

Hardbanding manufactures continue to invest huge amounts of money to develop more and more casing friendly hardbanding; operating companies spend incredible sums over dimensioning casing strings to account for predicted burst strength by the wear factor. If manufacturers start designing hardbanding materials with both low casing wear factor and high CPT values, casing wear would be sufficiently self limiting and the reduction in strength

would be low. Drilling time in terms of casing wear would be no longer an issue for operating companies.

5 Parameters affecting casing wear

There are many parameters that will affect drill string and casing interaction.

From trajectory parameters, such as dogleg severity and dog leg location, operational parameters, including number of drill string revolutions and trips, over to mud properties, BHA design, hardbanding solutions, formation parameters and many more.

In the following chapter major and minor parameters affecting casing wear are outlined.

Eliminating all these causes is impossible. But it must be clearly stated: casing wear can be controlled and reduced. Knowledge of the drilling engineer is crucial to successfully approach this problem; experience is vital to develop best field wide practices and best practices for individual wells.

The "general casing wear model" by R.W. Hall[11] suggests a proportionality between volume of casing removed and sliding distance, lateral force and the casing wear factor:

$$V = WF \cdot \phi \cdot SD = WF \cdot \phi \cdot \pi \cdot OD_{tj} \cdot N \cdot 60 \cdot t \cdot f \qquad \text{[Eq. 5]}$$

Wear is a function of the side force acting between casing and tooljoint, the geometry of the tooljoint, the number of revolutions per minute and the rotating time the tooljoint is in direct contact with the casing. Additionally it is a function of the wear factor, which is related to the friction factor.

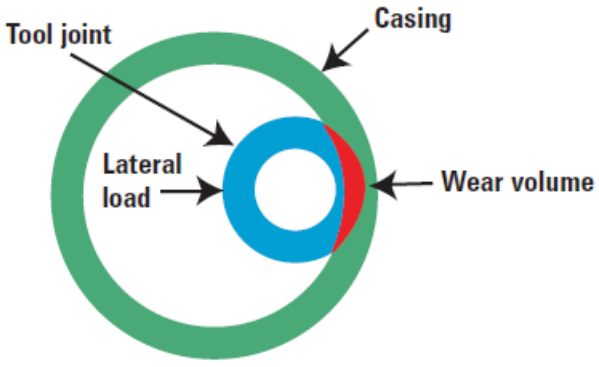

Fig. 23 Lateral load pushes the drill string towards the casing

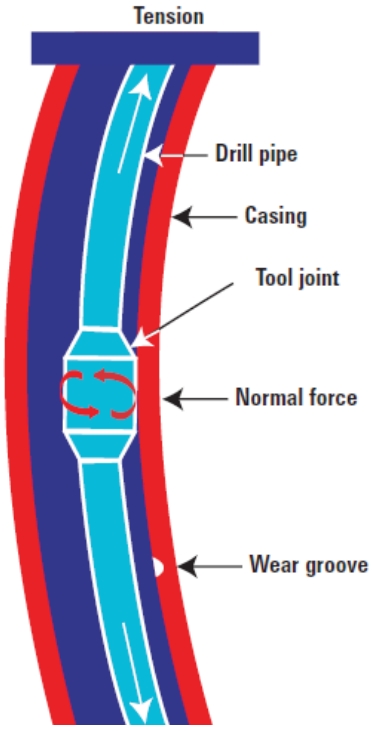

Fig. 22 Drill string rotating in the inner/high side of a dogleg

5.1 Trajectory parameters

The need to reach deeper and more remote hydrocarbon reservoirs has required a dramatic change in drilling programs and well profiles. Extended reach drilling and ultra deep drilling techniques have made the wellbore trajectory ever more complex. Limited slots available on offshore subsea templates require a lot of multi lateral drilling.

5.1.1 Doglegs

Doglegs are crooked places in a wellbore where the trajectory of the wellbore in three-dimensional space changes rapidly.

Most doglegs are created unintentionally, however sometimes they cannot be avoided. Kickoff points are considered as doglegs, but are part of the planned trajectory.

Dogleg severity can be calculated by the following formula[14]:

$$DLS = \frac{30}{\Delta MD}\Theta = \frac{30}{\Delta MD}\cos^{-1}\left[\cos I_U \cos I_L + \sin I_U \sin I_L \cos(A_L - A_U)\right]$$

DLS...Dogleg severity [deg/30m]
Θ...Dogleg angle [deg]
I_U, I_L...inclination of upper / lower survey station [deg]
A_U, A_L...azimuth of upper / lower survey station [deg]
ΔMD...Difference in measured depth between upper and lower survey station [m]

[Eq. 8]

Apparent dogleg severity: The dogleg severity as it is calculated between two survey stations.

Real dogleg severity: The real dogleg in the well.

If direction change takes place over a smaller measured depth than between the two survey stations, the apparent dogleg severity is less than the real dogleg severity. Thus, the smaller the interval length between two surveys, the more accurate the determined dogleg severity (Fig. 24).

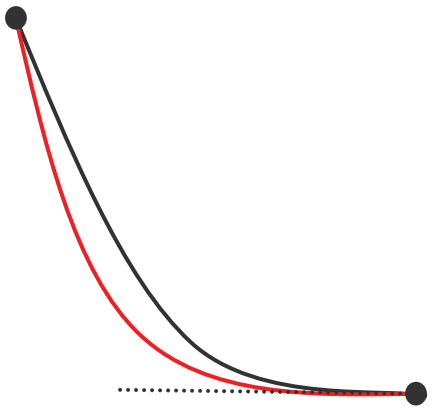

Fig. 24 Apparent DLS (black) and real DLS (red)

Apparently in doglegs the side force on the casing inner wall becomes larger (Fig. 22 and Fig. 23). Additionally the casing is subjected to higher bending stresses in the dogleg. The side force increases both with dogleg severity and the tension force caused by the drill string below.

If the string is in tension, wear is observed on the high side of the dogleg (0 or 360 degree wear in ultrasonic image logging) in build sections and on the low side (180 degree wear) in drop sections. A change in azimuth can cause wear on the left/right side of the casing.

5.1.1.1 Shallow part of the well

If tension load is high, the shallow part of the well is the most critical speaking about casing wear.

One should keep in mind that the shallower the well, the

- higher the observed tensional forces from the weight of the string below: As a result "on-spot wear" caused by the resulting high lateral forces can accumulate.
- more revolutions and sliding in the dogleg.
- longer the contact time between casing and tooljoint.

Reducing casing wear in this section is crucial, especially if the casing will be reused for later drilling operations and a sidetrack performed in a deeper part of the well.

5.1.1.2 Deep part of the well

Generally casing wear is not severe in deep parts of the well, but due to the many factors contributing it can be a serious problem here as well.

Deeper parts of the well are subjected to a different load case:

- Less tension load resulting in lower side force in a dogleg
- Often compressive load in horizontal or highly inclined sections: As a result wear is often observed on the low side of the well as a continuous wear groove

5.1.1.3 Transition zones

Transition zones are parts of the well, where the drill string initially was under compression and with ongoing drilling operations is subjected to tensional loading.

Casing wear is then observed on the high and the low side of the casing where doglegs exist. The same amount of casing volume removed spread evenly of the whole circumference is less severe than if casing is removed only on a single spot. A deep wear groove decreases burst rating more than a shallow one.

Transition zones occur during drilling out a long 8-1/2" reservoir section of a shallow set 9-1/2" production casing. First the casing is experiencing compressive loading and a shallow wear groove may be seen at low side in the area of the shoe. Near target depth the casing can be subjected to tensional forces and on-spot wear can occur on the high side of the casing.

5.1.1.4 Trajectory planning

Summarizing one can say doglegs should be avoided, especially in shallow parts of the well. The smoother the wellbore profile, the lower the side loading forces will be.

Not all wellbores can have a near-vertical trajectory, however longer and straighter tangents in planned directional holes will greatly reduce lateral forces. Where feasible, drilling to deeper depths prior to departure reduces the consequence of a dogleg.

5.1.2 Micro-tortuosity

Per definition *tortuosity* is the amount of excess curvature in the wellbore or in other words the amount of local dogleg severity variations. It is often associated with the slide/rotate action in the use of steerable motors.[15]

Total tortuosity is the sum of planned tortuosity, macro-tortuosity and micro-tortuosity.

Planned tortuosity is the summation of the total curvature (inclination and azimuth changes) in the planned well trajectory divided by the well depth.

Macro-tortuosity is the summation of the total curvature in the well as measured by MWD survey in dogleg severity subtracting the planned tortuosity.

Micro-tortuosity occurs on a much smaller scale and is created by small scale borehole spiralling, where the hole becomes a helix instead of a straight line.

Arthur Lubinski was the first one to come up with the idea of borehole spiralling realized its impact on casing wear[16]:

"*A 2-deg hole following a tight spiral would be vertical but far from straight; if it held steadily to 2-deg, there would be no objectionable rate of change in angle, yet the spiral hole might develop serious, key-seating difficulties, drill pipe wear on intermediate casing, etc.*"

The question whether hole spiralling actually exists could be solved with MWD acoustic calliper tools, advanced wire line survey techniques and interpretation of back calculated friction factors.[17]

Only rotary steerable systems in combination with long gauge bits can reduce or nearly eliminate the many problems associated with crooked boreholes. [17], [18] A state of the art 3-D near-bit mechanical calliper image while drilling tool[19] can take measurements 4 ft from the bit. This allows immediate corrective action. Conventional MWD/LWD tools are positioned 50/100 ft away from the bit.

No detailed studies or investigations on the effect of micro tortuosity on casing wear exist up to date.

5.2 Operational parameters

Long it was thought that the major cause of casing wear is due to tripping of the drill string and wire line logging. Bradley and Fontenot[20] were the first to prove experimentally that wear is primarily caused by drill string rotation.

5.2.1 Drill string rotation

Wear due to drill string rotation depends on a whole set of parameters, such as rotation time and speed, abrasiveness of the drilling fluid, wear resistance of the casing, dogleg severity, tension in the drill string at the wear point and tooljoint design.

Keeping all the non-operational parameters in the wear volume equation constant, rotation time and speed would be directly proportional to worn volume of casing:

$$V = WF \cdot \phi \cdot SD = WF \cdot \phi \cdot \pi \cdot OD_{tj} \cdot N \cdot 60 \cdot t \cdot f = Const. \cdot N \cdot t \qquad \text{[Eq. 5]}$$

This leads to the conclusion that wear is greater, the:

- higher RPM
- the longer the contact time between tooljoint and casing

According to Bradley and Fontenot wear is independent of rate of penetration (ROP). By doubling ROP, the wear volume removed per tooljoint would only be half, but for the same rotation time twice as many tool joints would pass.

This conclusion is true for constant ROP only. Varying ROP may cause severe on-spot wear.

5.2.2 Tripping and wire line wear

Tripping and wire line wear cannot account for the wear observed in field[20].

Comparing laboratory test results and field observed wear caused by tripping with rotating operations (Tab. 1) clearly shows that tripping wear is orders of magnitude smaller than wear due to rotation.

Well	Wear Point (ft)	Dogleg Severity (degrees/100 ft)	Mud Type for Logging	Measured Wear Depth (in.)	Estimated Wear Depths (in.)		
					Total Joint Rotating Wear	Pipe Body Tripping Wear	15/32-in. Diameter Wireline Wear
2	15,793	13.9	Invert (20.0 lb/gal)	0.194	0.7	0.001	0.008
4	9,000	10.8	(17.8 lb/gal)	0.360	0.5	0.002	0.013
6	2,822	8.4	Sea-water gel (12.0 lb/gal)	0.400	0.3	0.010	0.020
7	650	8.0	Salt-water gel (12.6 lb/gal)	0.380	0.3	0.008	0.020

Tab. 1 Comparison of tripping, wire line and rotating wear[20]

Obviously the more wire line and tripping runs, the higher casing wear.

Results show that wire line wear can be reduced by reducing the mud solids and sand content in the mud.

5.2.3 Reaming and backreaming

Reaming and backreaming causes additional wear due to drill string rotation. Lowering the amount of reaming, will lower the total drill string revolutions and decrease casing wear. Reaming can be reduced by a sufficient number of wiper trips.

5.3 Casing material selection

Different steel grades have different wear characteristics, but due to other constraints (minimum required strength, corrosion resistance) not always the desired steel grade can be selected.

The effect of abrasive and adhesive wear on different steel compositions and metals has already been addressed in Chapter 3.

In the wells that will be discussed in this thesis, Statoil uses P110 steel and for corrosive environment L80Cr13 steel. General information on CO_2 corrosion and background information concerning CO_2 corrosion for the later following Troll casing wear analysis is presented in Chapter 8.

Concerning abrasive wear resistance the main difference between the two steel grades is the different hardness. Casing steel with added 13% chrome cannot have a higher hardness than 23 HRc. The limit for P110 is 32 HRc.

Stainless steels such as 13%Cr steel have in general poor tribological properties and are very susceptible to adhesive wear as outlined in Chapter 3.

5.4 BHA and drill string parameters

5.4.1 Tooljoint hardbanding

Because of the larger tooljoint diameter compared to drill pipe diameter, the tooljoint is constantly in contact with either the casing or the open hole and worn off rapidly.

Hardbanding is a technique designed to extend the life of drilling tools and reduce wear on casings, marine risers and BOPs.

It is applied in one inch bands around the circumference of the tool joints and centre wear pads to protect the drill pipe tool joints and centre wear pads from excessive wear while drilling (Fig. 25).

Hardbanding of drill pipes has been around since more than 80 years. The first hardbandings consisted of a mild steel matrix with crushed sintered tungsten carbide (TC) particles[21]. In 1967, R. W. Lewis[22] conducted experiments with various hardbandings and concluded that TC hardbandings cause the most severe casing wear.

The complex drilling techniques today (ERD, super-ERD, deep drilling offshore, deep sidetrack multilaterals) require to protect both the tooljoint and the casing, as well as riser and BOP, against wear due to drill string rotation and tripping. They are called "casing friendly" hardbanding or "wear resistant alloy" hardbandings.

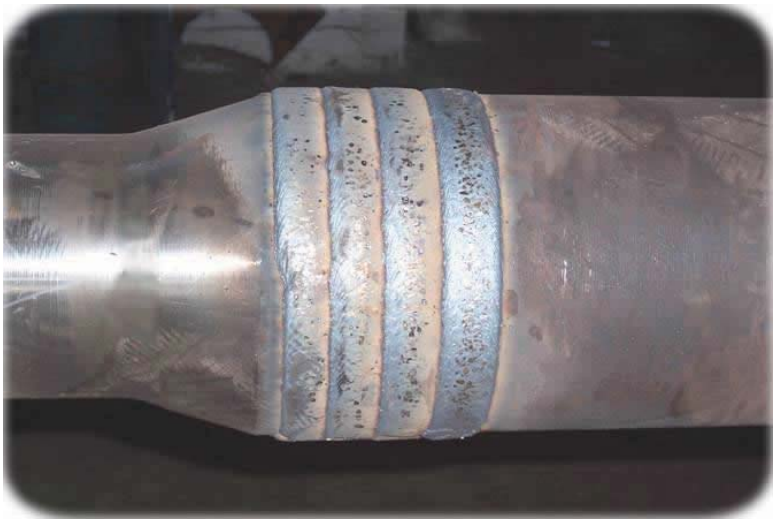

Fig. 25 Arnco 100XT[23]

5.4.1.1 Applications

5.4.1.1.a Flush application

Flush hardbanding is applied so that no increase in external diameter is experienced due to the hardbanding (Fig. 26).

As a result, the entire length of the tooljoint, as well as the hardbanding, will contact the casing wall.

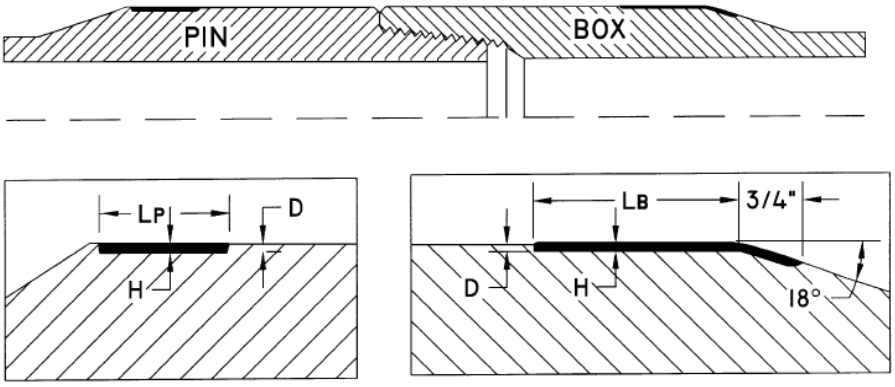

2"	L_P	L_B	3"
3/32" ,+0, - 1/32" (2,38mm +/- 0,80mm)	D		3/32", +0, - 1/32" (2,38mm +/- 0,80mm)
Flush with O.D., + 1/32", -0" (+0,80mm,-0)	H		Flush with OD, + 1/32", -0" (+0,80mm,-0)
Apply hardbanding flush with 18° shoulder, +0, - 1/32" (+0mm, -0,80mm) If not specified, the Taper Weld Bead width shall be a minimum of 3/4" (19mm)			

Fig. 26 Arnco 200 XT in flush application[23]

5.4.1.1.b Raised or proud application

Application of hardbanding in a proud condition leads to a larger external diameter. As it takes longer to wear off the hardbandings, it is thought to protect the tooljoint better against wear than applied flushed.

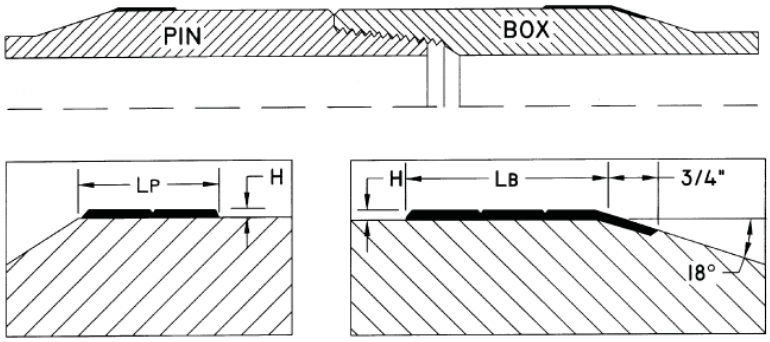

2" (~50mm)	L_P	L_B	3" (~76mm)
4/32", +0", - 1/32" (3,17mm, +0mm, -0,80mm)	H		4/32", +0", - 1/32" (3,17mm, +0mm,-0,80mm)
** Apply hardbanding flush on 18° shoulder, +0, - 1/32" (+0, -0,80mm); The taper groove should be machined to a depth that equals the finished applied thickness (H) for the raised hardband on the OD. When specified, the Taper Weld Bead width shall be a minimum of 3/4" (19mm)			

Fig. 27 Arnco 200 XT in raised application[23]

5.4.1.1.c As welded vs. ground application

Hardbandings are usually welded onto the tooljoint.

To run a hardbanding *as-welded* means to run it in the state it is after the welding procedure. A *ground* hardbanding is treated after the welding process to reduce the surface roughness.

Surface roughness of hardbanding crucially influences the wear rate. Two body abrasive wear can be reduced by smoothening the harder one of the two rubbing surfaces, here the tooljoint.

Supported by laboratory testing and field experiments, Trio OilTec, a hardbanding manufacturing company, observed severe increase in casing wear when using as-welded hardbanding compared to ground (factor up to four times) [24].

Their explanation is that new longer lasting hardbanding materials remain as-welded for a longer period of time than older ones.

5.4.1.2 Casing friendly hardbandings

The first hardbandings' short come to protect the casing from could be improved somehow by using fine TC particles instead of crushed and sintered TC.

In 1989, Amorphous Technologies, Inc. developed a chromium hardbanding, ArmacorM™ that significantly reduced casing wear. It was an amorphous (work-hardened) type material that had a very low friction coefficient, but had a very low resistance to the high stress abrasion during drilling in open hole[25]. This resulted in high tooljoint wear rates and soon reduced the popularity of this product among service companies.

In late 1992, Arnco Technology introduced a chromium alloy hardbanding, Arnco 200XT™, that first successfully protected both casing and tool joints. It has a crystalline structure and a consistent through-wall hardness of 45-60 HRc[ii] and a high tolerance for stress abrasion in open hole. It should be applied in a proud condition for maximum performance[26].

5.4.1.3 Hardbanding benchmark tests

Approximately 20 years ago the Drilling Engineering Association (DEA) conducted a study (DEA 42) with the intent to categorize competitive hardbandings and their relationship to casing wear. All tests were conducted on the Maurer Engineering test apparatus and a 2.0 casing wear factor established as a benchmark. Anything below 2 was considered casing friendly. The Maurer test apparatus changed a couple of times and today tests in the Mohr Engineering laboratories in Houston are performed. Just like the tests also the benchmark criteria deviate greatly from DEA 42 and the wear factor of 2 is no longer the benchmark criteria.

The casing wear test standards and procedures are being reviewed by API with the intent to publish a standard. The result of changes in the test has caused confusion on which

[ii] HRc....Rockwell hardness

hardbanding can be regarded as casing friendly. Until API publishes a specification, the industry is confined to their own interpretations of the Mohr Engineering Test data and many manufacturers run test on their own hardbanding apparatus.

Tests on the Maurer apparatus were done for Arnco 200XT[iii] and the later developed Arnco 100XT and Arnco 300XT that even outperformed the first product. Those tests and field tests support the "casing friendly" performance of the hardbanding[25].

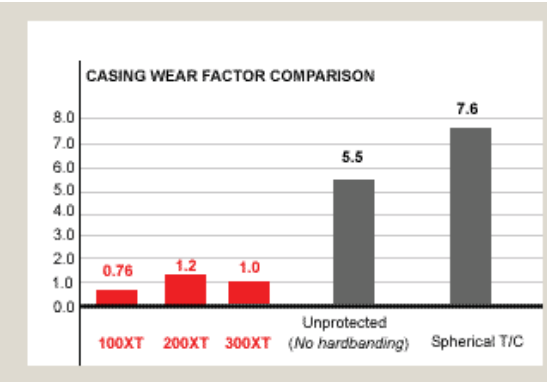

Fig. 28 Casing wear factor comparison[23]

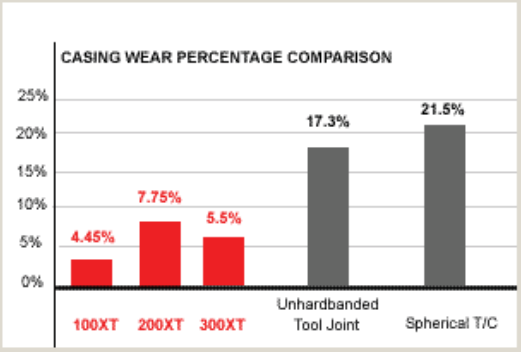

Fig. 29 Casing wear percentage comparison[23]

New promising hardbanding solutions are developed by Trio OilTec. The results of in-house testing are shown in Fig. 30. It should be mentioned that Arnco 100XT™ is not included in the test. The products provided by Trio OilTec are MX5, MX24, OTW-12[iii] and OTW-16[24].

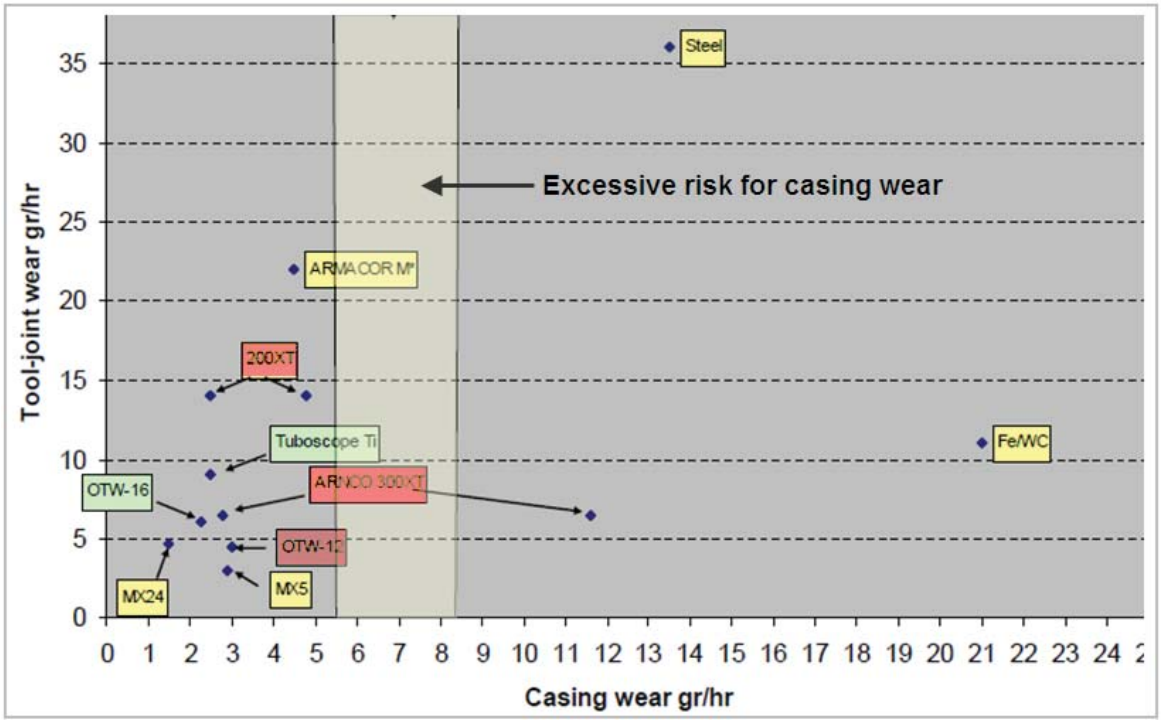

Fig. 30 Results wear from tests by Trio OilTec

[iii] Arnco 200XT and 300XT are used by Statoil on 5" drill pipe

5.4.1.4 Selecting the proper hardbanding

Selection of an appropriate hardbanding should not solely be based on casing wear factor, but also consider:

- Tool joint wear rate
- Friction factor
- Field experience
- Cracking, spalling and other failures
- Availability of application and reapplication
- Ability of application over existing tungsten carbide, other alloys or itself
- Ease of application
- Cost

Quality control of hardbanding is crucial to avoid unexpected high casing wear with casing friendly hardbanding.

The most common reported problem is cracking due to the metallurgical structure of the hardbanding. These cracks often lead to premature failures, spalling, large porosity and other reapplication problems.

Hardbanding manuals teach how worn hardbanding should be inspected and demonstrate the acceptable criteria. For most hardbandings it is not necessary to remove them before reapplication over themselves, providing that the worn hardbandings are free from gross defects. Previously worn hardbandings should be investigated cautiously as reapplications are only as good as the previously worn hardbandings' condition.

In case cracks or spalling is detected, immediate reapplication of hardbandings is necessary.

5.4.2 Drill string design

5.4.2.1 Bearing surface of the tooljoint or hardbanding

The greater the bearing surface of the tooljoint or hardbanding for a given diameter, the more volume of casing is removed. This can be reasoned by the longer contact time between casing and tooljoint in a dogleg and explains why raised hard facings are likely to outperform flush hard facings in terms of casing wear. This is especially true if the lateral force is the same for both situations.

If one correlates wear rate with contact pressure rather than contact force, two counteracting effects can be observed. For a given contact force the pressure on a larger bearing surface will be lower, but contact time increases compared to a smaller bearing surface (Fig. 31) [12] [26].

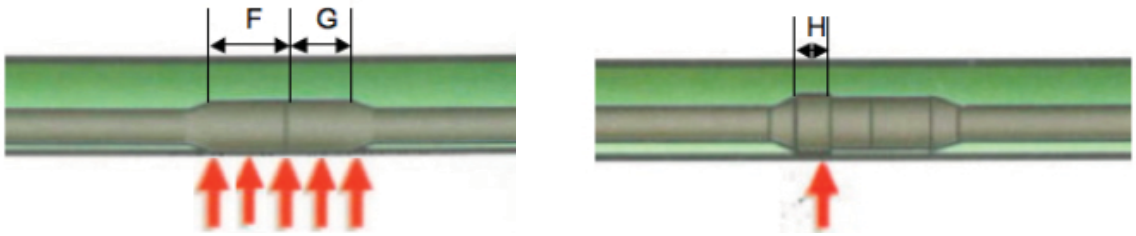

Fig. 31 Large bearing surface area versus low bearing surface area

5.4.2.2 Casing / drill string clearance

The diameter relationship between drill string and casing affects casing wear in a similar way as stated under 5.4.2.1. A smaller casing to drill string diameter for a given drill pipe unit weight causes a larger contact area and a lower contact pressure. For a given contact time or tooljoint length a small annular clearance, hence a larger drill string OD, is preferable to a large clearance, as the wear will be distributed more evenly along the circumference of the casing. The wear groove will be rather shallow and strength reduction lower.

A stronger drill string will additionally decrease the accumulation of drill string fatigue, reduce buckling and improve wellbore hydraulics[27].

5.4.2.3 Length of the drill pipe

An additional source of wear may also be caused by using Range III drill pipes with a length of 13.5-14.8 m compared to Range II drill pipe with 9.2-10.2 m. The additional length of each range III joint creates a large contact area in the middle of each joint caused by gravity-based sag in highly inclined boreholes[28].

5.4.2.4 Geometry of drill pipe

By the use of specialized drill pipe with stakes or helical sections, the side load in dog legs can be distributed more evenly over the drill string, lowering the load concentration on the tooljoint and as a consequence reducing wear. However, this benefit coincides with the original objective of specialized drill pipe – to improve hole cleaning. Specialized drill pipe is placed in designated sections of the hole to improve cleaning and this is not often where high severe dog legs are encountered.

5.5 Drilling fluid parameters

Mud as the intermediate medium between tooljoint and casing is another important parameter affecting casing wear.

It is difficult to determine how a specific mud ultimately affects wear under certain conditions. This is due to the many types of different mud and mud additives and the fact that mud properties and composition will change down hole due to a changing pressure and temperature regime. Additionally drilled solids will mix with the mud and change it's original design.

Small scale equipment and measurements fail in describing field observations [29]. Only full scale test machines and field testing can reveal certain trends how mud affects casing wear.

Several studies, aimed to describe the influence of mud, exist. Unfortunately, non standardized testing equipment makes comparison of those studies difficult. Sometimes the results are in contradiction to other results.

It should be emphasized to develop a standardized testing equipment and procedure to facilitate interpretation and comparison.

5.5.1 Oil based mud

Several studies and field observations indicate that oil based mud systems have a higher slipping effect between the tool joints and the casing, thus providing better lubrication and decreased friction. This in terms reduces casing wear.

The amount of wear is generally low and nearly the same for unweighted and barite weighted mud [29].

In contrary to all other studies, White and Dawson [30] observe an increase in friction / wear rate in oil based mud (OBM).

5.5.2 Water based mud

5.5.2.1 Mud weight and weighting material

A general observation of laboratory tests is that with increasing mud weight, casing wear rates decrease [20,29]. Most weighting additives are able to form a protecting film that hinders severe adhesive wear.

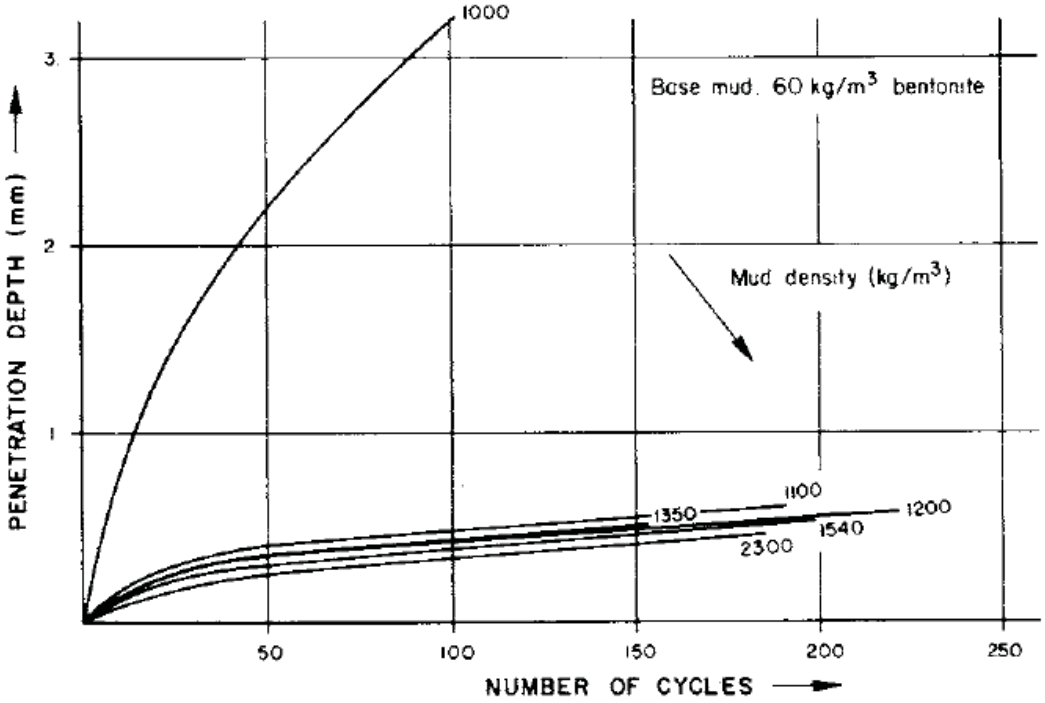

Fig. 32 Effect of mud density on casing wear for barite-weighted muds at a contact load of 8 kN [29]

Fig 32 shows the effect of barite weighted mud: Apparently, barite is able to form a protective layer that decreases casing wear. Unweighted bentonite mud causes severe adhesive wear[iv], because bentonite seems to be unable to form a protective film between casing and tooljoint.

When using barite as weighting material lower wear rates are observed compared to using hematite or quartz (Fig. 33). This can be explained by the higher hardness of quartz and hematite which will increase abrasive wear. Nevertheless, the observed wear rates are less than for unweighted mud[11,29].

[iv] indicated by wear debris in the form of flakes

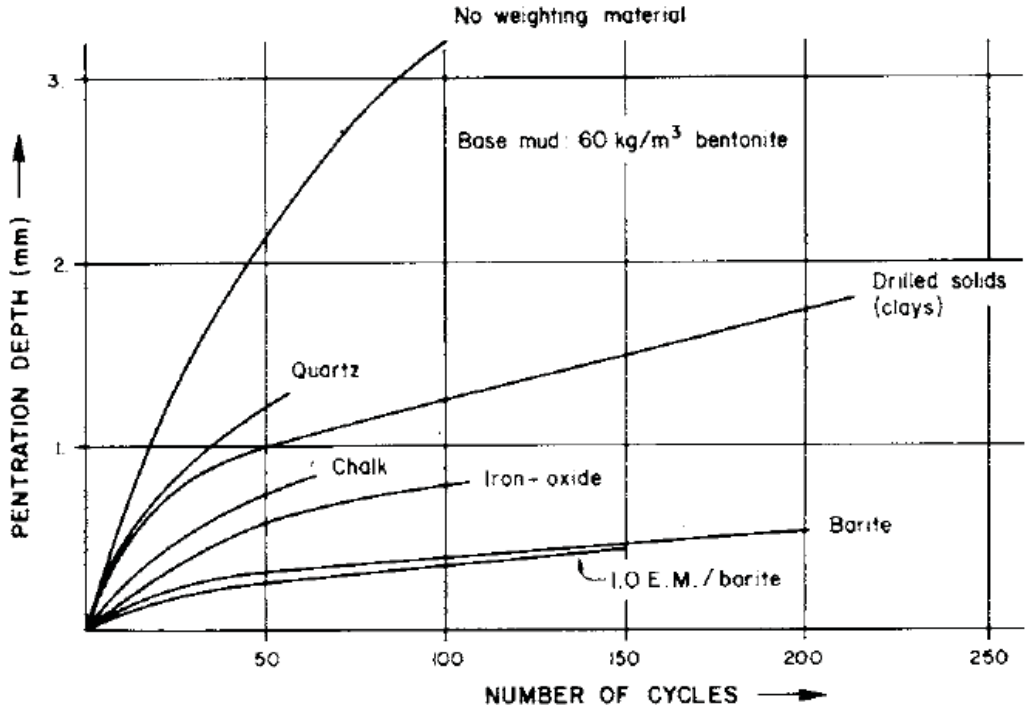

Fig. 33 Results of casing wear experiments with 1.15 – 1.2 SG muds with various weighting materials at a contact load of 8 kN. [29]

In contrary to all other studies, White and Dawson[30] observed an increase in friction / wear rate in weighted WBMs.

5.5.2.2 Other mud additives

The effect of other mud additives is strongly dependent on the mud weight. Generally, for weighted mud, no effect is observed; for unweighted muds the following results were made:

- Drilled solids: According to Bol[29] drilled solids entering the mud system have particle sizes significantly larger than weighting materials. This hinders the formation of a protective film between casing and tooljoint and therefore reduces wear resistance. Bradley and Fontenot[20] observed an increase in wear resistance due to drilled solids.
- Polymers: Bradley and Fontenot found the addition of polymers to be detrimental to casing wear. However Bol observed a slight reduction in casing wear.
- Salts: Addition of salt can reduce casing wear, as film formation in encouraged[29].
- Diesel: Addition of diesel has no influence as it contains no reactive components to form a protective film.

5.5.2.3 Lubricants

To avoid casing wear sometimes lubricants are added to the mud in order to create a film between casing and tooljoint surfaces with a low gliding resistance (reduction in adhesive wear). It must be stressed that the effect of lubricants strongly depends on the actual

surface conditions of the casing and tooljoint at the time of addition and on the type and amount of solids in the mud[29].

In full scale testing equipment and field testing no significant influence of lubricants on weighted WBM could be observed. With an increasing amount of solids in the mud, these solids will penetrate the lubricant film and make it inefficient. Overtreatment with lubricant (normally occurring at 2-5%) will decrease wear rate/ friction. This is thought to be due to surfactants in the lubricator changing the wettability of the solids in the mud from water wet to oil wet. If the oil wet solids reach the tooljoint/casing contact area, friction will decrease dramatically. In bentonite muds this is not observed, apparently due to the negative charge on the clay platelets preventing them from being oil wetted.

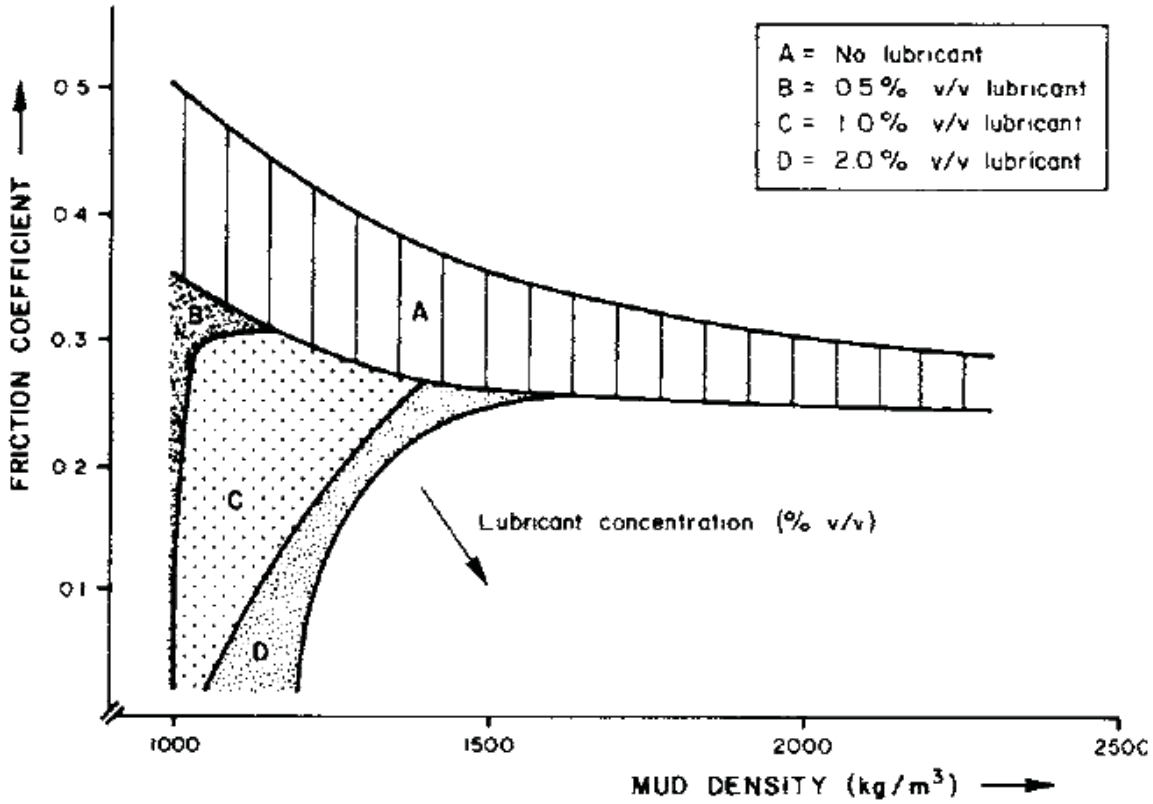

Fig. 34 Friction coefficient as a function of mud density and lubricant concentration in barite-weighted muds (general trends) [29]

If the mud weight exceeds 1.5 SG no effect could be observed at all. For unweighted muds and muds with low mud weight (1.0-1.3 SG) a decrease in wear rate could be observed if lubricant was added in a concentration of 1-2 %[29].

5.5.2.4 Sand and silt content

In unweighted muds adhesive wear seams to be so high that abrasion due to sand has no influence on casing wear[29,30].

In film forming weighted muds (salts and lubricants) sometimes a slight increase in friction / wear rate is observed.

5.6 Formation and parameters

Formation parameters have only an indirect influence on casing wear. Their effect is reflected in operational parameters, such as ROP, RPM and WOB and slightly changes the composition of the mud.

5.6.1 Formation hardness

Average ROP is generally low in hard formations.

Such hard formation are for instance calcite stingers through the reservoir section as being present in the Troll field: Calcite nodules and stringers up to several meters thick, derived from shell material within the sands, occur throughout the reservoir and can create difficulties while drilling. Depending on the dip angle, the orientation of the calcite stringer surfaces, the condition of the bit and the drilling parameters when entering or exiting the calcite stringer, the bit can be forced aside into the more drillable loose sand. This behaviour can potentially result in high local doglegs[3].

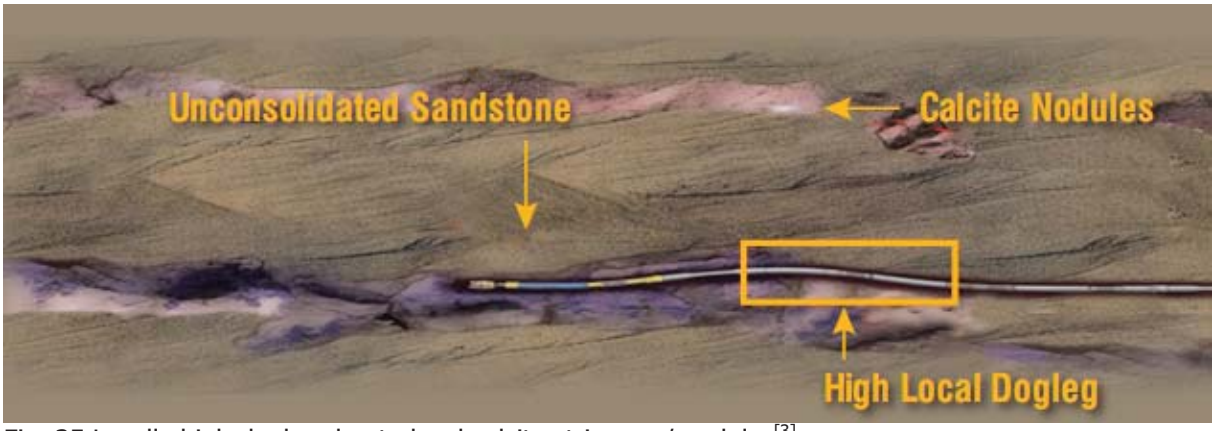

Fig. 35 Locally high dogleg due to hard calcite stringers / nodules[3]

While drilling through hard rocks often strong drill string vibrations are experienced.

5.6.2 Interbedded formations

Interbedded formations of alternating soft and hard layers can act as natural whipstocks.

The miniature whipstock theory is based on drilling experiments made by Hughes Tool Company in which an artificial formation composed of glass plates has been drilled with the hole inclined to the laminations[31]. In these tests the plates fractured perpendicular to the bedding plane, creating miniature whipstocks. If such whipstocks are created when laminated rock fractures perpendicular to bedding planes, this could cause up dip drilling.

The higher the *anisotropy index* of a formation, the more corrective action must be taken to follow the planned trajectory. This increases the likelihood of creating doglegs.

The rock anisotropy refers to the differences in physical properties of rocks as related to the directional characteristics; for example, "strength" or "drillability" may be different when measured in different directions through the rock.[31]

6 Casing wear logging

Casing wear monitoring and/or logging serves two purposes: Firstly, to detect the presence of casing wear and secondly, to assess the severity of the problem in order to ensure that all safety requirements are met.

Quantitative measurements can be done by logging the casing with various logging tools, e.g. ultrasonic imaging tool and multifinger calliper.

Ditch magnets can be used to identify the presence of casing wear.

6.1 Ditch magnets

Ditch magnets are junk retrieval tools designed to remove metal particles from drilling mud and are only used for a qualitative check on casing wear debris metal.

They comprise of a series of extra strength magnet elements encapsulated in a high quality stainless steel.

Ditch magnets give no information about where casing wear has taken place. The amount of metal returned depends strongly on drilling hydraulics: Fluid velocity, circulation rate and drill string revolutions. The cumulative amount of metal flakes and debris returned can be correlated to drilling hydraulics to give an estimate of how much casing wear has taken place.

The magnet should be used any time metal particles may accumulate in the mud. The tool has special application during milling and wash over operation and will be positioned in the mud return line before the shale shaker or directly on the drill string. All metal particles passing by the magnet will then be caught and retained, protecting the shale shaker, mud pumps and other costly component of the mud system.

Regular inspection of the magnet by rig personal is vital to detect casing wear problems.

6.2 Ultrasonic/acoustic imaging tools

Ultrasonic or acoustic imaging tools serve two different purposes.

Firstly, they allow interpretation of cement coverage in the annulus, thus channels in the cement and the quality of zonal isolation can be verified. Secondly, the condition of the casing can be checked and pipe integrity determined.

Statoil currently uses the UltraSonic Imaging (*USI*) tool provided by Schlumberger. For this reason the tool shall be discussed in more detail including tool description, measurement principle and uncertainty parameters involved.

Fastcast and *Cast-V* supplied by Halliburton have more or less the same features.

6.2.1 Tool description

The USI tool comprises a single transducer mounted on an ultrasonic rotating sub on the bottom of the tool. Ultrasonic pulses in a frequency range of 200 and 700 kHz are emitted by a transmitter, which measures the reflected waveforms from the internal and external casing interfaces.

As the transducer is mounted on the rotating sub, the entire casing annulus can be scanned (Fig. 36).

The emitting frequency (number of shots) at one depth (in USI logging referred to as "cross-section) can be either five or ten degree radial sampling. Vertical sampling rate is manufacturer dependent and usually in the range of 0.6 – 6 inches.

Centralisers are mounted on the tool to avoid eccentricity, which would affect quality and accuracy of the logging results.

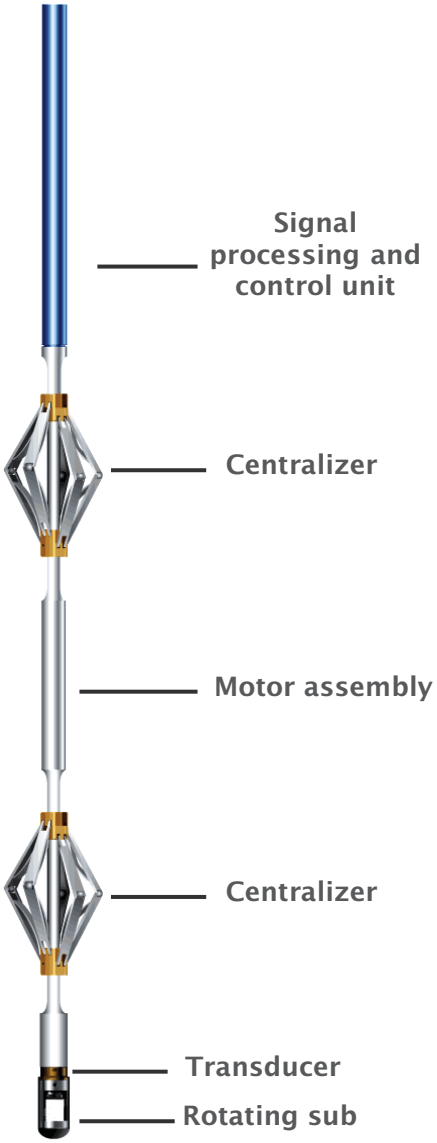

Fig. 36 USI tool by Schlumberger

6.2.2 Measurement principle

The measurement output consists of four measurements that are made from the echo received by the transducer:

- Travel time of the primary reflection: gives internal radius
- Amplitude of primary reflection: gives rugosity (surface condition) of cement
- Resonance frequency: gives casing thickness through processing
- Resonance decay: gives cement impedance through processing

The two main parameters influencing casing wear inspection are the casing thickness value and rugosity; internal radius measurement is of value as well, but usually less accurate than casing thickness measurement. The ultrasonic bursts (shots) are about 10 µs short.

To derive an accurate measurement of internal radius and cement the wellbore fluid travel time, the tool must be run in the fluid properties measurement mode (FPM), where the transducer is stationary and oriented towards a built in plate with known thickness. The speed of sound in fluid (FVEL) can be obtained by dividing the transit time measurement through the known distance between emitter and target plate.

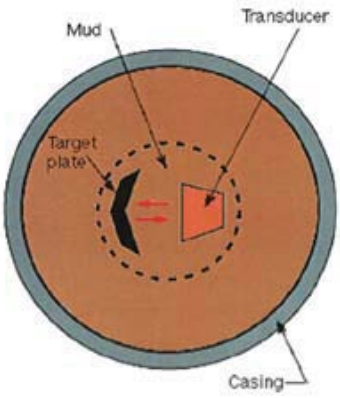

Fig. 37 USIT in FPM mode

In the casing measurement mode the transducer is flipped by 180 deg and the sub rotated. When the pulse hits the casing wall, energy is transferred into the casing and some is reflected back. As the casing resonates, energy is transmitted into the cement and also back into the casing fluid. The energy transmitted back into the mud is picked up by the transducer and then processed (Fig. 38).

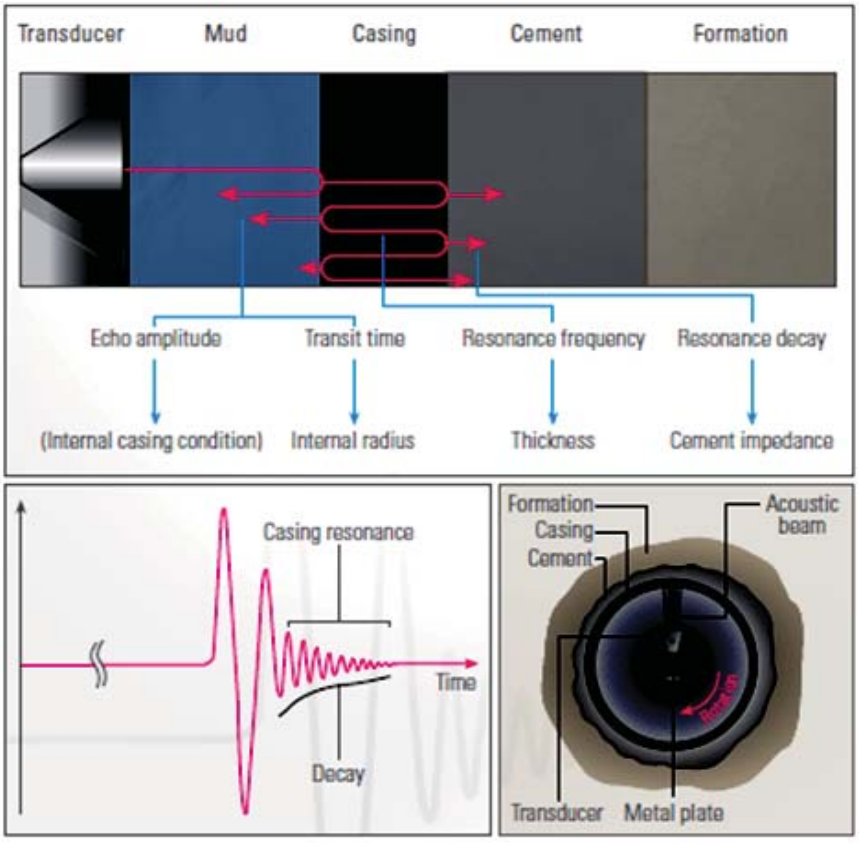

Fig. 38 Casing measurement principle of USIT[32]

The logging results are presented as easily readable, colour coded images (Fig. 39).

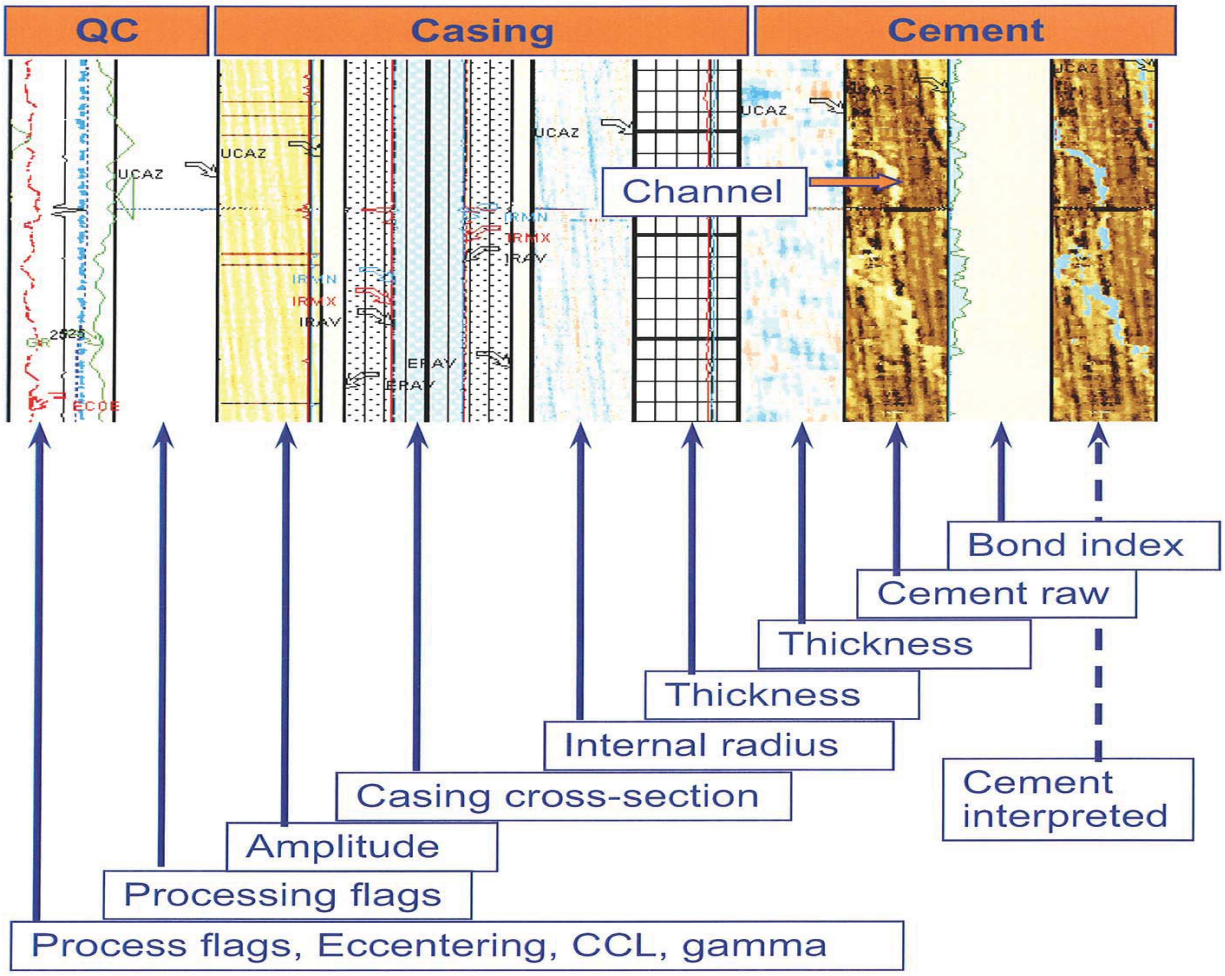

Fig. 39 Logging output of ultrasonic imaging tool [32]

6.2.3 Uncertainties in USIT logging

As with all logging tools several measuring uncertainties are involved that lead to uncertainties of the actual condition of the casing.

Those include uncertainty about the original wall thickness of the casing, tool inaccuracy, tool centralization and the proper choice of radial sampling values. The absolute accuracy of the obtained measurement is +/- 2%.

6.2.3.1 Casing nominal wall thickness versus original wall thickness

Often the original wall thickness of the casing is not the same as the nominal wall thickness stated by the manufacturer. The drift diameter is the inside diameter that the pipe manufacturer guarantees per specifications. Nominal inside diameter is always slightly larger than drift diameter. Additionally, the casing can be radially distorted (casing ovality).

If the original casing geometries are not known, the difference between nominal and original wall thickness can be interpretated as wear.

To avoid misinterpretation a quality check base run should be performed prior to any drilling condition to know the actual casing geometry. The critical unknown is the original inner diameter that can lead to errors in casing wear calculations afterwards. The outer diameter is usually less affected by drilling operations.

Running a base log is associated with higher costs and time and usually not done.

6.2.3.2 Fluid velocity

The fluid velocity is measured along the logging interval and will vary with fluid composition in the wellbore. The more homogeneous the composition of the fluid is the lower deviation between the values.

Often a decrease of sonic travel time with depth is observed due to relative accumulation of solids in the lower part. For lower sonic travel times the internal radius may seem to be larger than it truly is.

Also debris in between or on the reference plate and the transducer as well as oil films on the transducer can lead to inaccurate measurements.

To avoid high inaccuracy the logging results should be divided into sections and several fluid velocity values picked. This however is rarely done.

6.2.3.3 Tool eccentricity

Two centralisers above the transducer shall keep the tool centred in the well. Nevertheless, eccentricity can occur, especially:

- In high local doglegs: This in terms means that eccentricity can give an indication of doglegs
- If the tool is passing the casing collars
- In case a wear groove is in the casing and the centralisers are sliding through the wear groove

The USIT automatically can correct for tool eccentricity, but only up to a certain degree. A maximum of 2% of casing OD is the tolerance limit.

6.2.3.4 Radial sampling and frequency range

Radial sampling can be between 36 (360 deg / 10 deg) and 72 shots per vertical level. This involves a small uncertainty as not the whole circumference of the casing is logged. Especially if the base of the groove is located between two measurement points wear might be underestimated if one picks one of the two measurement point. A way to avoid picking the wrong thickness value, is to plot all the thickness values for this cross-section and extrapolate to a value which might correspond better(Fig. 40).

This can also be done if the measurement was poor in the wear groove due to the limited frequency range of tool. To obtain an accurate thickness measurement the tool sends out pulses in a frequency range in which the resonance frequency of the casing is. If the casing has a wear groove, the resonance frequency will change. The tool can detect wall thickness losses up to max. 54%[v] if post processing methods are applied. In post processing methods the thickness search window is narrowed down: this gives better results for points with high casing wear, but poor results for the rest of the casing.

Post processing allows also generating a 3D model of the worn casing.

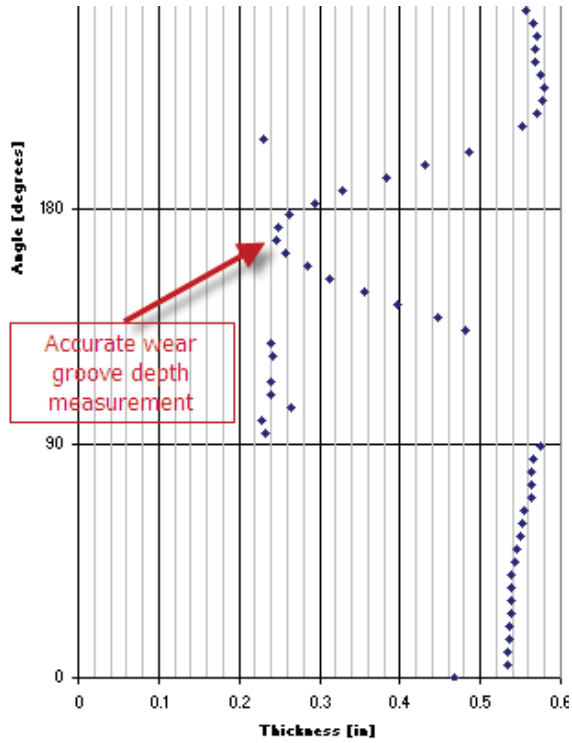

Fig. 40 Good measurement of min. wall thickness

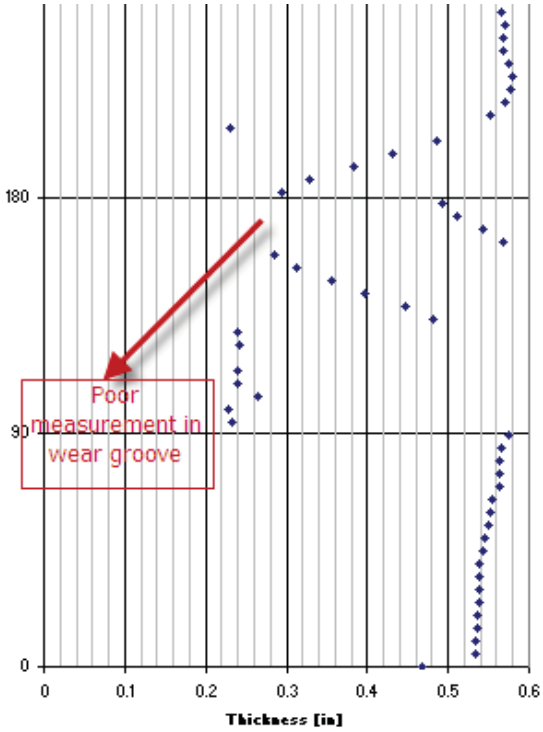

Fig. 41 Poor measurement of min. wall thickness

6.3 Multifinger calliper tools

An alternative to ultrasonic imaging tools is the multifinger calliper tool (MFT), which is run and retrieved on wire line and comprises surface read out.

Multifinger callipers originally were designed to measure changes to tubulars within a well and served only as mechanical devices. Around 1995 the first electronic based versions of these tools were introduced and with them the ability to produce logs with greater resolution allowing generation of 3D images of the interior of the well[33].

[v] In Troll field wear up to 60% can occur.

With a set of arms or fingers it can measure the internal diameter. A base log is required to compare the original internal diameter to the new one.

Life monitoring during running ensures measurement quality. The data are stored in a memory module and can be downloaded and processed as soon as the tool is retrieved.

In contrast to the USI tool, multifinger calliper tool cannot measure the original outer diameter and detect external corrosion, but only the inner diameter. For casing wear logging the thickness is a more stable value than the inner radius, as it is not affected by ovality.

Fig. 42 Multifinger calliper tool

Fig. 43 Tungsten tipped fingers

6.3.1 Measurement principle and tool description

Fig. 42 shows an illustration of the MFT. The fingers make up a circular array of sensors providing a number of simultaneous independent radius values around the circumference of the inside of a tubular at a single depth.

For a 7″ casing: $7'' \cdot \pi * \frac{2.54cm}{1''} = 55.86cm \quad \frac{55.86cm}{60\,finger} \approx 0.9cm$

This would mean one measurement point each 9mm. This data is updated 38 times a second for every finger. The amount of data is big enough to generate high quality 3D visualization of the inner casing string.

The fingers are tungsten tipped and measurements are not affected by any wellbore fluids, apart from very thick mud or highly viscous oils. The high hardness is required to avoid wear on the calliper fingers leading to false measurements.

The measurement principle is based on an actuator arm moving in and out of the sensor coil along with each calliper arm. The output signal is transmitted via the electrical logging cable and finally to surface computers where the signal is decoded. Down hole temperature and tool inclination are sent along with the measurements. After decoding and processing the data on surface, finally a 3D image of the casing can be obtained.

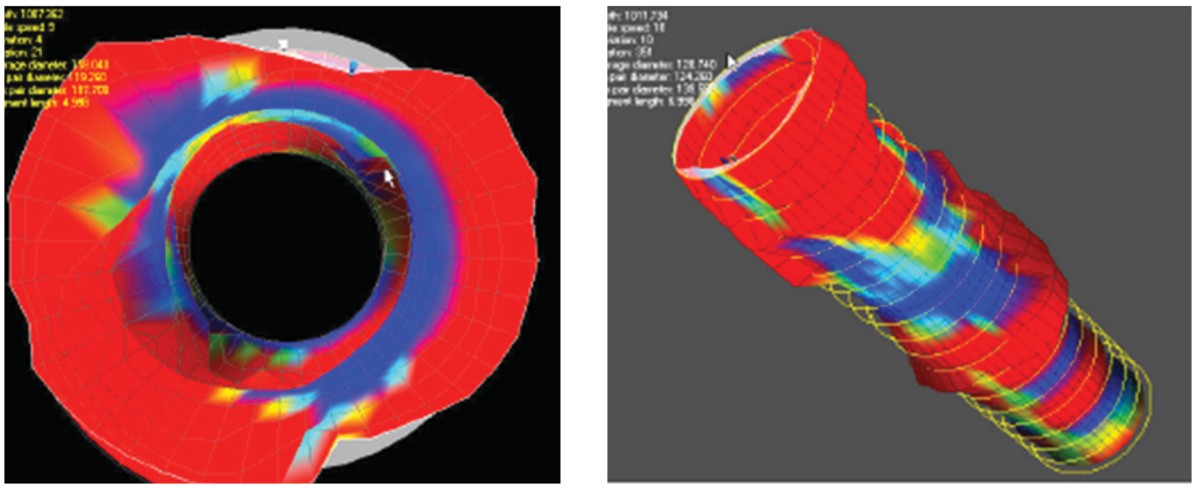

Fig. 44 MLT 3D images from inside and side of the casing

6.4 Magnetic thickness tool (MTT)

This relatively new invention was brought onto the market in 2004 and has an array of twelve miniature sensors mounted on a bow spring (Fig. 45). It works on magnetic flux principle.

The sensors sample 100 times per foot. This allows 100% coverage of a well's casing. The tool is able to close down to 43 mm ($1\ ^{11}/_{16}$") and easily passes through tubing.

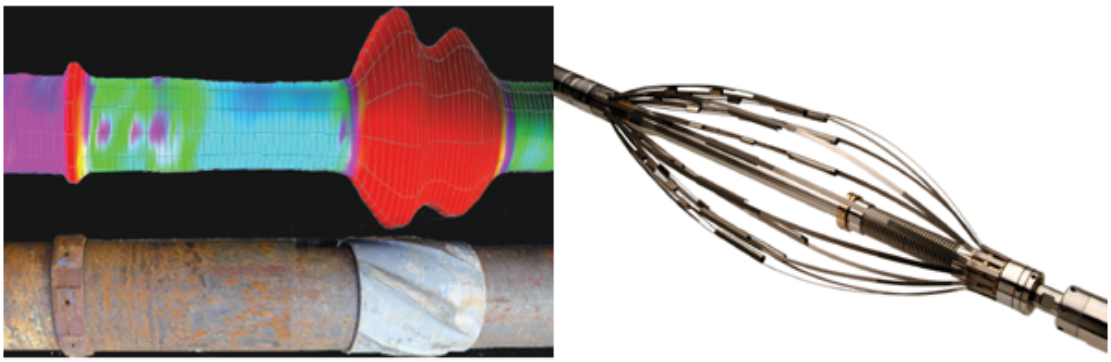

Fig. 45 3D image generated of MTT measurement (left) and MTT sensors on a bow spring (right)

Compared to earlier tools operating on magnetic principles (e.g. magnetic flux leakage MFL tools) it gives the most accurate data (Fig. 46).

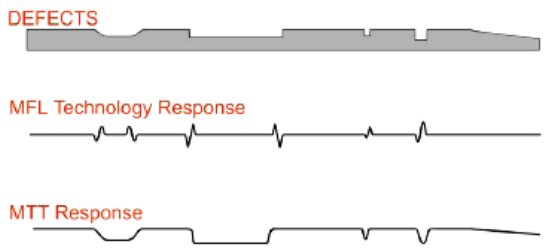

Fig. 46 Responses of MTT and MFL

6.4.1 Measurement principle

An alternating magnetic wave is emitted from the tool. The magnetic wave permeates through the casing wall and then travels a short distance along the outside before passing back through the wall and being detected by the sensors. The velocity and amplitude of the emitted wave are affected by the metal thickness: thinner walls resulting in faster wave propagation and less attenuation. These differences are used to detect and quantify variations such as pitting and metal loss. The internal diameter must first be determined with a multifinger calliper tool. Reference to the multifinger calliper tool data determines whether the metal loss found with the MTT is internal or external.

It is not affected by any fluids in the well.

7 Problems related to casing wear

Casing wear by drill string is an increasing problem for drilling deep wells and/or extended-reach wells. This chapter briefly outlines which consequences worn casing may have and will then present methods to determine the remaining burst and collapse strength of worn casing.

Loosing well integrity is probably the main concern of any operator in regard to casing wear. Casing leaks impose a serious safety hazard for people, environment and equipment.

Reusing existing wells and casings may not be possible if the casing is worn out already.

Problems in the completion phase include packer setting problems

Casing wear costs. Many casing failures cost operators millions of dollars in repairs, sidetracks and even well abandonment; protecting the casing with inappropriate hardbanding costs drilling contractors equally as much in drill string repair and/or replacement. Those costs will be given back to the operators.

7.1 Casing burst strength reduction

Casing wear leads to a reduced wall thickness of the casing. This in term requires that the reduced burst resistance of the casing needs to be crosschecked with the required burst resistance to meet safety requirements.

If the *safety factor* for burst determined with the reduced burst resistance is less than the *design factor*, an additional casing needs to be set before drilling can be continued in a safe way.

- The design factor is the specified requirement (input) for the minimum distance between a load case and the defined limit of the pipe. It must be verified after drilling a section, e.g. with formation integrity test (FIT), leak-off test (LOT) or a fracture test (FT).
- The safety factor is the resulting (output) actual distance between load case and the defined limit of the pipe.
- $\text{Safety} = \dfrac{\text{safety factor}}{\text{design factor}} \geq 1$

The safety must always exceed the minimum value of 1.

A common approach is to use the API burst strength equation with a linear reduction by the remaining wall thickness or the wear percentage. This approach is a very simple, but also a very conservative one. To cost-optimize more accurate solutions to this problem are at hand.

7.1.1 Casing burst strength without wear

Pressures acting on a cylindrical casing (hollow cylinder) can be easily decomposed into three directions using cylindrical coordinates.

The stress tensor is then made up by three components:

- *radial stress* σ_r: acting towards or from the centre of the casing
- *tangential* or *hoop stress* σ_θ: acting perpendicular to both the radial and the axial stress around the casing
- *axial stress* σ_a acting in direction of the casing length axis

The Van Mises yield criterion for casing triaxial stress condition:

$$\sqrt{\sigma_\theta^2 + \sigma_r^2 + \sigma_a^2 - \sigma_\theta^2\sigma_r^2 - \sigma_\theta^2\sigma_a^2 - \sigma_a^2\sigma_r^2} = \sigma_y \qquad \text{[Eq. 9]}$$

For a casing without wear and zero axial stress on which a burst pressure is acting a hoop stress is induced that can be expressed by the Lamé equation[34]:

$$\sigma_\theta(r) = \frac{p_i r_i^2 - p_o r_o^2}{r_o^2 - r_i^2} - \frac{1}{r^2}\frac{(p_i - p_o) r_i^2 r_o^2}{r_o^2 - r_i^2} \qquad r = \{r_i; r_o\}$$

[Eq. 10]

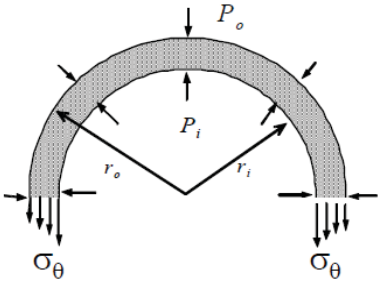

Fig. 47 Casing hoop stresses[34]

The pressure differential or burst pressure can be expressed as:

$$\Delta p = p_i - p_o \geq 0 \qquad \text{[Eq. 11]}$$

For a burst pressure acting on the casing, the induced hoop stress will be a tensile stress with decreasing magnitude with increasing distance from internal radius (Fig. 47)

If the pressure differential exceeds a certain value, the casing material will start to yield.

Fundamental mechanics require that all forces are in equilibrium. To satisfy this condition the burst load must be equal to the load acting in the tangential direction.

$$2(p_i r_i - p_o r_o) = 2\int_{r_i}^{r_o} \sigma_\theta dr \qquad \text{[Eq. 12]}$$

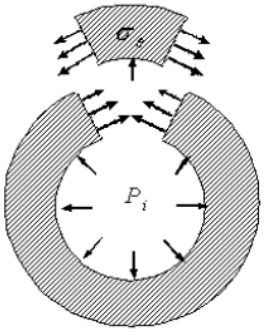

Fig. 48 Casing hoop stress balance for a casing without wear[34]

Fig. 48 depicts this graphically (note: here p_i equals the burst pressure).

API adopted this formula to represent casing burst strength with an approximation of casing yield under internal pressure and called it as internal yield pressure[35] (the maximum allowed pressure differential to avoid casing material yield):

$$p_{API} = 0.875 \frac{2\sigma_y t}{D} \quad \text{[Eq. 13]}$$

σ_y…yield strength [psi]
t…wall thickness [in]
D…casing outer diameter [in]

The factor 0.875 derives from the wall thickness tolerance of 12.5% less than nominal wall thickness. Obviously the thicker the casing wall thickness t, the higher the burst strength.

7.1.2 "API linear wear model" / Uniform wear

The simplest approach to calculate burst strength for a worn casing is by linear reduction of the API burst strength with the remaining percentage of casing wall thickness. It is very conservative and often underestimates the remaining strength. This can be misleading and lead to wrong decision making involving huge amounts of cost.

$$p_{API,w} = (1-w) \cdot 0.875 \frac{2\sigma_y t}{D} \quad \text{[Eq. 14]}$$

w…wear factor

7.1.3 Analytical solution: "Slotted ring model"

Assuming a worn casing with wear depth w[34], the loss of hoop stress plus the internal pressure acting now on a thinner casing, changes the hoop force.

The resulting hoop force F acting on a casing now is:

$$F(r) = 2\int_{r_i}^{r_i+w} (p_i + \sigma_\theta) dr \quad \text{[Eq. 15]}$$

$$F(r) = p_i w + \frac{p_i r_i^2 - p_o r_o^2}{r_o^2 - r_i^2} w - \frac{w}{r_i (r_i + w)} \frac{(p_i - p_o) r_i^2 r_o^2}{r_o^2 - r_i^2} \quad \text{[Eq. 16]}$$

Casing hoop stress increases by:

$$\Lambda\sigma_\theta = \frac{F}{(t-w)} \quad \text{[Eq. 17]}$$

To maintain momentum balance

$$M = \Lambda \sigma_\theta (t-w)(r_o - \frac{t-w}{2}) - F(r_i + \frac{w}{2}) = \frac{F}{2}t \qquad \text{[Eq. 18]}$$

The momentum can be converted expressed as an equivalent hoop stress, which is a tensile hoop stress at the inner diameter, ID, and compressive hoop stress at the outer diameter location:

$$\Delta\sigma_{\theta,m}(r) = \frac{M}{ID}\left(r - \frac{r_i + w + r_o}{2}\right) = \frac{3Ft}{(t-w)^3}\left(2r - r_o - r_i - w\right) \qquad r = \left\{r_i + w; r_o\right\}$$

[Eq. 19]

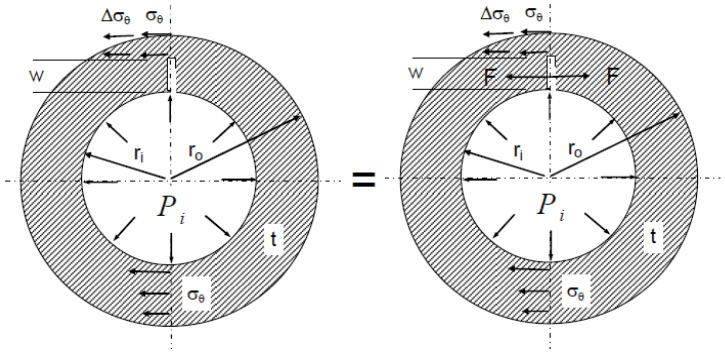

Fig. 49 "Slotted ring" model – pressure balance[34]

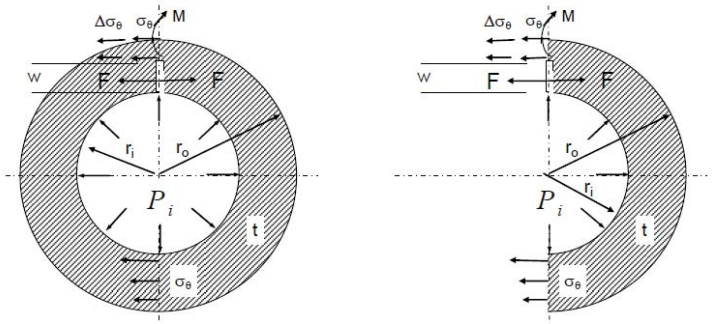

Fig. 50 "Slotted ring" model – momentum balance[34]

Summing up all the additional terms and adding them to the original equation, gives the equation for hoop stress for a worn out casing:

$$\sigma_{\theta,w}(r) = \frac{p_i r_i^2 - p_o r_o^2}{r_o^2 - r_i^2} - \frac{1}{r^2}\frac{(p_i - p_o) r_i^2 r_o^2}{r_o^2 - r_i^2} + \frac{F}{(t-w)} + \frac{1.95F\left(2r - r_o - r_i - w\right)}{(t-w)^3}$$
$$r = \left\{r_i + w; r_o\right\} \qquad \text{[Eq.20]}$$

A correlation factor of 0.65(1-w/t) is added to the bending hoop stress to account for wear shape geometry and casing deformation.

7.1.3.1 "Slotted ring" versus finite element analysis (FEA)

Comparing maximum, minimum and average hoop stresses in the worn casing with FEA modelling for a 9 $^{5}/_{8}$" T-95 casing subjected to a burst pressure of 1,000 psi, gives the following result (Fig. 51). The minimum hoop stress at the outer diameter decreases due to bending.

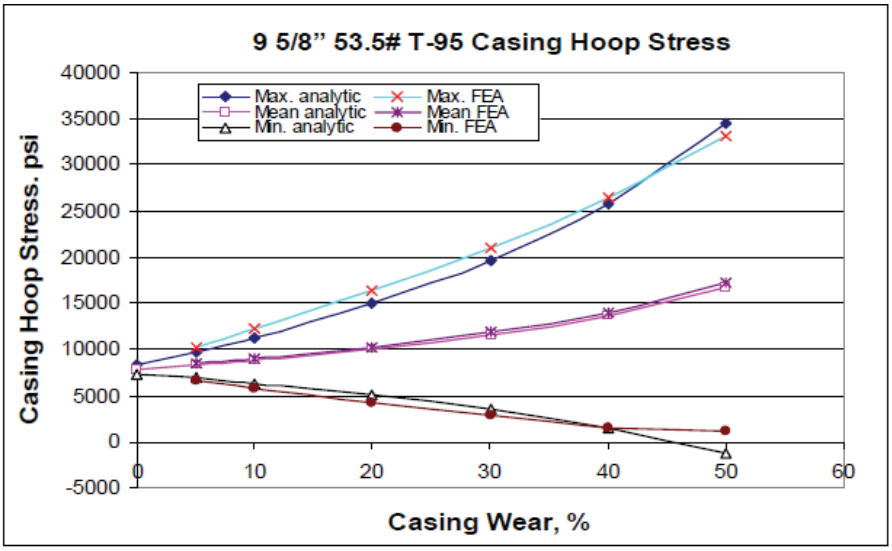

Fig. 51 Worn casing hoop stress: FEA and Slotted ring[34]

7.1.3.2 "Slotted ring" versus "uniform wear"

Comparing maximum hoop stresses in the worn casing with the maximum hoop stress by a uniform wear model for a 9 $^{5}/_{8}$" T-95 casing subjected to a burst pressure of 1,000 psi, gives the following result (Fig. 51):

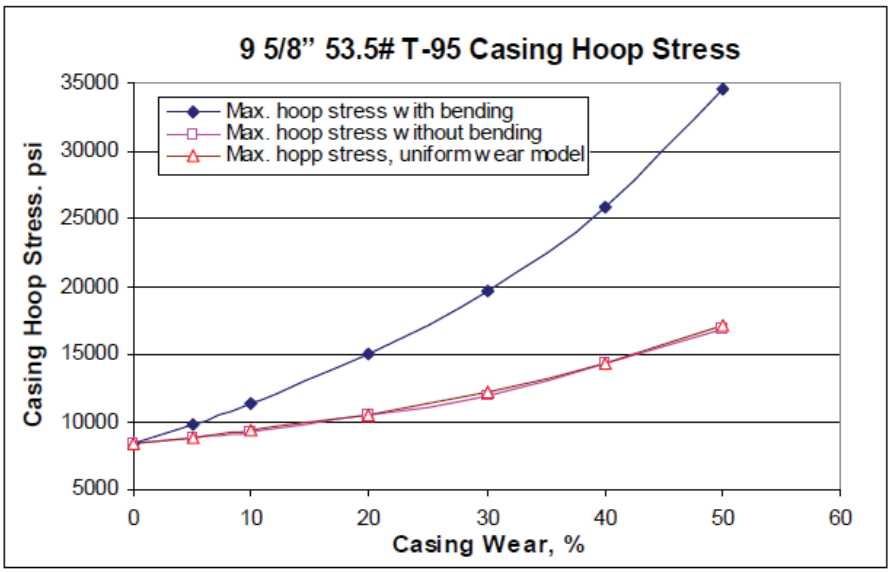

Fig. 52 Max. Hoop stress: Uniform wear and slotted ring[34]

The simple approach, which does not included the influence of bending, fits good if the bending term is neglected in the slotted ring model. It strongly deviates if bending is included and underestimates casing strength.

7.1.4 Other wear models

Based on triaxial analysis other casing burst strength equations[34] exist. These include the the (a) initial yield burst equation, (b) full-yield burst equation and (c) casing rupture burst equation, which are derived from casing triaxial stresses analysis.

(a) $$p_{IY} = 0.875\frac{2\sigma_y}{\sqrt{3}}\frac{2t}{D}\left(1-\frac{t}{D}\right)$$ [Eq.21]

based on casing yield at casing inner diameter

(b) $$p_{FY} = 0.875\frac{2\sigma_y}{\sqrt{3}}\frac{2t}{D}\left(1+\frac{t}{D}\right)$$ [Eq.22]

based on casing yield across entire wall thickness

(c) $$p_{DR} = 0.875\frac{2\sigma_{ult}}{D-t}$$ [Eq.23]

based on casing ductile tensile failure[36]

Equation (c) is based on tubular capped-end testing. It is not based on the yield criterion, but on tensile failure as the internal pressure will impose a tensile load on the capped ends. Furthermore, burst pressure is not inversely proportional to casing OD, but to the mean diameter.

The worn casing burst strength can then be defined when:

(a) the maximum new hoop stress at the inner diameter reaches casing yield strength.

$$\sigma_{\theta,w}\left(r = r_i + w\right) = \sigma_y$$ [Eq.24]

(b) the average new hoop stress in the middle of the remaining casing reaches material yield strength.

$$\sigma_{\theta,w}\left(r = \frac{r_i + w + r_o}{2}\right) = \sigma_y$$ [Eq.25]

(c) the average new hoop stress in the middle of the remaining wall reaches casing material tensile strength.

$$\sigma_{\theta,w}\left(r = \frac{r_i + w + r_o}{2}\right) = \sigma_{ult}$$ [Eq.26]

Where σ_y is defined as:

$$\sqrt{\sigma_{\theta,w}^2 + \sigma_r^2 + \sigma_a^2 - \sigma_{\theta,w}^2\sigma_r^2 - \sigma_{\theta,w}^2\sigma_a^2 - \sigma_a^2\sigma_r^2} = \sigma_y$$ [Eq.27]

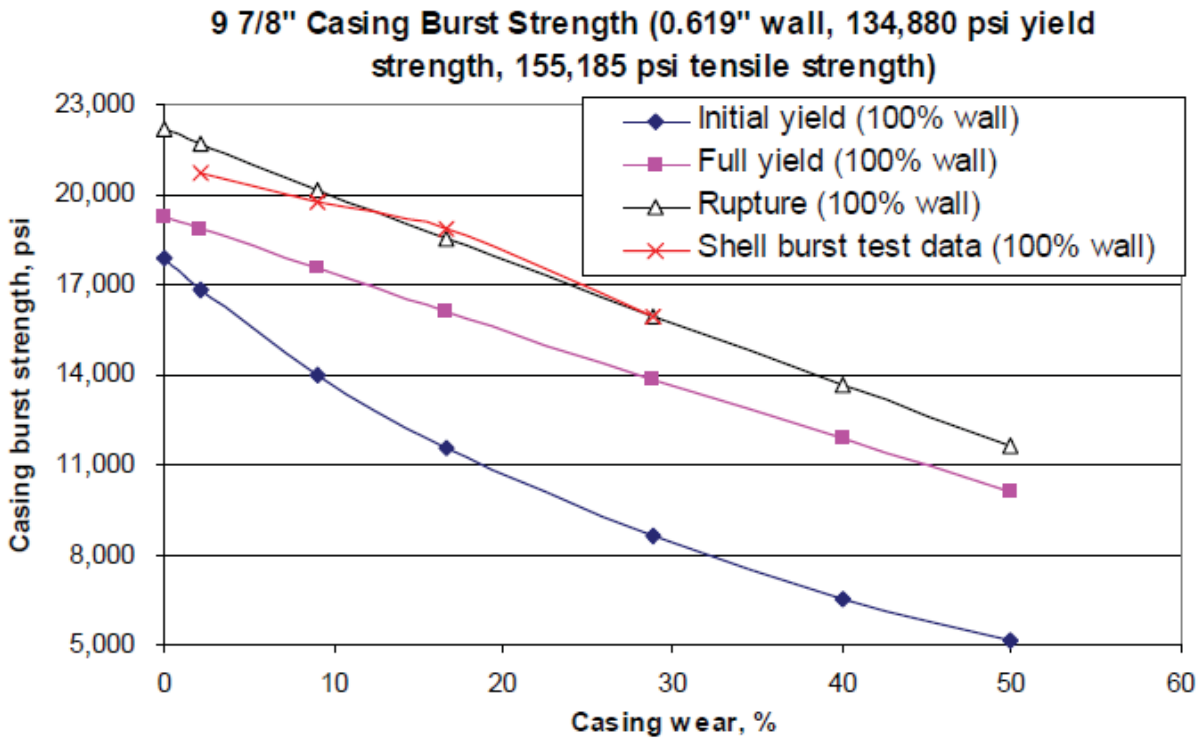

Fig. 53 Worn casing burst strength prediction: The rupture burst equation gives the most accurate and least conservative prediction[34]

7.1.5 Applicability of the different models

Decision making is finally based on the reduced casing burst strength, which gives quite different values for the different models. Depending on service condition, different models should be applied to not over- or underestimate the remaining strength.

- The highest remaining casing burst strengths are obtained by full yield or rupture burst model (Fig.). They are applicable for casing wear in sweet service condition. Here linear reduction from API equation is a way too conservative model.
- Remaining burst strength in sour wells should be estimated from the slotted ring model to prevent an "earlier" casing burst from hydrogen sulphide stress cracking. The more simple API approach can be used here as well, but only for low wear conditions.

7.2 Collapse strength

To clarify the mechanism of the collapse strength reduction, collapse tests were performed by using steel pipes with internal wear [37]. Empirical formulas for the prediction of collapse strength under wear and bending allowing ovality, eccentricity and residual stress were derived.

Three tests were conducted with P110 (7″) and N80 (5-1/2″ and 7″) pipes with a D/t ratio in the plastic collapse region and thickness loss between 20 and 35 percent. Uniaxial and bi-axial collapse testing was done.

The results for the 5-1/2″ casing under uniaxial load show a correlation between wear ratio and reduction of collapse strength. The ratio of worn to unworn collapse pressure is almost proportional to the ratio of minimum to original casing wall thickness.

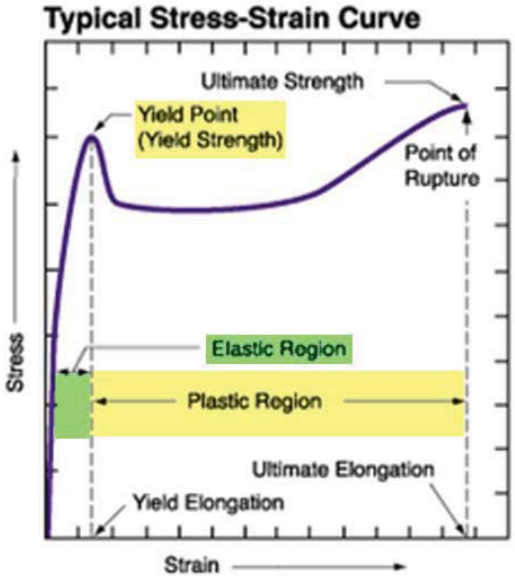

Fig. 54 Typical steel stress strain curve[38]

The mechanism of collapse strength reduction was found to be yield onset as the experimental data for different $D/t_{reduced}$ for 5-1/2″ casing are parallel to the yield onset curve. The unworn casing (D/t=18.1) is in the plastic collapse region (Fig. 54 and Fig. 55).

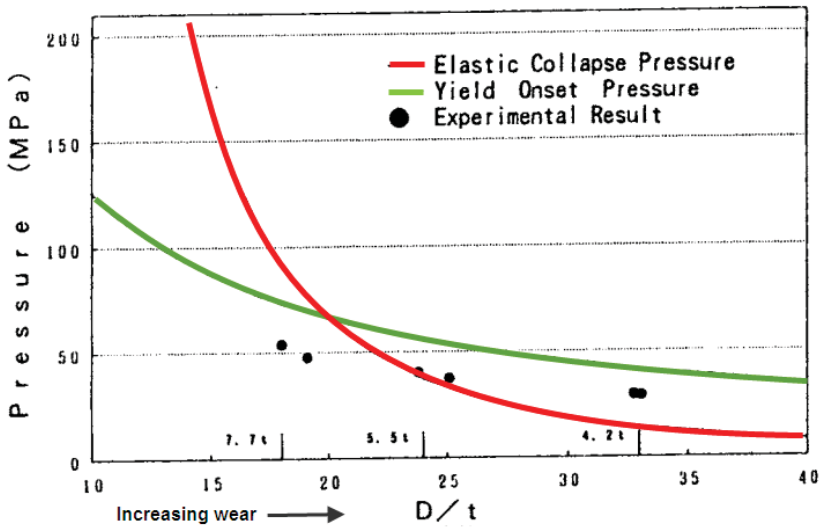

Fig. 55 Ideal tube (7.7t) collapse pressure and worn casing collapse pressure (5.5t, 4.2t) [37]

Elastic collapse pressure (Timoshenko) and plastic collapse pressure[vi]:

[vi] Yield onset pressure is a bit lower than plastic collapse pressure, but a good approximation

Elastic:	$P_e = 2E\frac{(D/t - 1)^3}{1 - v^2}$	Plastic:	$P_{yield} = 2S_y \frac{D/t - 1}{(D/t)^2}$
	E...Young's modulus [N/mm²] v...Poisson's ratio [-] t...wall thickness [mm]		Sy...Yield strength [N/mm²] D...Outside diameter [mm]

[Eq.28] [Eq.29]

To determine the tangential stress in the worn casing, the wear groove may be approximated by an eccentric cylinder.

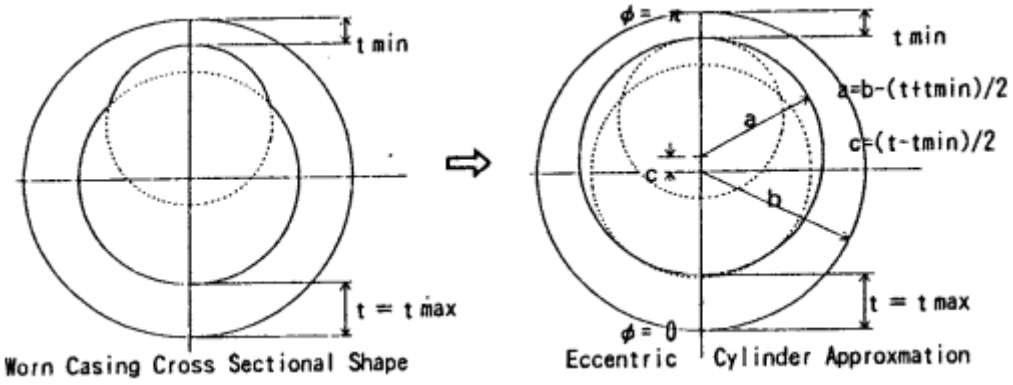

Fig. 56 Modelling of worn shape[37]

The circumferential stresses can then be calculated for uniformly worn casing for a casing with wear groove:

$$\sigma_t(\phi) = -2p\frac{b^2}{a^2+b^2}\frac{\left(b^2-c^2\right)^2 - a^2(a+2c\cdot\cos\phi)^2}{\left(a^2+b^2-c^2\right)^2 - 4a^2b^2} \qquad \text{[Eq.30]}$$

$$b = D/2;\quad a = b-(t+t_{min});\quad c = \frac{t-t_{min}}{2}$$

At worn portion circumferential stress is:

$$S = -2p\frac{b^2}{a^2+b^2}\frac{\left(b^2-c^2\right)^2 - a^2(a+2c\cdot\cos\phi)^2}{\left(a^2+b^2-c^2\right)^2 - 4a^2b^2} \qquad \text{[Eq.31]}$$

Yield onset pressure of worn casing by eccentric cylinder model:

$$P_{y,worn} = -S\frac{a^2+b^2}{2b^2}\frac{(a^2+b^2-c^2)^2 - 4a^2b^2}{(b^2-c^2)^2 - a^2(a-2c)^2} \qquad \text{[Eq.32]}$$

Uniformly worn casing gives a slightly higher circumferential stress at the worn side.

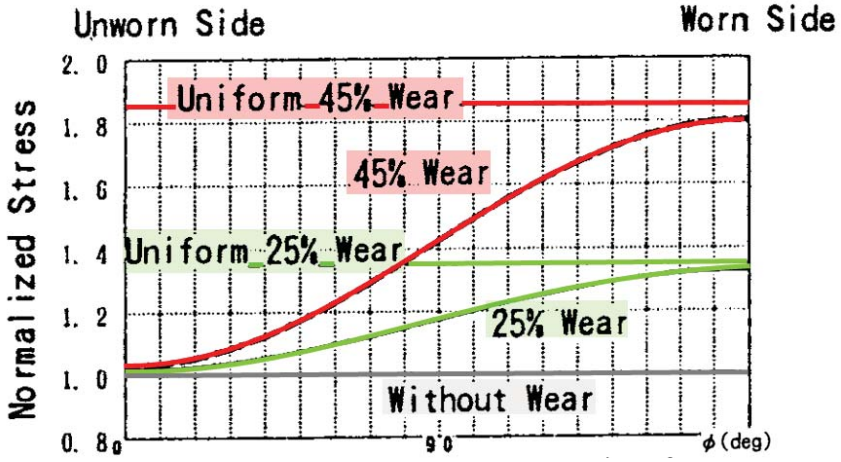

Fig. 57 Stress distribution of worn tube normalized by unworn tube stress[37]

An analysis of worn casing elastic collapse pressure was made with FEA using the measured shape. The FEA results of ideal tube and collapse pressure are in good agreement with Timoshenko's equation (Fig. 58).

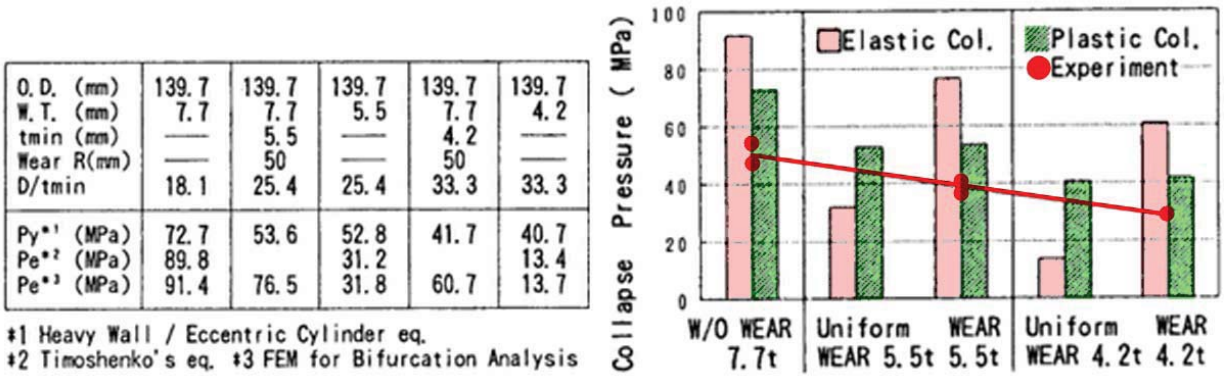

O.D. (mm)	139.7	139.7	139.7	139.7	139.7
W.T. (mm)	7.7	7.7	5.5	7.7	4.2
tmin (mm)	—	5.5	—	4.2	—
Wear R(mm)	—	50	—	50	—
D/tmin	18.1	25.4	25.4	33.3	33.3
Py*1 (MPa)	72.7	53.6	52.8	41.7	40.7
Pe*2 (MPa)	89.8		31.2		13.4
Pe*3 (MPa)	91.4	76.5	31.8	60.7	13.7

*1 Heavy Wall / Eccentric Cylinder eq.
*2 Timoshenko's eq. *3 FEM for Bifurcation Analysis

Fig. 58 Worn casing dimension and pressure (5.5" OD x 7.7t N-80); elastic/plastic collapse strength of ideal pipe and experimental results[37]

Unworn tube is in the plastic collapse region. Uniformly worn tube with wall thicknesses 5.5t and 4.2t will fall into the elastic collapse region with large reduction of collapse strength. Locally worn tube with minimum wall thickness 5.5t and 4.2t still fall in the plastic collapse region with higher remaining collapse strength. Evaluation of worn tube with uniform wear model would lead to an underestimation of remaining collapse strength.

The lowering ratios of experimental collapse strength to yield onset pressure are almost the same for unworn and more or less worn tubes. Deviation from yield onset in experimental and calculated results derives from imperfections of the real pipe

Thus collapse pressure of worn casing can be estimated by combination of the estimation of yield onset pressure worn casing by eccentric cylinder model and the estimation of the effect of imperfections, such as ovality and residual stress.

First the collapse pressure of unworn tube is evaluated, then the worn casing collapse pressure using K_{int}. Collapse pressure of worn tube can be evaluated by a set of empirical formulas developed by T. Tamano et al.:

$$Pe = 2E/(1-\nu^2)/[(D/t)(D/t-1)^2]$$

$$Pgy = 2Sy(D/t-1)/(D/t)^2[1+1.47/(D/t-1)]$$

$$Pga = Pgy[\sqrt{1-3/4(Sa/Sy)^2}-1/2(Sa/Sy)]$$

$$H = 0.0808u(\%)+0.00114e(\%)-0.1412Sr/Sy$$

$$Pest = 1/2(Pe+Pga)-\sqrt{1/4(Pe-Pga)^2+PePgaH}$$

where Pe :Clinedinst's elastic collapse pressure
Pgy :general yield pressure,
Pga :general yield pressure under axial load,
H :deviation from ideal tube
Pest:collapse pressure of actual tube

$$Pw = Pest/Kint$$

$$Kint = Py/Pyw$$

where Pw:collapse pressure of worn tube
Py:yield onset pressure of unworn tube
Pyw:yield onset pressure of worn tube

Kint stands for the ratio of how fast yield onset starts comparing with the unworn tube.

[Eq.33]

Fig. 59 Equations to calculate collapse uniaxial and biaxial strength of worn casing[37]

The effect of wear on collapse uniaxial and biaxial strength with the above presented empirical formula for cylinder model and FEA is in good agreement with experimental results. The reduction in collapse strength is much smaller than predicted by uniform wear model.

8 Carbon dioxide corrosion fundamentals

This chapter shall give some general information on CO_2 corrosion and some background information on the CO_2 corrosion history on Troll.

CO_2 corrosion is one the most studied form of corrosion in oil and gas industry. This is generally due to the fact that the crude oil and natural gas from the oil reservoir / gas well usually contains some level of CO_2 (and H_2S – hydrogen sulphide). The major concern with CO_2 corrosion is possible equipment failure, especially the main downhole tubing or production casing and transmission pipelines. Thus, it can disrupt the oil/gas production and imposes safety and environmental risks.

If the corrosion rate of carbon steel becomes too high, the use of corrosion inhibitors should be taken under consideration. Corrosion inhibitors form a protective film on the corroding metal.

Gas-lift oil wells are more susceptible to general and localized corrosion than pumping wells because of the higher temperature and the higher concentration of CO_2 (provided that CO_2 has not been removed from a working gas, so that the solution at the well bottom shows low pH) and a lot of water and O_2 is present in the injected gas.

Corrosion protection of gas/condensate lines is challenging due to the low pH of condensed water. The corrosion rate can be controlled by using pH stabilizers which react to form a passivity film on the corroding surface. The disadvantage of pH stabilizers is the formation of scale products (e.g. $CaCO_3$, Fe_3O_4) after water breakthrough. Injection of pH-stabilizer in combination with a chemically compatible scale inhibitor is required from then on.

8.1 Reactions

CO_2 corrosion can be described by the following reactions: Carbon dioxide dissolves in water and is partly hydrated to form carbonic acid:

$$CO_2 + H_2O \Leftrightarrow H_2CO_3 \qquad \text{[Eq.34]}$$

Carbonic acid is diprotic and dissociates in two steps:

$$H_2CO_3 \Leftrightarrow H^+ + HCO_3^- \qquad \text{[Eq.35]}$$

$$HCO_3^- \Leftrightarrow H^+ + CO_3^{2-} \qquad \text{[Eq.36]}$$

Concerning the cathodic reaction, the overall reaction is:

$$Fe + 2\ H_2CO_3 \rightarrow Fe^{2+} + 2\ HCO_3^- + H_2 \qquad \text{[Eq.37]}$$

The reaction creates bicarbonate which shifts reaction (3) to the right and formation of iron carbonate can take place if the solubility product of iron carbonate is exceeded.

$$Fe^{2+} + CO_3^{2-} \rightarrow FeCO_3\ (s) \qquad [Eq.38]$$

The formation of iron carbonate has a large influence on the corrosion rate since it forms a protective film.

8.2 Factors influencing CO_2 corrosion

8.2.1 CO_2 partial pressure

The higher the CO_2 partial pressure, the more hydrogen carbonate (H_2CO_3) is built which dissociates to HCO_3^-, CO_3^{2-} and H^+. At filming conditions an increased CO_3^{2-} concentration can promote the formation of iron carbonate, which protects the steel against corrosion and the corrosion rate will accordingly drop. Precipitation of iron carbonate scale is promoted in less sour environments.

8.2.2 Bicarbonate concentration / pH

Iron carbonate solubility increases with decreasing pH. Thus it precipitates to form a protective film in lower pH environments more easily. Increasing bicarbonate concentration also reduces the reduction of hydrogen ions and thus increases pH (Fig. 60)

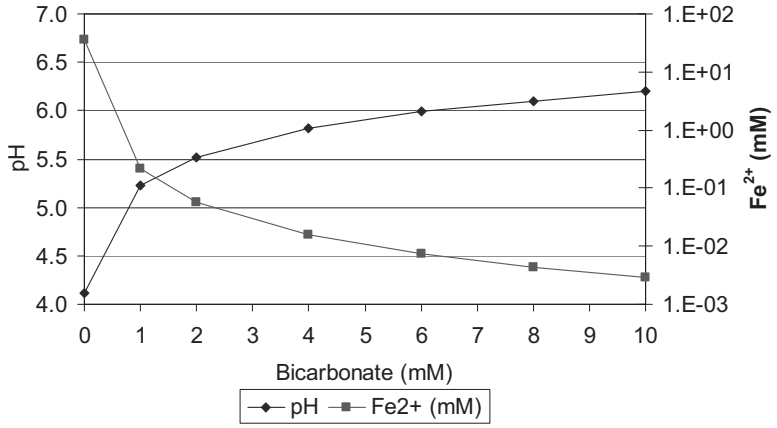

Fig. 60 The influence of bicarbonate concentration on pH and iron solubility at 1 bar CO_2 and 80°C[39]

The corrosion rate decreases with increasing pH. Condensed reservoir water has very low pH, whereas formation water has a pH of about 5.5 (Fig. 61).

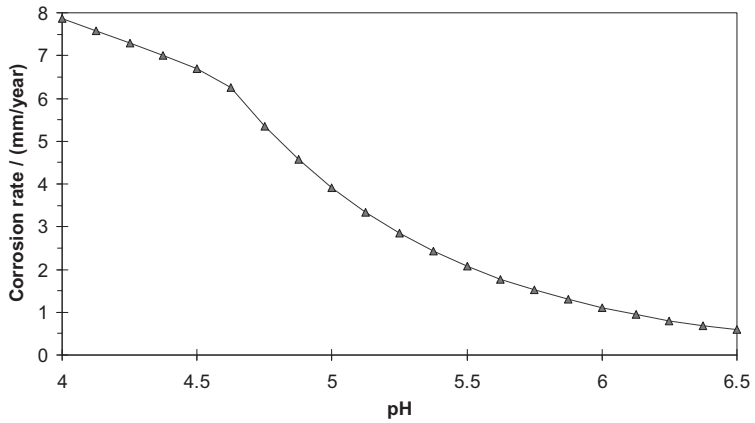

Fig. 61 Corrosion rate versus pH at 1 bar CO_2 partial pressure and 80°C [39]

8.2.3 Temperature

The corrosion rate generally increases with temperature, whereas the iron carbonate solubility decreases. The two mechanisms are competing: First the corrosion rate will increase until precipitation of iron carbonate scale is promoted and the corrosion rate starts to decrease at high temperature.

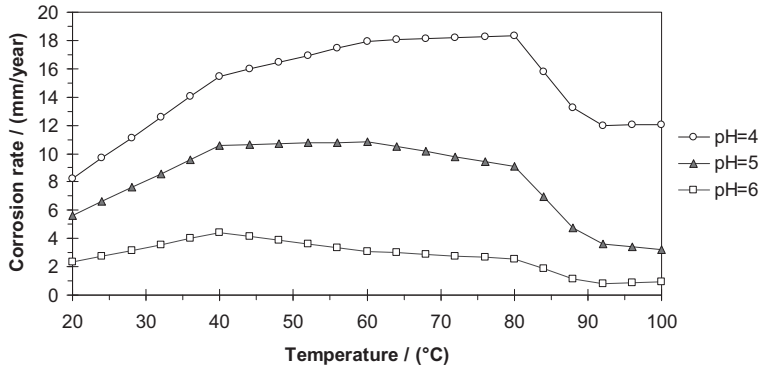

Fig. 62 The relationship between corrosion rate, temperature and pH [39]

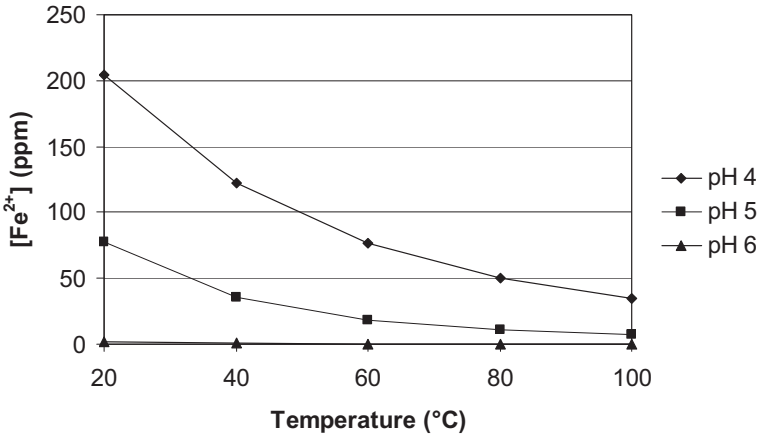

Fig. 63 The influence of temperature on the Fe^{2+} concentration that is necessary to obtain $FeCO_3$ saturation [39]

8.2.4 Organic acids

Actetatic acid is the most important organic acid in formation waters and natural gas. A second important acid is formate acid, which is formed by the reaction between CO_2 and formate based brine.

$$CO_{2(aq)} + H_2O + COOH^-_{(aq)} \Leftrightarrow HCO_3^-{}_{(aq)} + HCOOH_{(aq)} \quad [Eq.39]$$

Acetic acid can influence the corrosion process in two ways. It acts as a provider for H^+ and acetic acid can be reduced directly on the metal surface in the same way as carbonic acid. Acetic acid also influences the formation of protective films. At low pH a higher Fe^{2+} concentration is needed to reach $FeCO_3$ saturation when acetic acid is present, but at high pH acetic acid does not influence the Fe^{2+} concentration that is necessary to reach saturation. Crolet et al observed that iron acetate, which has higher solubility than FeCO3 is the major corrosion product (pH 5.18, 50°C) while at high pH and 80°C HAc had no significant effect on FeCO3 formation and its protectiveness. In summary, acetic acid will have a pronounced effect on the corrosion at low pH, but at high pH when acetic acid is present as acetate its influence is small. [39]

8.2.5 H_2S partial pressure

Hydrogen sulphide content has a large impact on the corrosion rate since it will influence pH and cause formation of iron sulphide films. Iron sulphide films are of low solubility, thus H_2S will influence the composition of the protective film and type of corrosion at quite low partial pressure. [39]

Kapusta et al[40] have proposed the following limits for when a system can be regarded as sweet or sour (Tab.2):

pCO_2 / pH_2S	Corrosion	Remarks
>5000	CO_2 corrosion	CO_2 corrosion prediction
20 – 5000	Corrosion in slightly sour environment	Low risk of localized corrosion. Corrosion rates will be lower than predicted in sweet wells
> 20	H_2S corrosion	Elementary sulphur precipitates at elevated pressures (>300 bars) and temperature (> 100degC). Localised corrosion rates can be very high, particularly in highly saline environments

Tab. 2 Influence of H_2S on CO_2 corrosion rate[40]

To predict the corrosion rate in the sour regime Pots et al[41] proposed to multiply the CO_2 corrosion rate with a pitting factor which is dependent on chloride concentration.

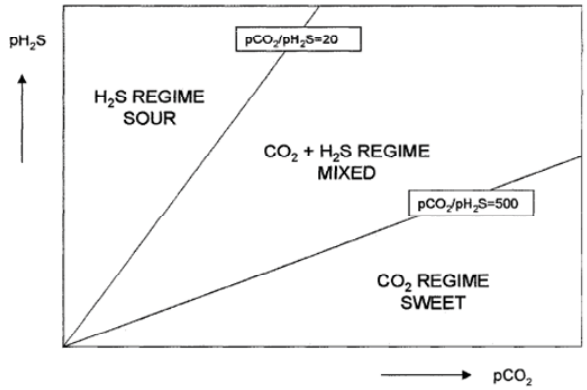

Fig. 64 Regimes for sweet and sour corrosion[41]

8.2.6 Wall shear stress

Under most well and pipeline conditions the wall shear stress only gives a gradual and low increase in corrosion rate due to increased transport of cathodic species to the steel surface. Additionally the flow can also partially / fully erode the protective iron carbonate film from the metal surface and slow down the build up of a protective film. In case of total film erosion high localized corrosion can take place.

8.2.7 Water wetting

Corrosion is not taking place if water cut is less than 40% and flow velocity above 1.5 m/s. Above 40% water cut partial protection applies, but only if the flow velocity is above 1.5m/s. At lower flow velocity separation of oil and water will take place.

Another approach is to use the oil/water inversion point. The inversion point is the water cut where the fluid goes from oil continuous to water continuous. Above the inversion point full water wetting and high corrosion rate should be assumed while below inversion point a gradual decrease in corrosion rate will take place.

The use of water wetting should be restricted to vertical wells, as local flow conditions (e.g. bends and obstacles) can promote oil/water separation too.

8.3 Corrosion facts and completion on Troll

CO_2 corrosion is an issue on Troll. Bottomhole temperature is about 69 ºC and pressure 145 bars.

In February 2000 a leakage in well 31/2-E-4H in Troll oil province was discovered. Investigations[42] showed that a PUP joint of about one metre connected to the X-mas tree and the production tubing was made of carbon steel. The PUP joint was penetrated due to

CO_2 corrosion. 23 other wells had the same material in the PUP joint. CO_2 corrosion calculations have been performed for all the wells with carbon steel PUP joint. Based on the results from the calculations the following conclusions and recommendations were given:

- The composition of formation water and the CO_2 content in the oil and gas vary from place to place in the Troll field (Fig. 65)

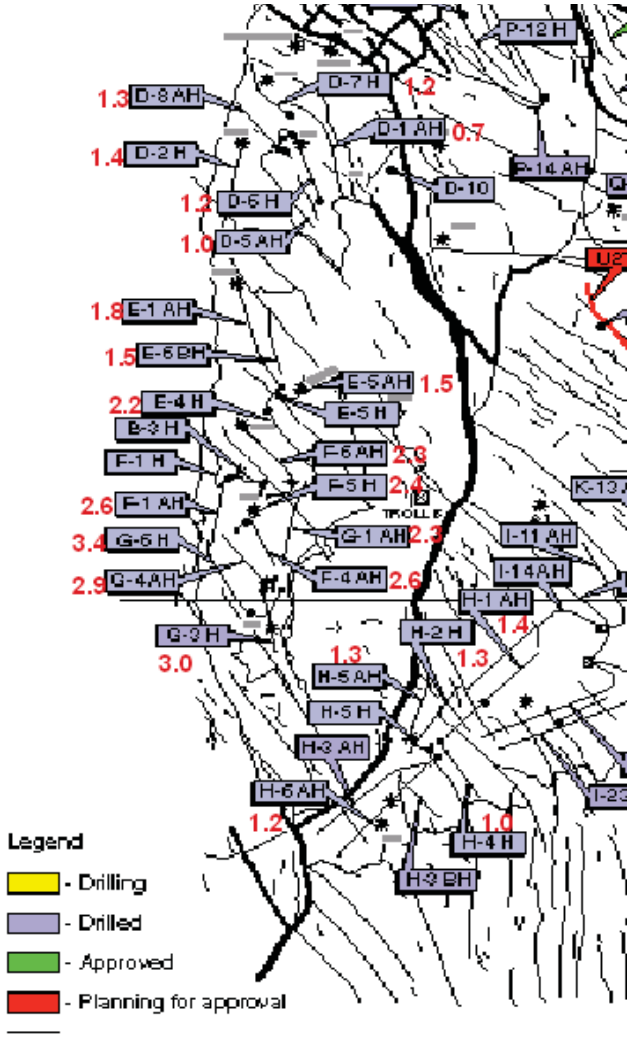

Fig. 65 CO_2 content in gas. The red number beside the well identification show the mole % CO_2 measured in the gas phase at test separator conditions for all the wells. The measurements were done in the first one or two years of production for each of the wells [42]

- The composition of formation water and the CO_2 content in the gas phase have changed with time. The change results in a lower pH in the formation water which gives higher corrosion rates than at the beginning of production.
- Calculation of accumulated corrosion showed that well E-4 was not the most corrosive of the wells. This indicated that factors like water wetting and production rates have been important factors for the real corrosion rate in the PUP joint in well E-4.
- Visual inspection of the PUP joint from well E-4 indicated that mesa corrosion had occurred (Fig. 66). It is assumed that mesa corrosion occurs when the water cut is

above 40% and at the same time the wall shear stresses is above 20 Pa. A mesa corrosion rate of 5.9 mm/y was estimated for well E-4.

Fig. 66 PUP joint in well E-4 failed due to severe mesa corrosion

It was recommended to do a new evaluation regarding time for repair of the remaining wells when results from the repaired and/or inspected wells were available.

Recently (Mar, 2010) pulled steel pup joints in three wells have experienced far less corrosion than predicted by the study in year 2000. The investigated steel PUP-joints of wells F-1, H-3 and H-6 where exposed to flowing corrosive production fluids for approximately five years (1996-2001) before a pipe was inserted in the pup joint to protect it from further corrosion. In well F-1 the CO_2 percentage is highest with 3.0 %. Predicted corrosion rate is 12mm/yr; Ultrasonic measurements conducted in April 2010 showed that after 5 years exposure the wall thickness decreased from 9.2mm to a minimum of 8.5mm[43]. The two other wells experienced similar low corrosion.

A new evaluation was never done and recent inspections show that the assumptions of the study in year 2000 may be too conservative and the calculations should be redone.

8.3.1 Where can carbon steel be used?

8.3.1.1 Above the perforations

If corrosion shall take place water has to condense above the perforations.

A gas is considered dry when the water dew point at the actual pressure is at least 10 °C lower than the actual operation temperature for the system [44]. On Troll water dew point is approximately 2°C lower than gas temperature. Isothermal reduction of pressure yields a hydrocarbon condensate, while isobaric cooling yields condensation of water. If both

pressure and temperature is reduced, hydrocarbons will always condense, while water may or may not condense, depending on the magnitudes of the reductions. Troll gas should therefore be regarded as corrosive.

Fig. 67 shows the corrosion rate between the production packer and isolation packer if water condenses.

The corrosion rate will be between 2 and 5.5 depending on the mole % CO_2. Even with only 0.5 mole % the corrosion rate is too high for use of carbon steel, i.e. a 10 mm casing may be penetrated in 5 years.

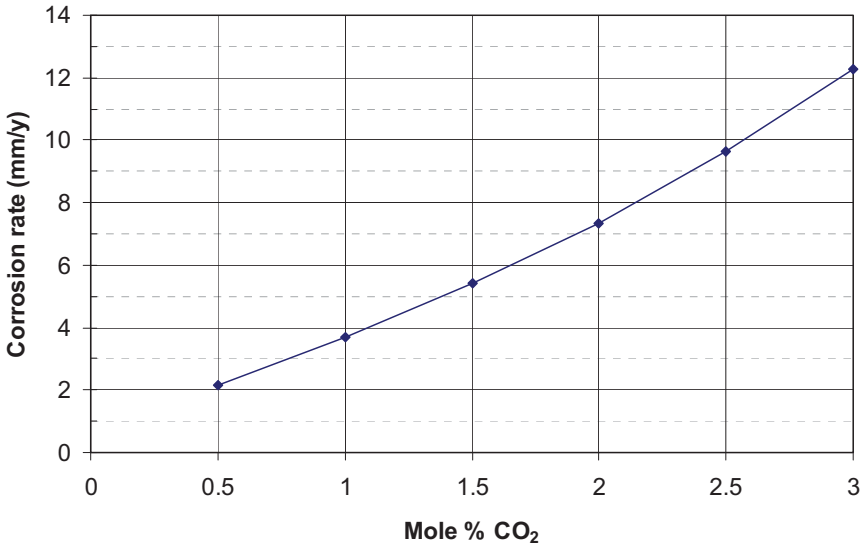

Fig. 67 Corrosion rate versus mole% CO_2 between production packer and isolation packer if water is condensing

8.3.1.2 Below the perforations

There will be completion fluid below perforations. CO_2 in the lift gas will dissolve in the completion fluid and cause corrosion. The corrosion rate will be limited by the transport of CO_2 in the completion fluid. The corrosion rate will therefore be highest close to the lift gas/completion fluid interface and decrease with increasing distance from the interface. For diffusion of CO_2 in water the mean diffusion length is estimated to be about 1 m for a period of 20 years. If the transport of CO_2 in water is controlled by diffusion the region of corrosive water is rather small. In a well at production there exist temperature differences between the tubing, the annulus and the formation, which could generate convection cells as illustrated in Fig. 68. The convection forces decrease as the temperature difference decreases deeper in the well. At very low heat transfer rates the convection stops and the transport is only controlled by the diffusion. This means that 13%Cr steel should be used for the section of the casing which is close to the interface, but further below carbon steel can be used.

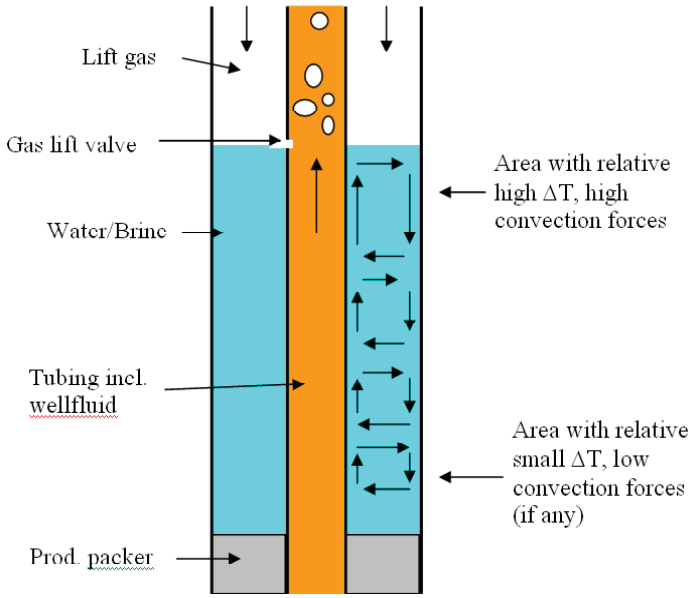

Fig. 68 Transport of CO_2 in annulus completion fluid

8.3.1.3 Between isolation packer and screen hanger packer

The corrosion rate depends primarily on mole percent CO_2 and formation water composition (pH). Basis for the predicted corrosion rates for the horizontal section are the calculations done in the course of the steel pup joint corrosion incident. Similar assumptions are used with full water wetting assumed in the horizontal section due to complex geometry with zones which will enhance local water separation. The predicted corrosion rates vary between 2.3 and 4.9 mm/y.

8.3.2 Typical Troll completion design, 2 branch well

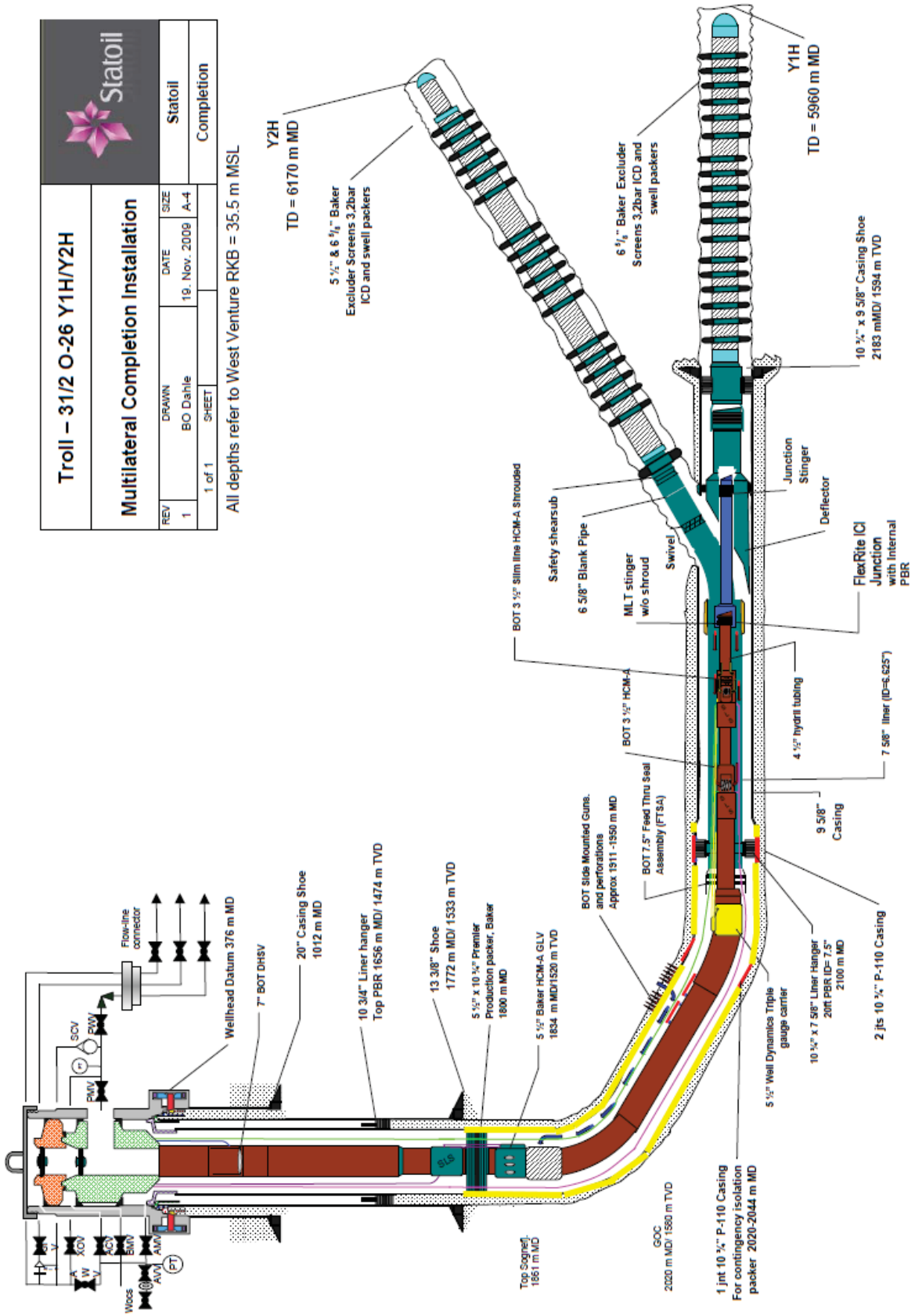

Fig. 69 Troll two-branch multilateral completion; Chrome joints marked in yellow

The two-branch multilateral horizontal oil producing wells are completed with sand screens and blank pipe / swell packers to blank off water horizons.

The top completion consists of two flow single lines control valves (TRFC-HN-AP and TRC-HN-LP), isolation packer, side mounted guns (SMG), LPZ packer with gas lift screen, hydraulic operated gas lift valve (HMP GLV), one production packer, one safety valve (DHSV) and tubing hanger. The gas cap is perforated with the side mounted guns and gas flow can be hydraulically adjusted from the surface through a control line, which operates the gas lift valve. The branch control completion can control the flow from the two individual branches.

A tubing hanger is run with preinstalled isolation sleeve. An internal tree cap is installed to ensure correct landing of the tubing hanger before setting packers and pressure testing the completion. The isolation sleeve is pulled before installing shallow tubing hanger and internal tree cap barrier plugs. After the marine riser and BOP have been pulled, a corrosion cap will be placed on top of the XMT.

The 13Cr section is marked in yellow. The packer setting area for the isolation packer consists of P110 black steel. Based on corrosion rate calculations black steel can also be used further down the perforations.

Due to the design of the tree cap corrosion inhibition with a chemical injection line is not feasible in Troll wells.

9 Casing wear analysis

9.1 Problem statement

Due to hard calcite stringers in the reservoir section Statoil ever experienced casing wear to a certain degree on Troll wells.

The amount of wear is thought to be linked closely to the presence of calcite stringers, as total drilling time will increase, due to low rate of penetration in the hard stringers and nodules.

Today the expected wear in Troll wells is forecasted based on a more or less accurate proportionality between total drilling time (circulating and drilling) maximum wear. Commercially available software, such as CWEAR by Petris, is not suitable to predict wear on Troll as the simulations underestimate the wear significantly.

This analysis is to study casing wear on the 10-3/4" production liner in Troll wells. It is the task to assess parameters contributing to excessive casing wear. In specific, it shall be investigated whether common parameters govern the wear problem or Troll wells do not follow a general casing wear trend. The occurring deviations in any case shall be investigated. Finally solutions for future Troll wells shall be given.

The study was initiated after in two recently drilled wells 31/2-F-1-BY1H/BY2H & 31/5-I-21-BY1H/BY2H unexpected high casing wear was seen on the USIT logging results. A third well 31/5-H-3-CY1H/CY2H, where drilling time was approximately the same as for the two other wells has seen about 15 % less wear (Fig. 70). A presentation of the USIT logging results and results of the reduced burst pressure ratings for these wells is given in the Appendix (16.1).

Due to the reduced pressure rating drilling is limited due to well integrity concerns and Statoil faces problems especially during the completion phase.

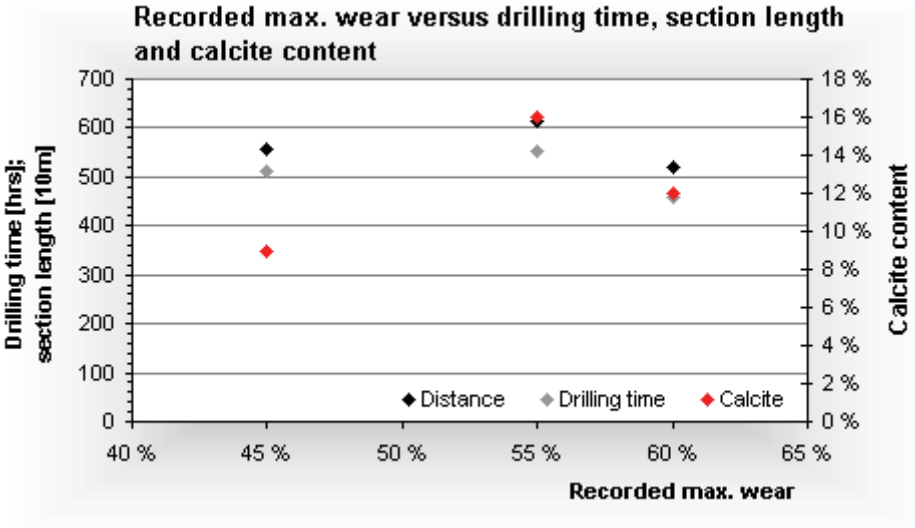

Fig. 70 Drilling time, cumulative 8 ½ branch length and calcite content for H-3 (45% max. wear), F-1 (55% max. wear) and I-21 (60% max. wear)

9.1.1 Problems related to casing wear in Troll wells

Though it is difficult to classify the technical condition and specification of worn casing, the ultimate consequence is lower reliability and significant cost impact in case of shut-down of wells.

9.1.1.1 Re-entry and deep side tracking with the potential of cost saving

In case a re-entry is planned in one of the wells a huge amount of costs can be saved by side tracking out of the existing 10-3/4" liner compared to side tracking out of a more shallow part of the well. With an already substantially decreased casing wall thickness, drilling out one or more additionally branches will further decrease the wall thickness and eliminate this possibility of saving costs due to well integrity concerns.

9.1.1.2 Completion problems

Due to the high casing wear often problems in the completion phase arise.

9.1.1.2.a Firing the side mounted perforation guns

Troll wells are completed with gas lift and there has to be sufficient pressure integrity in the casing to withstand the pressure needed to fire the perforation canons. If the burst rating of the 10-3/4" inch liner has been reduced too close to the pressure required for firing the perforation guns between the isolation and the production packer, the gas zone needs to be perforated in a separate run. Thus it will be exposed to the flow of hydrocarbons during the installation.

9.1.1.2.b Packer setting problems

In some wells leakages during pressure testing of the packer was observed due to the lacking ability of the packer to seal against the worn crescent shaped casing. This resulted in a sub-optimized completion design:

The production packer was moved up into the carbon steel which is basically not worn. The isolation packer was replaced by a swell packer. The problem with the swell packer is that it needs approximately 14 days to seal in Troll oil and will not seal if exposed to only Troll gas. It is therefore necessary to set mechanical packers that hold the pressure.

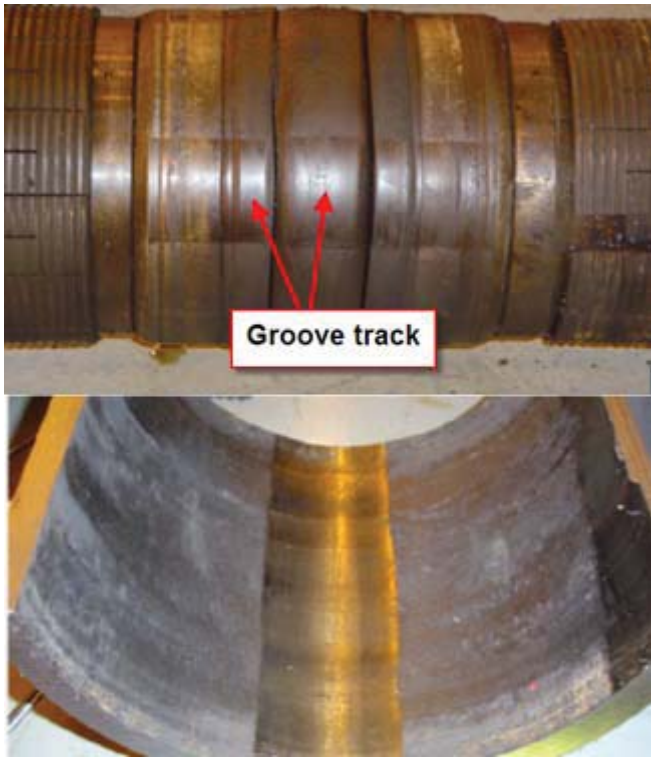

Fig. 71 Retrieved swell packer set in severely worn casing

In the interval where the packers are placed, the hydrocarbons will not flow straight to the casing, but 20 m above and below these packers. The change in the completion was approved after experimental testing showed that in this more or less stagnant hydrocarbon environment the CO_2 corrosion rate is significantly lower than in a flowing hydrocarbon environment. Up to date no problems related to corrosion behind those packers have been reported.

9.2 The typical Troll well and observed wear

All Troll wells drilled within the last five years have a similar trajectory and casing design (Fig. 72).

The 17-1/2" section is kicked off from a cement plug below the 18-5/8" shoe of an abandoned well. The section is drilled at low inclination (30 deg) followed by a tangent section and then builds inclination to about 60 deg. After setting the 13-3/8" casing, the 12-1/4" section is drilled and opened to 13-1/2" landing horizontally in the formation.

The 10-3/4" liner is a combination of black steel (P110) and chromium steel (L80Cr13) joints and tied back to surface. The chrome joints are located at approximately 1800 – 2100 mMD in the build section from 60 to 90 degrees. Occasionally there are two to three steel joints within the chrome section for packer setting area.

The 8-1/2" branches are drilled out of the 10-3/4" liner and reach TD at between 4000-7000 mMD. The branches are drilled with 5" drill pipe and occasionally 5" drill pipe below 5-1/2" drill pipe, where the 5-1/2" drill pipe usually not intersects with the 10-3/4" chrome section.

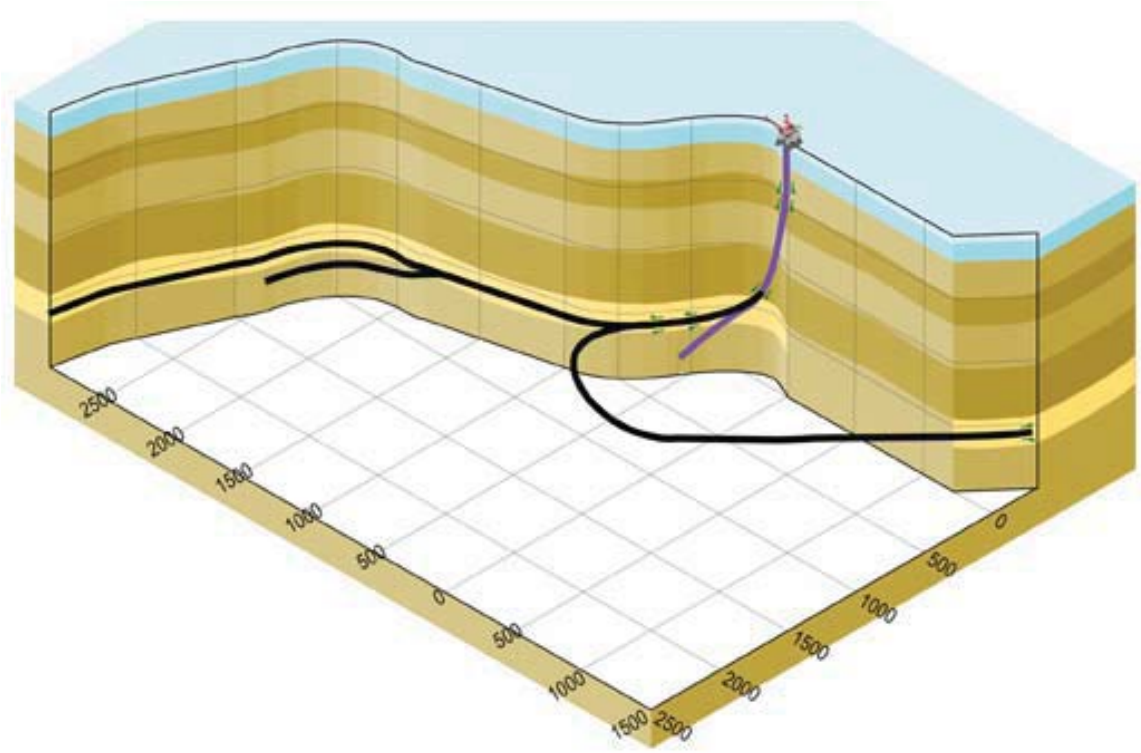

Fig. 72 The typical Troll well design[1]

9.3 Observed wear groove in Troll

The 10-3/4" liner is logged with an ultrasonic imager tool by Schlumberger.

The USIT reports only state the maximum amount of wear. After a short in-house USIT logging course, the logs were analysed by the author and with help of Statoil logging experts to estimate an average value.

Definition of average wear: Average of maximum wall thickness loss around the circumference of casing in all sampling points.

$$\text{Average wear} = \frac{1}{n}\sum_{i=1}^{n} \text{maximum wear around circumference of casing in sampling point}_i$$

n…number of total sampling points [Eq.40]

A correct average wear could be obtained for wells where the logs where available in a specific file output format (.dlis). For all other wells the USIT logs where studied and an average amount estimated by manually reading out the minimum remaining wall thickness values.

The average amount of wear can be used to study general wear trends. For detailed analysis the wear profile along the liner is more useful.

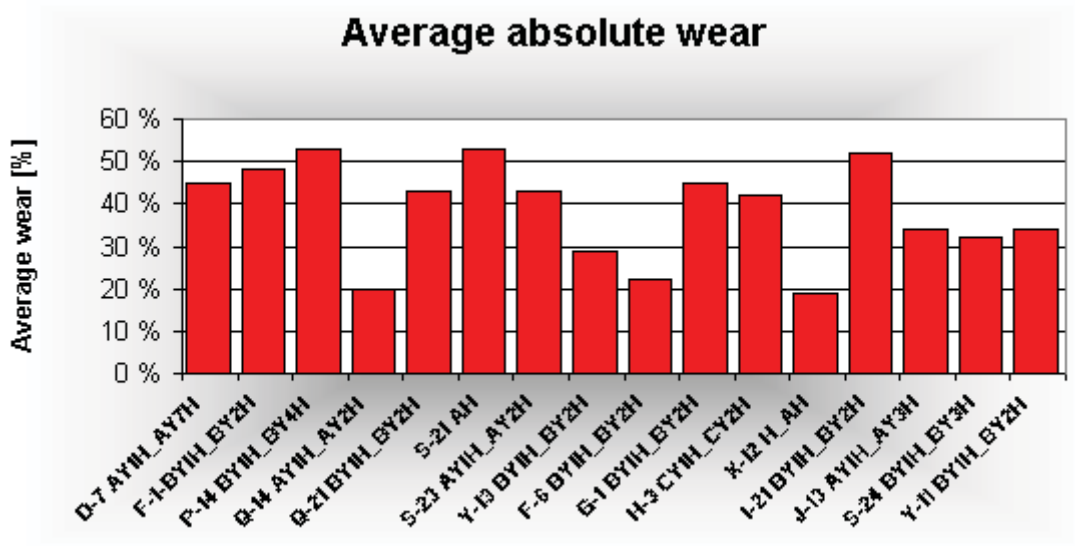

Fig. 73 USIT logging results for the analysed wells; USIT resolution ends at app. 54 % wear.

The USIT logs show the same wear pattern for all wells: a continuous wear groove on the low side of the well sometimes shifted a bit to the left or right side depending on the change in azimuth in the section.

Casing wear never appeared in the black steel casing[vii]: no matter whether only 20 % wear or up to 53 % wall thickness loss occurred on the chrome joints (Fig. 74).

[vii] No wear: percentage of wall thickness loss is smaller than 12.5%, which derives from the API min. wall thickness of 87.5% nominal thickness

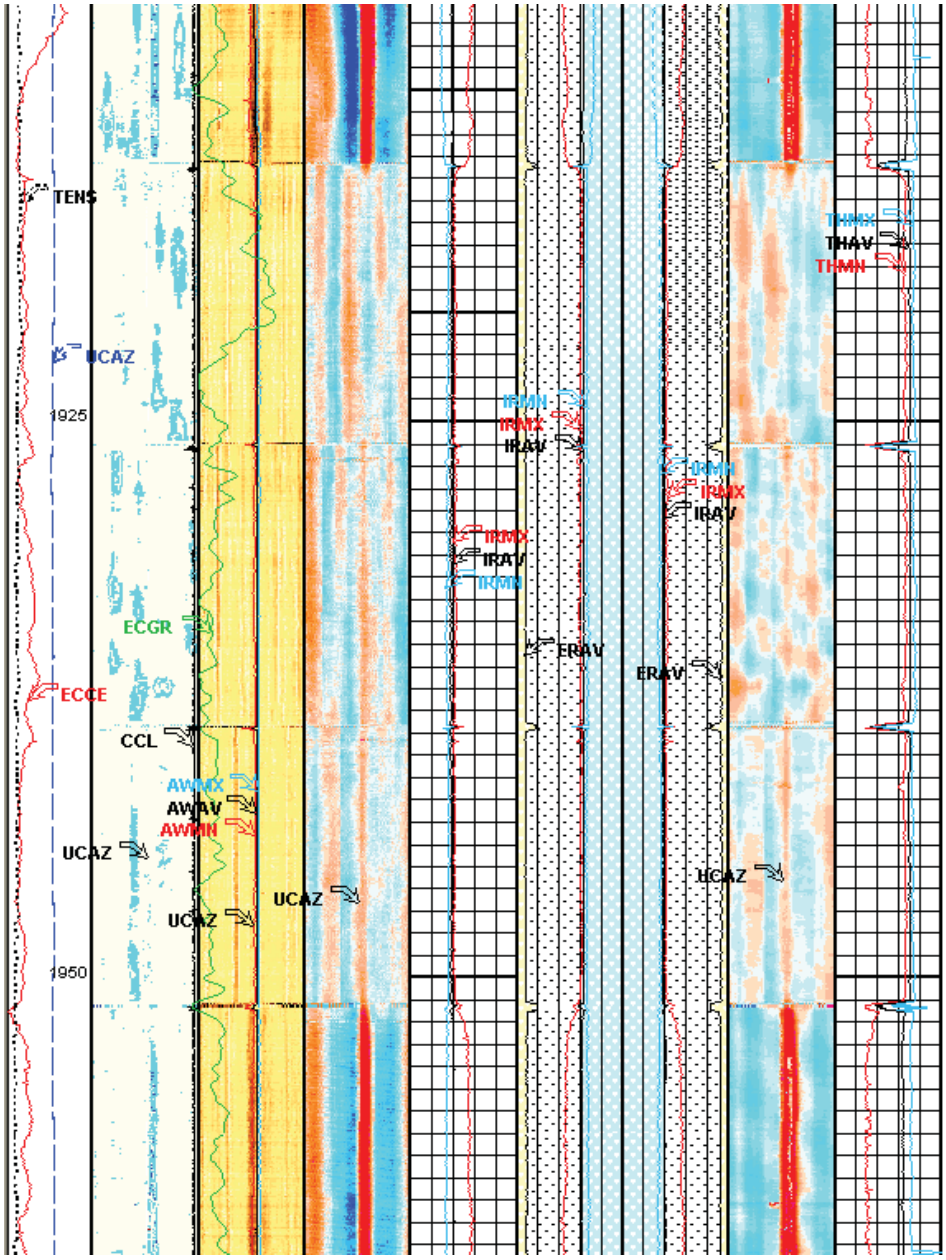

Fig. 74 USIT log Q-21 BY3H: Three joints of P110 between L80Cr13 joints

This observation is of vital importance, as it could mean that parameters causing casing wear may ultimately not be as severe as they seem to be.

9.4 Analysis approach and assumptions

The analysis approach is not an easy task as up to date no "valid" casing wear model exists for Troll and in general.

Literature states that casing wear is primarily caused by the rotation of the tool joint in the casing and tripping wear is negligible. The formula behind this idea has been presented earlier in part I and can be simplified to:

$$\%wear = C \cdot WF \cdot Side\ \ force \cdot total\ \ drill\ \ string\ \ revolutions$$

C …geometry constant for the drill pipe and hardbanding

The geometry of the drill pipe and hardbanding is the same in all wells.

9.4.1 Basic assumptions

"There is no reason to assume that the proportions of mechanical energy converted to heat, particle deformation, casing wear and tool-joint wear will remain constant throughout the wear process."[29]

This means that the casing wear rate for each well will change during drilling. From experimental testing the typical wear rate behaviour can be described as follows: A high *initial wear rate* is followed by a less steep more or less *constant wear rate* for a given side force (Fig. 75).

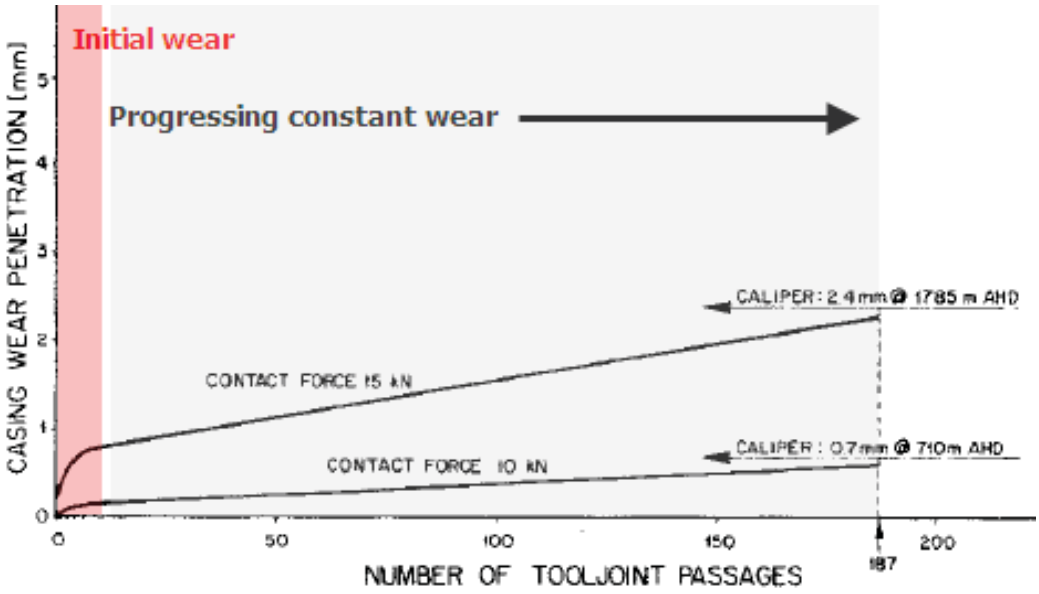

Fig. 75 Experimental casing wear behaviour: The slope of the curve defines the wear rate[45]

The initial wear rate can be determined in laboratory testing only. It is assumed to be the same in all wells.

The constant wear rate is constant only for a constant side force (and other parameters). The side force will change in the field:

- Parameters influencing the side force: real dogleg severity, weight on bit, bottom hole assembly, geometry of hardbanding, section length

It is assumed that the constant wear rate can be represented by a single side force value that has to be calculated individually for each well.

As the Troll wells are very similar in regards to casing design, mud composition and drilling strategy, one should expect to find a casing wear trend for all wells. The wells should follow

this trend if all other influencing parameters are constant. Minor or major deviation from the trend will be caused by other influencing parameters, such as:

- Drilling fluid parameters: concentration of lubricator, weighting additives, …
- Operational parameters: weight on bit, amount of reaming and backreaming, number of trips, …
- Other parameters: type of hardbanding, casing material, amount of calcite, …

9.4.2 Relative wear rate

To "measure" the deviation from the trend, a relative wear rate will be introduced. The relative wear rate (RWC) can be defined in various ways, e.g.:

- RWC 1: Relative casing wear percentage per drilling time[viii] or drilled metres
- RWC 2: Relative casing wear percentage per revolution or per revolution and side force
- RWC 3: Relative casing wear percentage per revolution, side force and hardbanding wear factor

By comparing e.g. RWC 2 with RWC 3 for a set of different wells, one should expect less deviation in between the wells for RWC 3. The more influencing factors can be revealed, the less deviation should occur.

Some of those influencing factors are unknown, the influence of others can be tested only in the laboratory.

9.4.3 Approach by a simple example

For better understanding, the analysis approach is illustrated by an example:

Three wells A, B, C in the same field have experienced casing wear. The side force and the number of tool joint passages (or total string revolutions) were calculated. The wear factors of the three different hardbandings are known.

Well	Wear [%]	Side force [kg/m]	Tool joint passages	Hardbanding / casing WF
A	35	39	50	1
B	40	33	80	0.9
C	45	37	60	1.2

Step 1: Plot wear against number of tool joint passages or total drill string revolutions

[viii] Based on this relative wear Statoil currently forecasts casing wear

Plotting the observed wear against number of tool joint passages, shows that Well C had less passages, but more wear. The relative wear rate[ix] is high for Well C and low for Well B. It is difficult to establish a trend for those wells, which means that more factors than just tool joint passages must be considered.

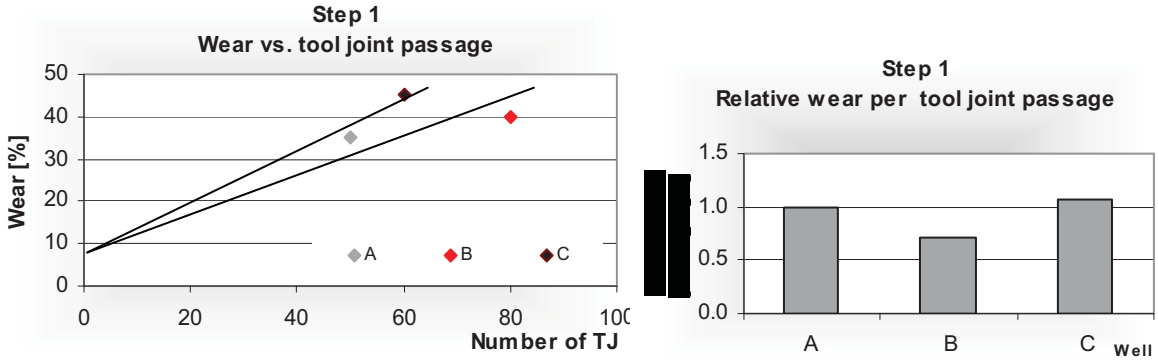

Step 2: Include the side force

An estimate of the average side force present during drilling the horizontal branches will be included in the next step. Including the influence of side force can help in finding a better base trend and relative wear rates also show less variance.

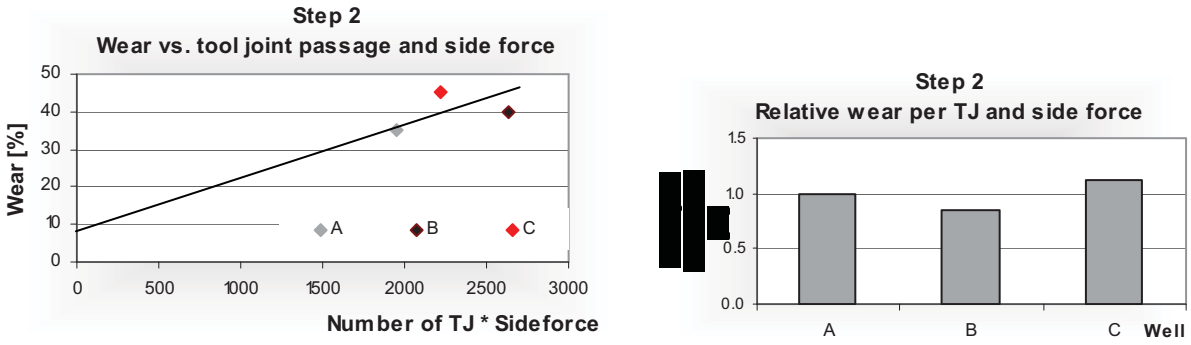

Still some deviation in the wear rates can be observed. Those are caused by all other parameters that have not been considerer so far.

Step 3: Include other known parameters that may have caused wear

If the main reason for different wear is the hardbanding wear factor, which is often true in practice, then again less variance should be observed.

[ix] Wear rate is normalized to well A to compare the calculated wear rate for the individual steps

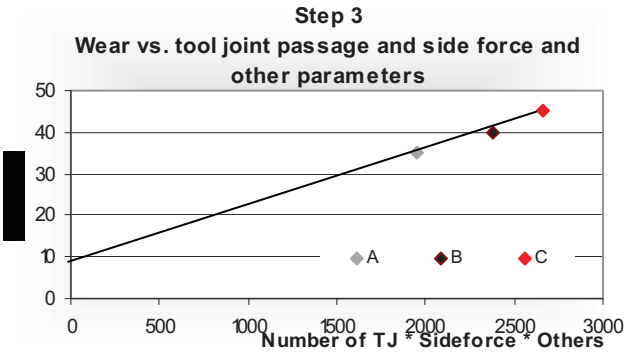

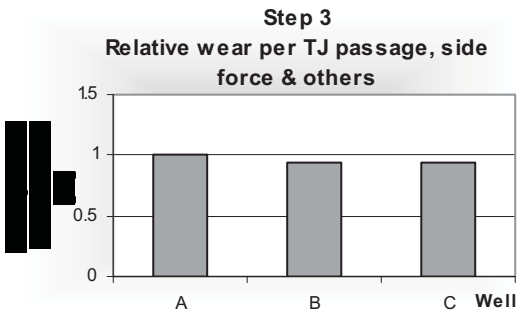

Finally a very good fit could be obtained indicating that the different hardbanding wear factors had a big influence in those three wells. The critical influence of hardbanding is often observed in "real" wells.

9.4.4 Further assumptions

As mentioned Troll wells are very similar and one should expect that they have many parameters in common. Thus a base trend can be established.

The composition of "Troll low solids KCl/$CaCO_3$/polymer mud" is more or less the same in all wells. Studies presented earlier show that weighting additives and lubricator concentration have a strong influence on casing wear beneath the mud properties. The mud specific gravity was the same in all wells drilled (SG 1.12), thus the influence of weighting additives will be more or less the same in all wells. Lubricator content in the branches was different and shall be studied.

Another factor that is assumed to be the same for all wells is the drill pipe and hardbanding geometry constant C. The hardbanding is generally applied in a 3/32" raised application over the tool joints with similar geometry.

The casing wear equation used in the model then simplifies to:

$$\%wear = WF \cdot Side\ \ force \cdot total\ \ drill\ \ string\ \ revolutions \qquad \text{[Eq.41]}$$

Considering the amount of involved (to a large extent unknown) parameters, it becomes obvious that three wells are not sufficient to detect any trend and more wells have to be taken into the analysis. Moreover it should be studied whether the three wells F-1, H-3 and I-21 significantly deviated from an already established trend (relative wear in terms of drilling hours). The number of wells is limited to those where a USIT log in the 10-3/4" liner was run and where reasonably good data is available.

As it is the primary aim of this field study to identify the reasons for excessive casing wear and explain deviations in wear, it will be more of a qualitative than quantitative study as the unknown parameters cannot be included.

9.5 Data base and general information on Troll wells

In order to do a comparative study a lot of data has to be collected.

A well database has been set up in order to facilitate the analysis.

9.5.1 General information

- Well name[x], rig name, drilling date from well reports
- Information on hardbanding on 5 inch and 5 ½ inch drill pipe from Statoil engineers
- BHA from Baker end of well reports

Rig	Well	Drilling date	Hardbanding on 5 in DP	Hardbanding on 5 ½ DP
Songa Trym	**D-7** AY1H / AH2H / AY3H / AY4H / AY5H / AY6H / AY7H	Mar, 2007	Arnco 300XT	Arnco 300XT
	F-1 BY1H / BY2H	Sep, 2009	OTW 12	OTW 12
	P-14 BY1H / BY2H / BY3H / BY4H	Nov, 2007	Arnco 300XT	Arnco 300XT
	Q-14 AY1H / AY2H	Mar, 2008	Arnco 300XT	Arnco 300XT
	Q-21 BY1H / BY1H T2 / BY1H T3 / BY1H T4 / BY1H T5 / BY2H / BY2H T2 / BY3H	Sep, 2007	Arnco 300XT	Arnco 300XT
	S-21 AH / AH T2 / AH T3 / BY1H / BY2H / BY2H T2 / BY3H / BY3H T2	Aug, 2005	Arnco 300XT	Arnco 300XT
	S-23 AY1H / AY2H	Nov, 2008	OTW 12, Arnco 300XT	OTW 12, Arnco 300XT
	Y-13 BY1H / BY2H	Feb, 2009	OTW 12, Arnco 300 XT	OTW 12, Arnco 300 XT
West Venture	**F-6** BY1H / BY2H	Aug, 2008	Arnco 200XT	TCS Titanum
	G-1 BY1H / BY2H	Feb, 2007	Arnco 200XT	TCS Titanum
	H-3 CY1H / CY2H	Nov, 2009	Arnco 200XT	TCS Titanum
	X-12 H / AH (X-12 drilled in 2002)	Aug, 2002 / Aug, 2007	Arnco 200XT For 2002: unknown	TCS Titanum For 2002: unknown
Polar Pioneer	**I-21** BY1H / BY2H	Oct, 2009	Arnco 300XT	ArmacorM
Songa Dee	**J-13** AY1H / AY2H / AY3H	Jan, 2009	Arnco 300XT	Arnco 300XT
	S-24 Y1H / Y1H T2 / Y2H / Y3H	Oct, 2006	Arnco 300XT	Arnco 300XT
	Y-11 BY1H / BY2H	Sep, 2008	Arnco 300XT	Arnco 300XT

Tab. 3 List of wells in the analysis

9.5.1.1 Hardbanding selection

A short description of the current hardbanding in use on the rigs is given below.

Arnco 300XT

- Ferrous-based alloy containing Nickel, Boron and Niobium

[x] E.g. I-21 BY1H/BY2H: First letter and number address the well, followed by branch name; T stands for technical sidetrack

- Additional alloy elements are used to control the mode of solidification to generate a fine-grained microstructure.
- Minimum 60+ HRc micro-hardness (61 – 64 HRc)
- Is applied in a raised application with a thickness of 3/32” (2mm)

Arnco 200XT

- Chromium based alloy hardbanding
- Crystalline hardbanding with a consistent through-wall hardness of 54 HRc
- It is applied in a raised application, 3/32" above the tool joint O.D.

Armacor M

- Alloy of iron, chromium and boron; chromium borides give the alloy its wear resistance.
- Hardness in the range 52 to 54 HRC
- ATI claims that during the wear process, Armacor M forms a very thin, very hard amorphous (metallic glass) layer on the surface, which enhances the wear resistance, reduces the coefficient of friction, and prevents galling
- Only on 5 ½ inch drill pipe

Tuboscope TCS Titanum

- Ultra-hard, titanium carbide microstructure, dispersed through a chrome martensitic alloy matrix
- Hardness of 55-57 HRC for 1 pass, with the hardness value increasing by 1-3 HRC points per additional pass
- Applied in raised application, 3/32" above the tool joint O.D.
- Only on 5 ½ inch drill pipe

9.5.2 Autotrak parameter reports

Autotrak parameter reports for each single branch and necessary sidetrack (after setting 10-3/4” liner) include beneath others the following information:

- Duration and mode: hold, steer, reaming and washing, backreaming, circulate, other
- Surface RPM
- Rate of penetration
- Weight on bit
- On and off bottom torque

- Mud weight: for all wells SG 1.12

An example is listed in the Appendix (16.4).

From the data the following number can be extracted for drilling the 8 ½ inch section in total and for each branch and sidetrack:

- Total number of drill string revolutions including rotating on and off bottom in the 10 ¾ inch liner
- Average weight on bit per branch / sidetrack and average weight on bit for the 8 ½ inch section
- Distribution of WOB
- Average RPM and distribution of RPM
- Average torque on bottom and off bottom
- Revolutions required to drill one meter
- Percentage of drilling, reaming, washing and backreaming and others

9.5.3 DBR well reports

From the Statoil DBR well database the following information can be extracted:

- Summary of operations for each branch / well
- Number of trips
- Casing / liner setting depth
- Location of chrome joints

9.5.4 Formation data

For each 8 ½ inch the following data is provided:

- Percentage of c-sand drilled
- Percentage of m-sand drilled
- Percentage of calcite drilled

From this number the total amount of drilling in c-sand, m-sand and calcite per section can be calculated, e.g.:

$$\%-\text{age calcite} = \frac{\sum_{i=1}^{m} \%-\text{age calcite}_i \cdot \text{branch length}_i}{\sum_{i=1}^{m} \text{branch length}_i}$$

m…denotes the number of branches

[Eq. 42]

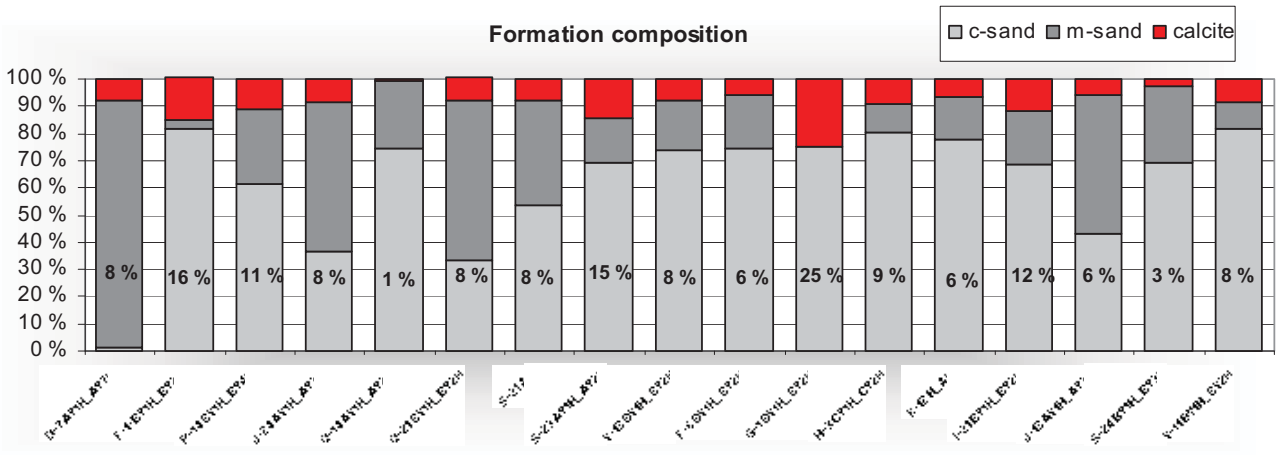

Fig. 76 Distribution of c-sand, m-sand and calcite

9.5.5 Information on lubricator

Baker drilling fluids provided information on the concentration of lubricator in the mud:

- Lubricator concentration: start of branch drilling
- Lubricator concentration: end of branch drilling

An average lube concentration based on the surface drill string revolutions per well was calculated. The results are listed in the appendix (16.5).

9.5.6 EDM Landmark compass

EDM Landmark compass was used to import the survey data for each branch into the database.

- MD, TVD
- Inclination, azimuth, dogleg severity, tortuosity

9.5.7 Percentage of drilling, reaming and others

- Drilling contains drilling in steering and hold mode as well as drilling cement
- Reaming includes reaming, washing and backreaming

- Others include circulating, downlink off bottom and ribs open

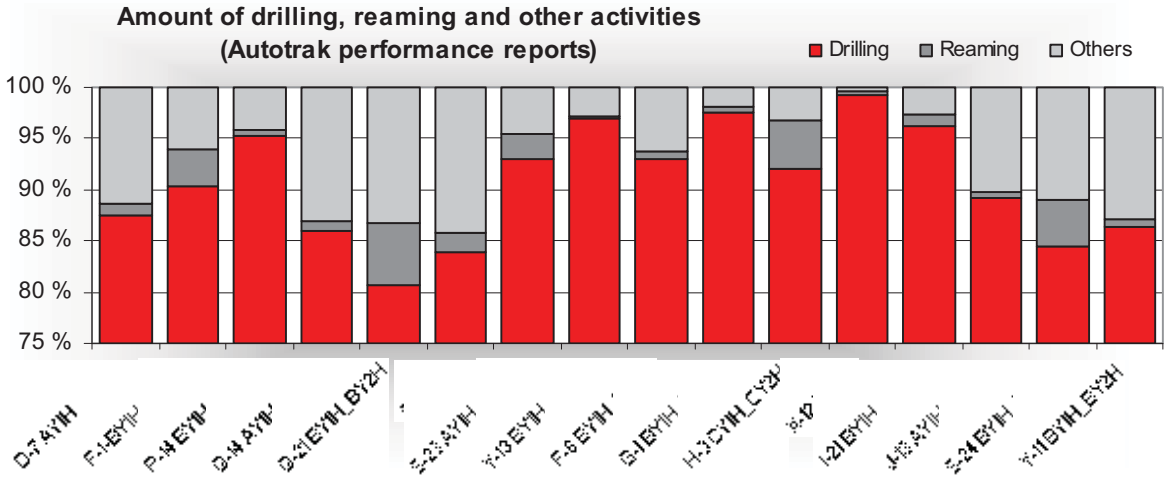

Fig. 77 Amount of drilling, reaming and other activities

9.6 Average RPM and total number of drill string revolutions

The surface speed of rotation will change throughout the drilling process and only a time averaged value can yield "correct" results. The time averaged value multiplied with the drilling time gives the total number of drill string revolutions. The time averaged rotational speed as well as the distribution of RPM for the wells can be taken from Fig. 78. To get the number the Baker Autotrak data for surface RPM and drilling time / mode is used.

$$Average\ section\ RPM = \frac{\sum_{i=1}^{m} RPM_i \cdot duration_i}{\sum_{i=1}^{m} duration_i}$$

m...number of time intervals [Eq. 42]

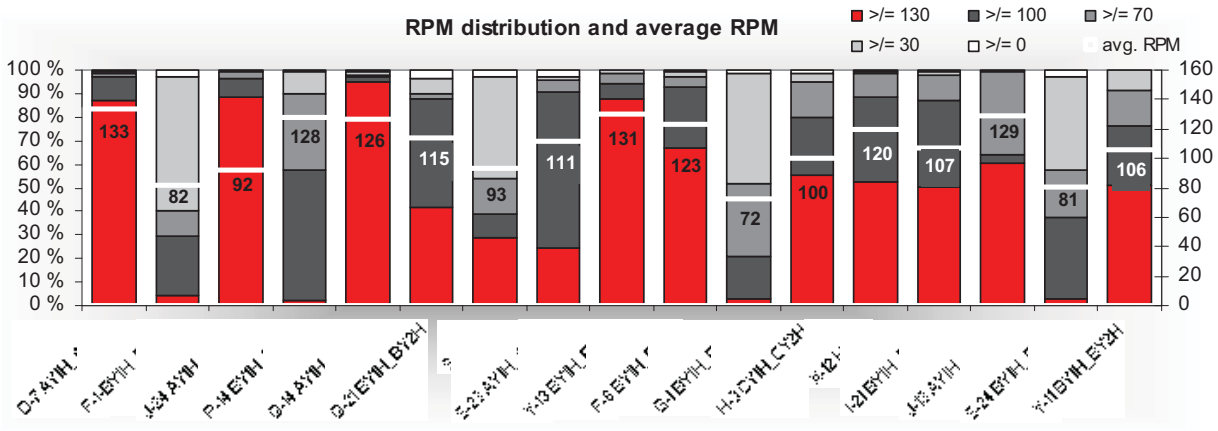

Fig. 78 Time weighted averages for RPM and distribution of RPM

9.7 Side force in the well

The side force of the drill string on the casing is a critical factor in the presented casing wear equation and a function of quite a few parameters:

- WOB
- Weight / type of the BHA
- Weight of the drill string: drill pipe grade
- Contact area between casing and drill string, which is changing over time
- Trajectory parameters of 13 ½ inch and 8 ½ inch hole section:
    - position/depth of the chrome casing joints
    - dogleg severity - especially in the chrome section

9.7.1 Choice of software

To get an approximate value for the side force two different software, EDM Wellplan from Halliburton and CWEAR from Petris, are available.

CWEAR is a powerful tool to forecast casing wear and provides a large list of different wear factors based on the largest casing wear data base available. Loading in the survey data from the drilled well allows better correlation of casing wear factor with actually observed wear. Statoil experience with CWEAR is that it cannot forecast wear on Troll wells, as only few wear factors for chromium steel casings are included. No experimental results for the combination with the hardbandings and drilling mud, Statoil currently uses, are available.

Originally EDM WellPlan is not built for casing wear analysis and cannot predict casing wear. However, it is a more suitable software to analyse the side force due to higher flexibility in stress and load analysis.

After doing some simulations with both softwares, the choice was made for WellPlan.

The first step in side force analysis included sensitivity analysis with WellPlan on parameters affecting side force and casing wear. The results of the sensitivity analysis justify the approach to replace the BHA by a short drill string section with larger outer diameter and higher unit weight and do all calculations in a separate database. The calculation procedure will be described before the results of the sensitivity analysis are presented.

9.7.1.1 Calculation procedure

All branch survey data for 56 branches were loaded in spreadsheets and calculations done with the formula for soft string model by Johancsik (16.6). The advantage of this approach was that different side force scenarios could be studied quicker.

The BHA is replaced by a section of pipe which is as long as an average Autotrak G3 rotary BHA (123m). A corresponding unit weight is chosen as well.

Troll low solids/KCl/Polymer mud with a specific gravity of 1.12 is used for all wells drilled. Thus the buoyancy factor is the same for all wells.

To check the validity of this approach a comparison of calculated and simulated (WellPlan) side force is plotted in Fig. 80.

In order to include the side force in the analysis a single representative value for each well has to be extracted out of the data. The difficulty in getting this value arises not only from a changing lateral load with drilling depth, but also from the fact that the side force was different in each branch and so was the average WOB. This "problem" is approached by calculating the average revolution weighted WOB for each branch and then calculating the corresponding branch side force. Then an average side force over the chrome section is calculated. The contribution of each branch to total wear is based on percentage of branch revolutions to total well revolutions. From this the final well side force can be calculated.

The procedure to get an average well side force value is illustrated graphically in Fig. 79.

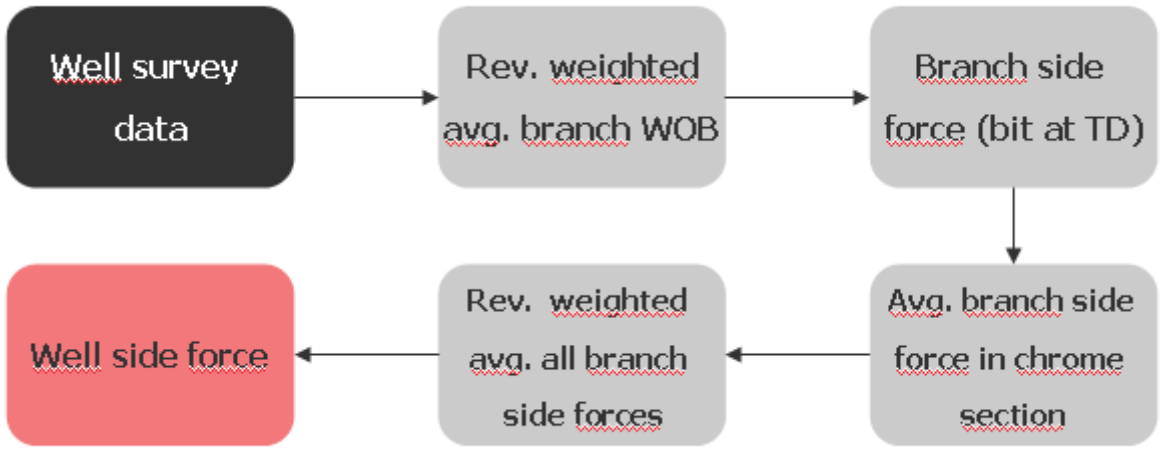

Fig. 79 Calculation steps to estimate side force

Calculated side force profile nearly perfectly overlaps with side force profile in WellPlan (Fig. 80).

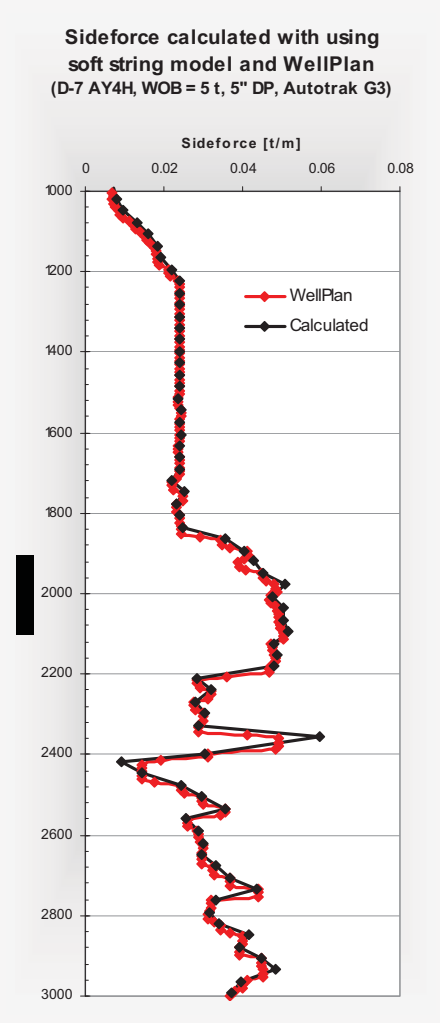

Fig. 80 Side force profile comparison: Calculated (black) and simulated in WellPlan (red)

9.7.2 Sensitivity analysis on WOB

The higher the WOB the higher the compressional force on the lower part of the string will be. To account for this the revolution weighted average WOB for each branch was calculated and used in the simulation.

Fig. 81 shows that side force will increase almost linearly with increasing WOB. From this one could conclude that also wear rate will increase linearly, but casing wear tests show different results. The proportionality between an incremental increase in side force and the resulting change in wear rate will not be constant. Thus it is equally important to pay attention to the WOB distribution (Fig. 82), as for the same calculated average WOB the wear volume will be different depending on whether the WOB was more or less constant or the average derived out of a combination of sometimes high and sometimes low WOBs.

Different WOB during drilling the wide horizontal branches has an influence on side force and therefore affects casing wear. It is therefore not accurate enough to use the same WOB for all branches in side force calculation.

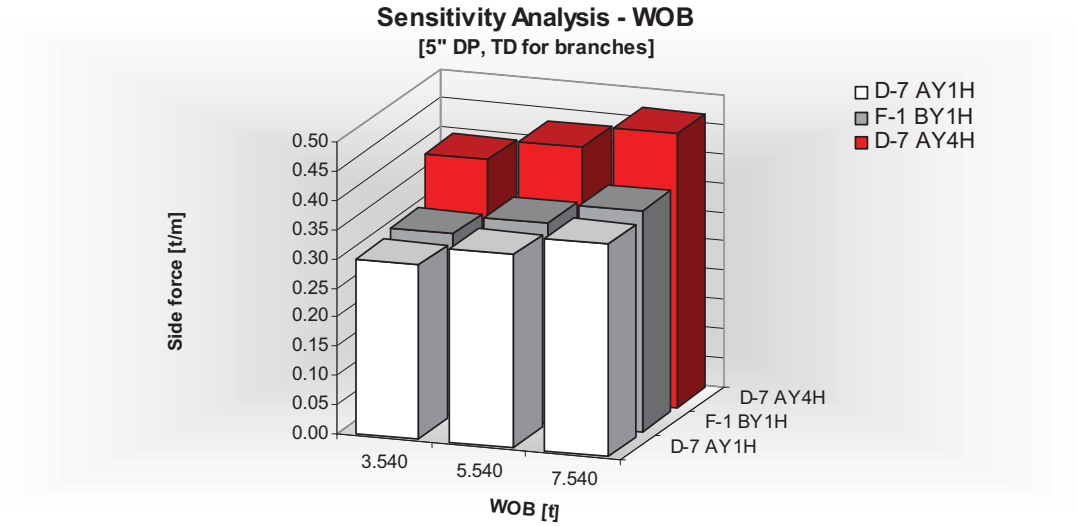

Fig. 81 Sensitivity analysis of the effect of different WOB in different wells

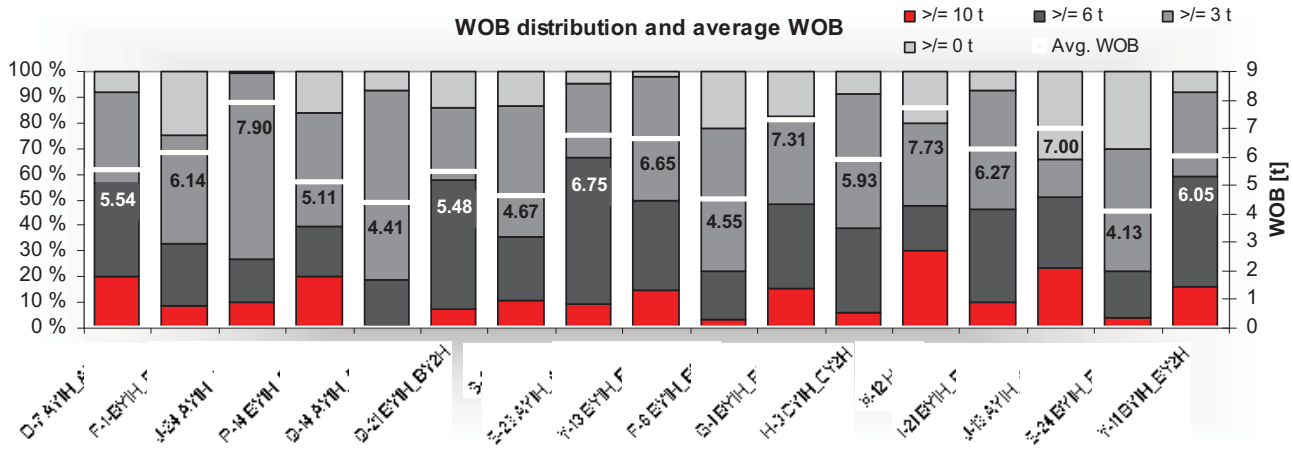

Fig. 82 Distribution of different weights on bit

9.7.3 Sensitivity analysis of BHA selection, drill pipe outer diameter and drilling depth

9.7.3.1 Different BHA

The set up of a typical Baker Autotrak and XTreme BHA used in Troll can be found in the appendix (16.7).

Particularly during tripping, when the BHA is pulled through the chrome section the side force on the casing will be very high, due to the high unit weight of the BHA. However, this will only be for a very short amount of time and tripping wear is not the primary source of wear. Additionally, the USIT logs show drill pipe induced wear and not BHA induced wear.

The influence of different BHA during rotating on bottom was studied with WellPlan. The results show that for a given drilling depth it has more or less no influence on side force and

therefore also not on casing wear (Fig. 83). It is therefore justified to replace the BHA by a drill string section with larger OD and higher nominal weight.

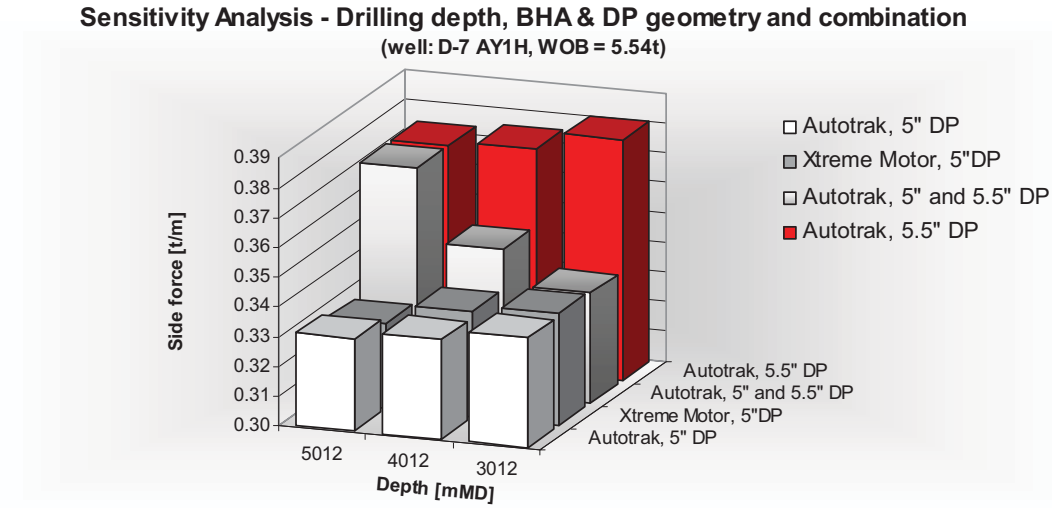

Fig. 83 Sensitivity analysis for drill pipe outer diameter, drilling depth and motor type[xi]

Statoil drilling engineers pointed out that a motor downhole could possibly reduce casing wear. Due to the additional power at the bit, less total drill string revolutions are required to drill with the same ROP. Additionally, engineers assume that during drilling with a motor the drill string will travel a bit more to the left and right side as it rotates. The wear volume perhaps is distributed more evenly over a larger area. This theory cannot be supported by any studies and also not by USIT logging results. The wear groove has the same geometry as in wells drilled without a motor.

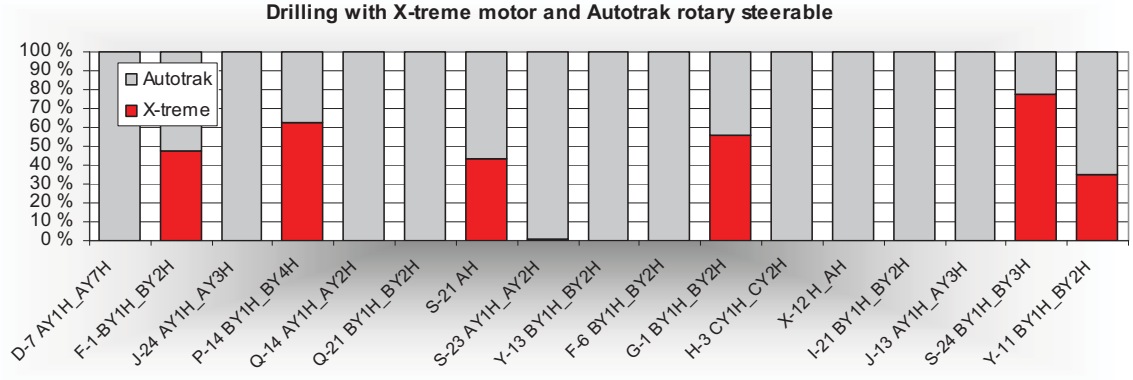

Fig. 84 Drilling with motor versus drilling with rotary steerable assembly

9.7.3.2 Different drill pipe OD

Also the weight / OD of the drill pipe will influence the lateral load on the casing. A comparison is shown in Fig. 83.

[xi] Note: Side force is in tons per 9.45m.

The red series shows the effect of drilling with 5-1/2" drill string. The side force is considerably higher than for drilling with a 5" drill string.

The light grey series shows the effect of drilling with combined string where at 3012 m only 5 " drill pipe is rotating in the chrome section, at 4012 m both 5" and 5-1/2" and at 5012 m only 5-1/2" drill pipe.

Different drill string design severely affects casing wear, but not in all wells and not for a long time 5-1/2" drill pipe were rotating in the chrome section.

To study the extent this phenomenon affected casing wear on Troll the daily drilling reports for the wells I-21– BY1H/BY2H and H-3 CY1H/CY2H were studied to find out when 5-1/2" drill pipe was laying in the logged chrome section. A more correct side force including the effect of 5-1/2" drill pipe was calculated. The result did not vary a lot from the "less accurate" one as 5-1/2" drill pipe did not overlap long enough with the chrome casing (Tab. 4). The influence on casing wear is therefore negligible for wells where 5-1/2" drill pipe was rotating in chrome joints. It is therefore justified to assume that only 5" drill pipe was rotating in chrome.

Well	Branch	branch WOB [t]	Rotation in chrome [drilling metres]	Revolutions		Sideforce [t/m]	
				5 1/2" DP	5" DP	5 1/2" DP	5" DP
H-3	CY1H	5.97	227	107063	1875527	0.0370	0.0353
	CY2H	5.88	0	0	1351635	0.0364	0.0347
I-21	BY1H	7.01	200	162680	1778923	0.0388	0.0371
	BY2H	5.31	0	0	1412713	0.0366	0.0349

Well	Resulting Sideforce [t/m]	
	neglecting 5 1/2" DP	including 5 1/2" DP
H-3	0.0350	**0.0351**
I-21	0.0362	**0.0363**

Tab. 4 Effect of 5 ½ inch drill pipe rotation on side force

9.7.3.3 Different drilling depth

Depending on whether the string is in tension or compression, the lateral load will increase or decrease with increased tension force due to the string below. Different drilling depth thus might influence casing wear.

Given the fact that most of the branches were drilled out horizontally, the tensional force due to the weight of the string below will remain more or less constant (Fig. 83). The marginal increase is caused by slightly different inclination angles and the effect of different drilling depth on side force and casing wear negligible. It is therefore also justified to calculate the side force for all wells at TD.

9.7.4 Sensitivity analysis on trajectory

Sensitivity analysis on the trajectory was done by calculating the soft string side force for a given weight on bit of 5 tons. Using soft string side force to investigate the influence of the trajectory has the advantage that dogleg severity does not influence results a lot. The influence of doglegs will be addressed separately in the discussion of the results.

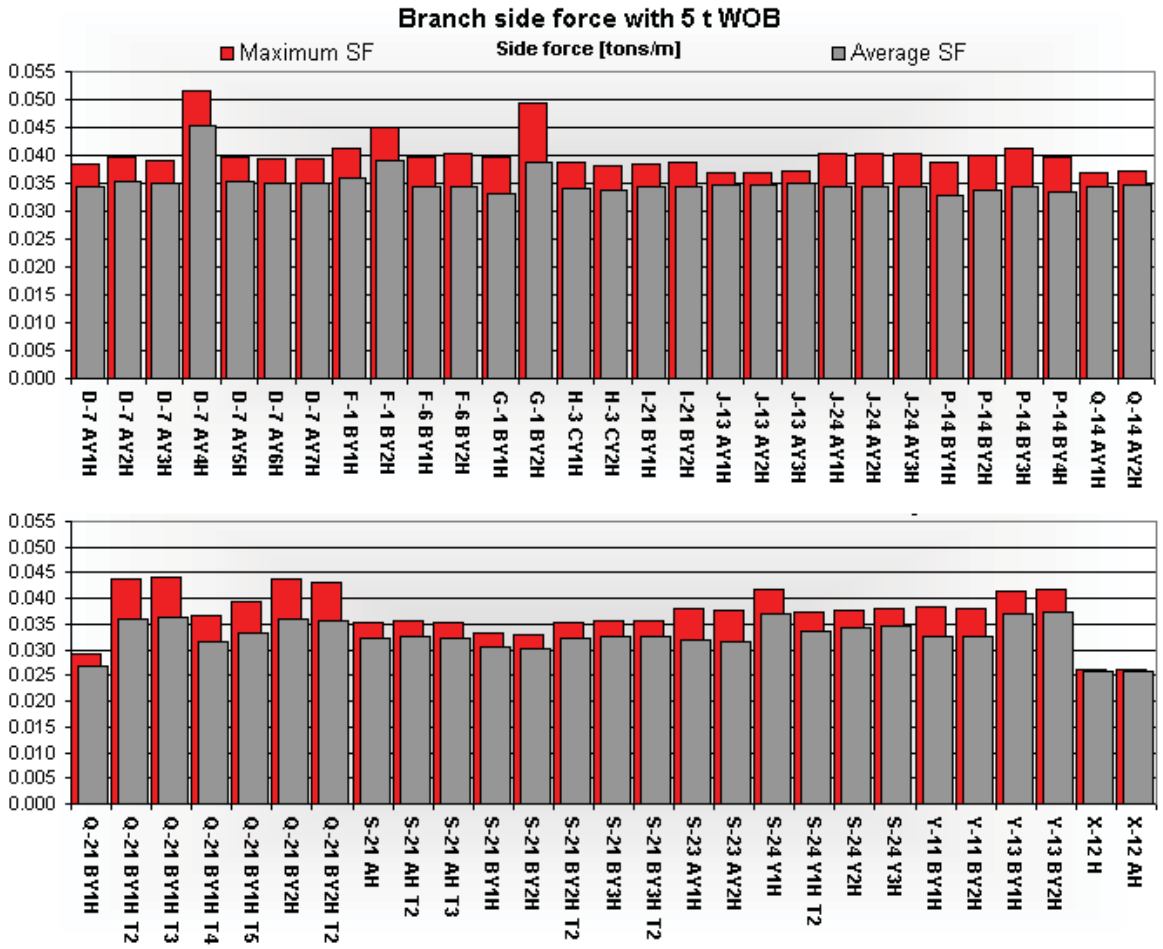

Fig. 85 Branch side forces using actual survey data for a given WOB of five tons

If all wells were drilled with the same weight on bit, the lateral load on the casing would be approximately the same.

However, some branches seem to have a lower, e.g. Q-21 BY1H, or higher side force, e.g. D-7 AY4H. All side forces were calculated assuming bit at TD: some branches had very short build or drop sections close to TD. Considerably higher values are caused by a short built section; lower values caused by a short drop section. This "falsifies" side forces, as those sections are not representative for the overall trajectory, which was in all branches (except X-12) horizontal (+/- 3 degrees).

The length of these build/drop sections was looked up for all branches where this occurred and considered negligible.

The side forces were than recalculated with horizontal landing sections (Fig. 86).

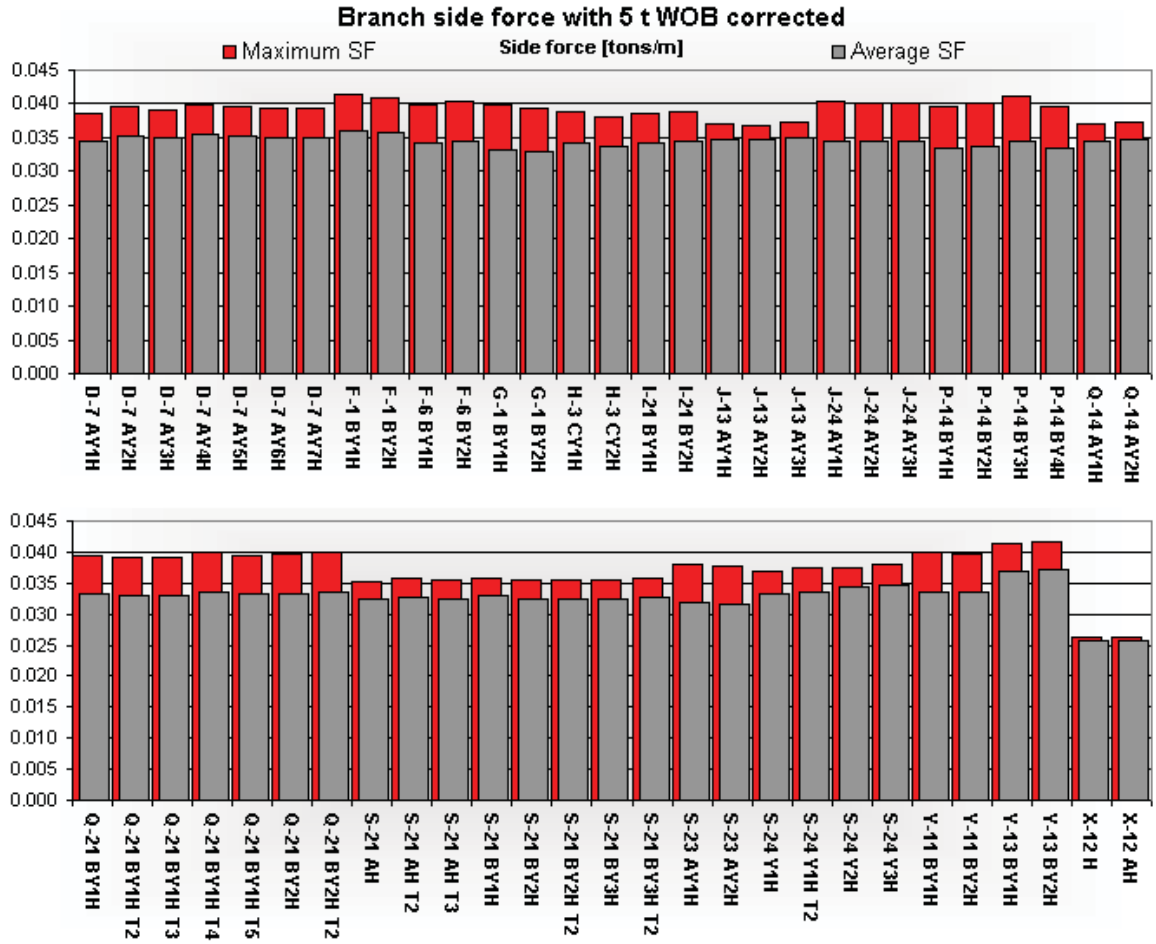

Fig. 86 Side forces with corrected survey data close to TD[xii]

The only well where trajectory caused a significantly different side force is X-12. The low side force is reasoned by the fact that the 8-1/2" was not built up to horizontal. As a result the string was in tension in the chrome section throughout drilling the 8-1/2" section in branch X-12 H, which did not build up to close to horizontal. In X-12 AH which soon builds up to horizontal, the string was in compression.

Apart from X-12 all Troll wells have a similar trajectory design with different 8-1/2" section lengths and slightly different inclination angles at start MD of the chrome section. The 8-1/2" section length and slightly different inclination angle had no big influence on side force and thus not on casing wear.

[xii] All side forces are compressive loads except X-12 H is a tension load

10 Results

10.1 The base trend

As mentioned in the introductory part of the analysis, the parameter which governs the base trend will be the one having the strongest influence on casing wear.

Various attempts to establish a base casing wear trend included investigation of total section length, calcite content, metres drilled through calcite and section drilling time.

The results are plotted below in Fig. 87.

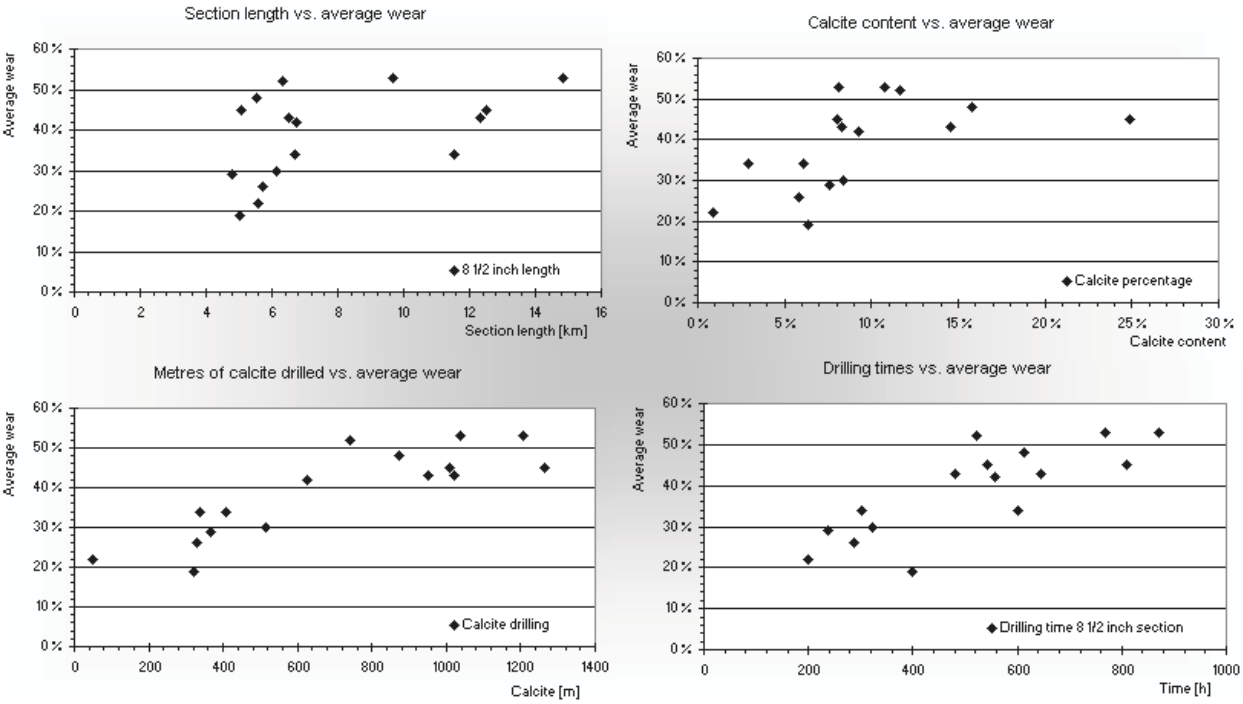

Fig. 87 Parameters studied to establish a base trend

Fig. 87 clearly shows that drilling time and metres of calcite drilled are closely linked to average wear on the chrome casing. This close relationship cannot be seen for the cumulative branch/sidetrack length and calcite content of the wells.

Slow drilling through calcite will certainly be reflected in total drilling time and metres drilled through calcite, whereas it has no influence on section length. From this one can conclude that the drillability of the formation will definitely have an influence on casing wear, especially when it comes to drilling through ultra hard calcite stringers and nodules.

Ultimately casing wear is caused by the number of tool joint passages or total drill string revolutions, which are plotted against average wear in Fig. 88.

Total drill string revolutions include both on bottom and off bottom drill pipe rotation for all branches and side tracks. The number was obtained through the time weighted average RPM.

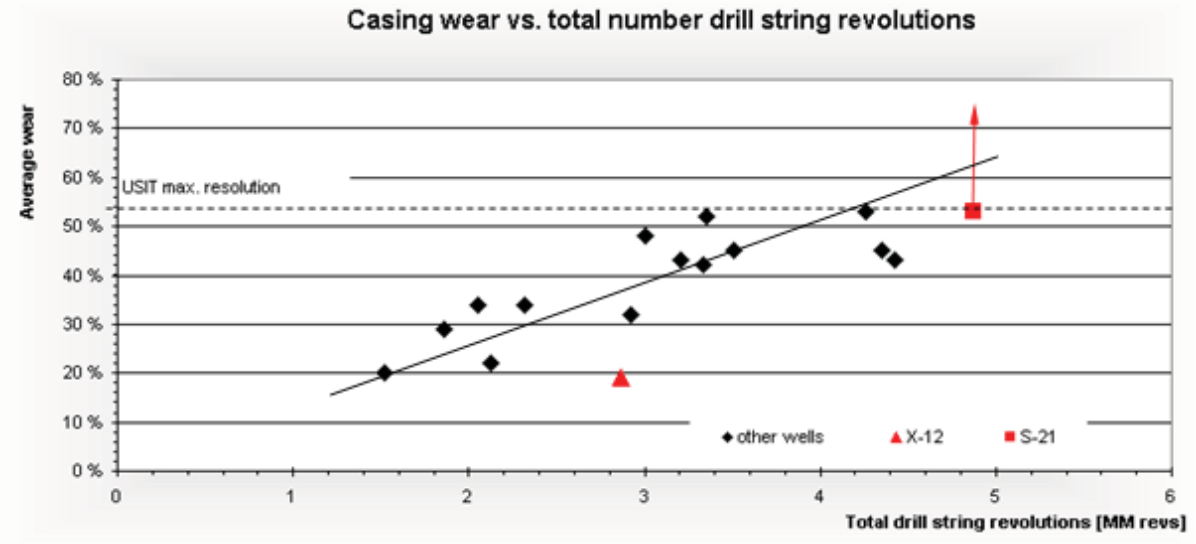

Fig. 88 Best fit with total number of drill string revolutions[xiii]

10.1.1 Main influencing factors governing the base trend

As the number of revolutions incorporates both the parameters section length and drilling of calcite, the direct influence of drillability is no longer visible in Fig. 88.

That a very distinct relationship between calcite content and number of revolutions required to drill the formation exists, can be seen in Fig. 89 and Fig. 90.

[xiii] In the final well report for S-21 the following remark on the USIT logging report is made: "Tried to pressure up to 235 bars, but observed sudden pressure drop when reaching 140 bars. A USIT log was run after the pressure tests. The log showed a worn casing with a groove on the low side. It was estimated that the leakage was due to holes in the 10 ¾ inch L-80, 13% Cr casing." Back-calculation of remaining wall thickness can be found in the appendix 16.8) and gave more than 70% wear.

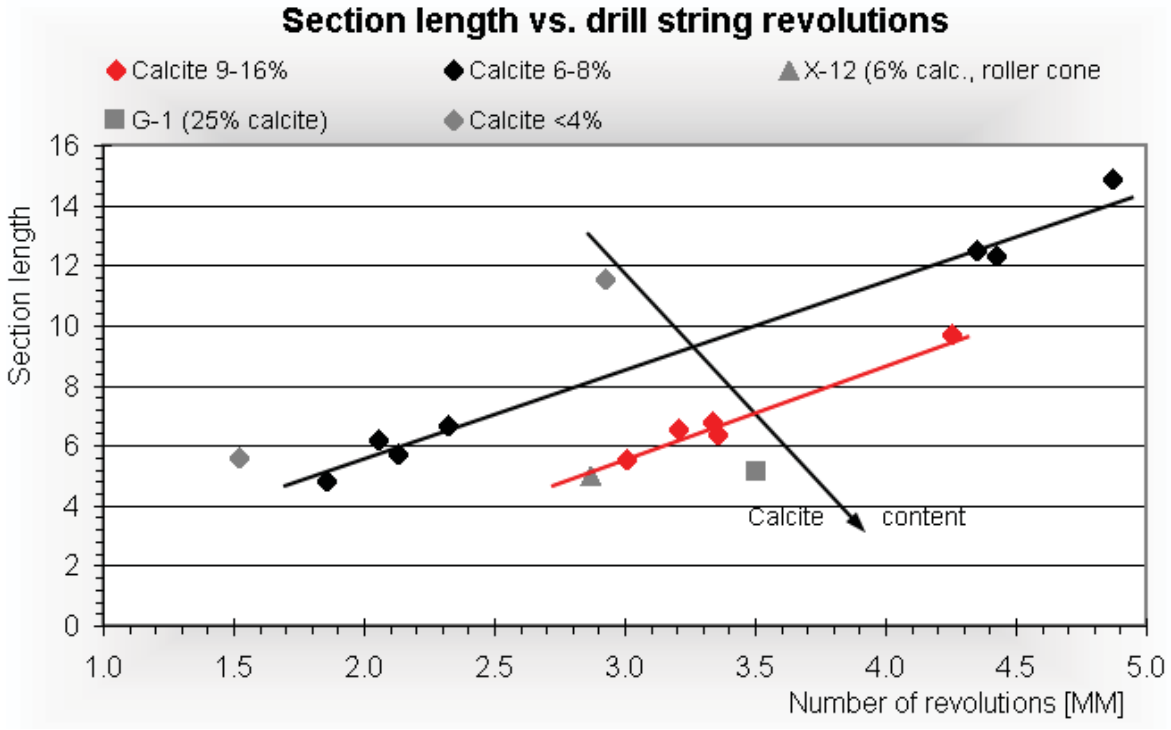

Fig. 89 Section length and calcite content influence on number of revolutions[xiv]

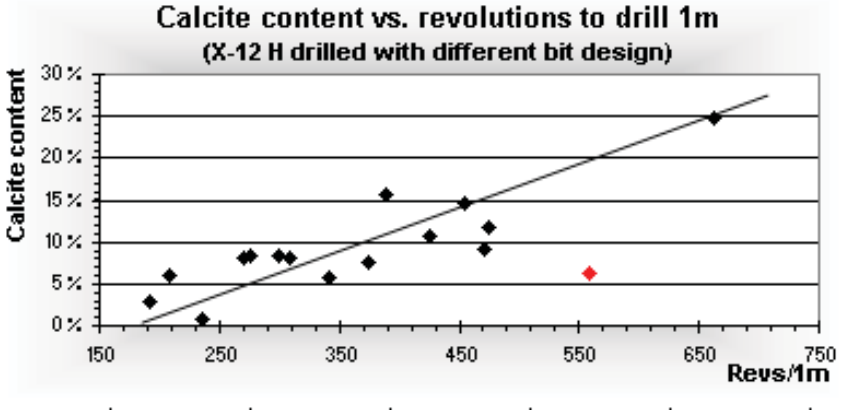

Fig. 90 Drillability of the formation[xiv]

In Fig. 90 the longest well required less drill string revolutions than considerably shorter wells. The longest well only had 1% calcite. Some deviation in this figure occurred due to neglecting the composition of the rest of the formation and the fact that ultra hard stringers (bulk density >2.6 g/cm3) are significantly harder to drill than "normal" stringers (bulk density >2.3 g/cm3). Also bit performance (PDC fixed cutter) contributes to some deviation.

[xiv] Well X-12, where branch X-12 H was drilled in 2002, does not follow the general trend: Unlike all other branches, X-12 H was a 9 ½ inch branch, built up to only 70 degrees and drilled with roller cone bit. Drilling with roller cone bit requires higher RPM and WOB.

Drilling with motor adds additional power to the bit for a given speed of rotation and thus should influence this trend as well (see also: 11.3.5)

Through the link of observed casing wear and number of revolutions and the relationship between number of revolutions, section length and calcite content, it can be concluded: Casing wear on Troll is significantly influenced by calcite content and section length. There is a close proportionality between those two factors and the amount of wear.

10.2 Including the side force in the analysis

The next step was to include the side force in the analysis to find out whether it can explain some trend deviation occurring in Fig. 88 (e.g. for the wells plotting at app. 35% wear and above 40% wear). From the results so far, one should expect that in general the side force shouldn't vary significantly in the wells.

10.2.1 Side force with actual WOB

The main parameter which influences the side force in the investigated wells, is the actual WOB. The actual weight on bit ultimately used was the revolution weighted average branch neglecting the influence of zero WOB revolutions. On one hand, the side forces with zero WOB are very low for all wells (app.16.9) and on the other hand, the neutral point of the drill string is within the chrome section in all wells during drilling with zero WOB. This means that the upper part of the string rotating in the chrome section will be in tension and the lower part in compression.

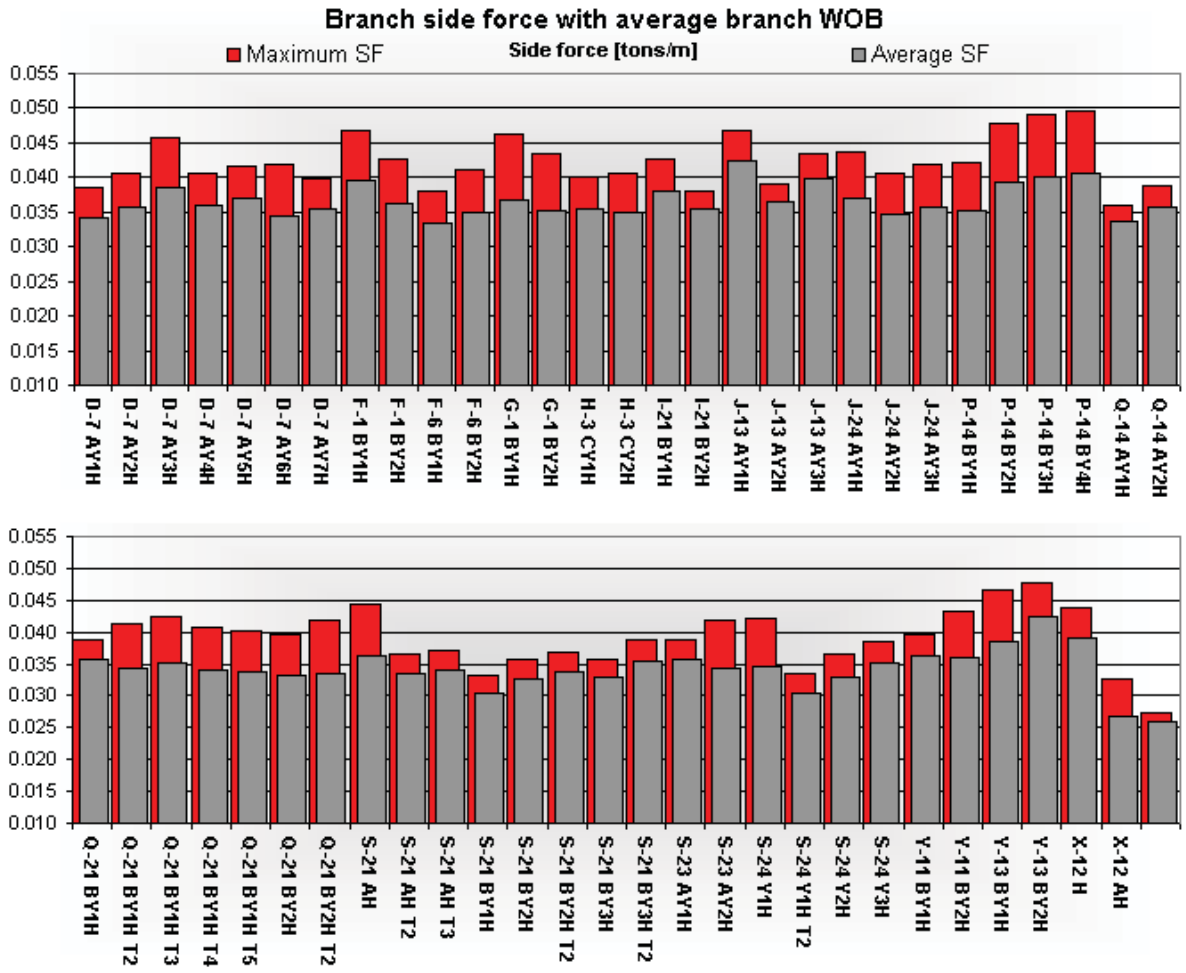

Fig. 91 Average and maximum branch side force accounting for the influence of WOB

As no logs where run after finishing each branch, an average well side force value was calculated based upon branch revolutions.

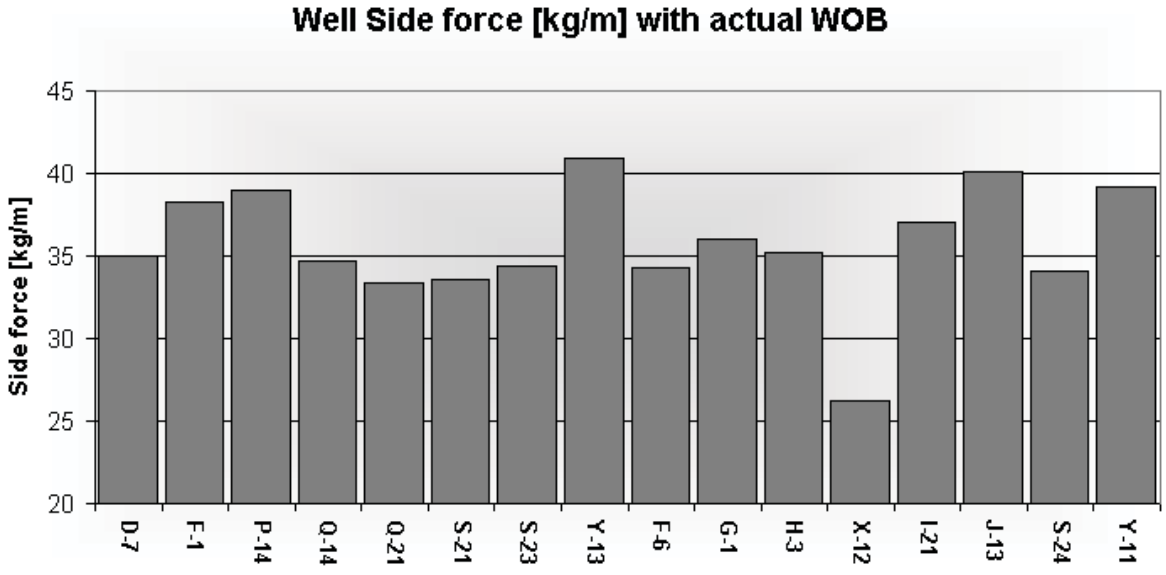

Fig. 92 Average well side force including the influence of WOB

As can be seen in Fig. 92 the well side forces did not vary a lot, which is not surprising as all wells where drilled horizontally.

The highest side forces occurred in the wells Y-13, J-13, P-14 and I-21. The lowest side force occurred in well X-12.

10.2.2 Influence of side force on wear

The average well side forces were than accounted for by multiplying with the total surface drill string revolutions and plotting the results against observed wear.

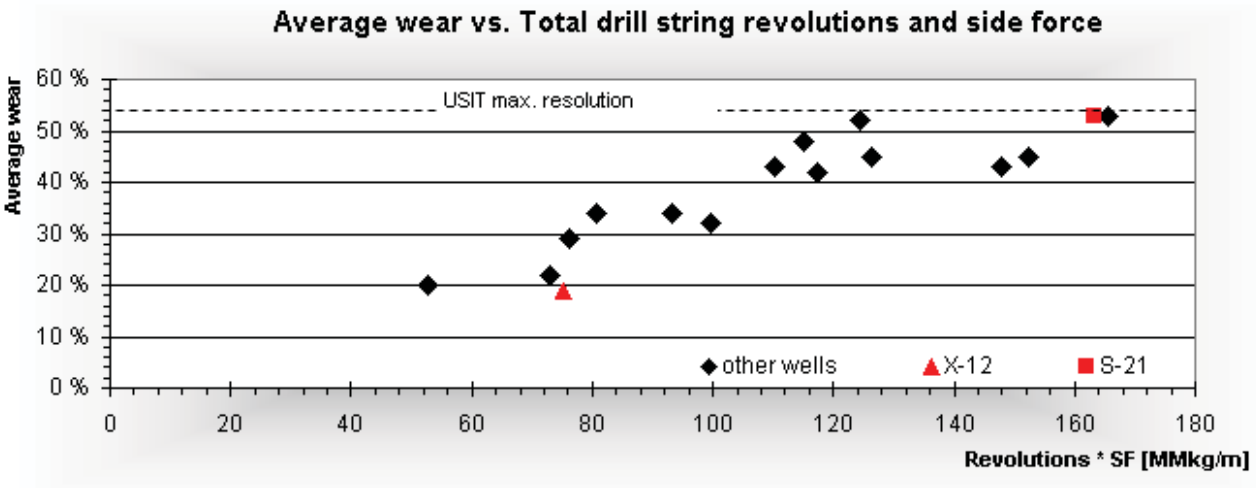

Fig. 93 Average wear vs. total number of drill string revolutions multiplied with well side force

Some additional information:

- S-21 had around 70 % wear
- The 8-1/2" section of branch X-12 H was 70 deg inclined, whereas X-12 AH landed horizontally. During drilling X-12 H the string was in tension all the time and wearing the casing at the high side. Theoretically this should be visible on the USIT log – unfortunately only the USIT logging report was available for this well. The reported wear groove on the low side should be caused by branch X-12 AH only and the number of revolutions should be corrected and decreased by approximately one million necessary to drill branch X-12.

Considering these findings shows that wear plotted against drill string revolutions multiplied with well side force follows a clear trend on Troll.

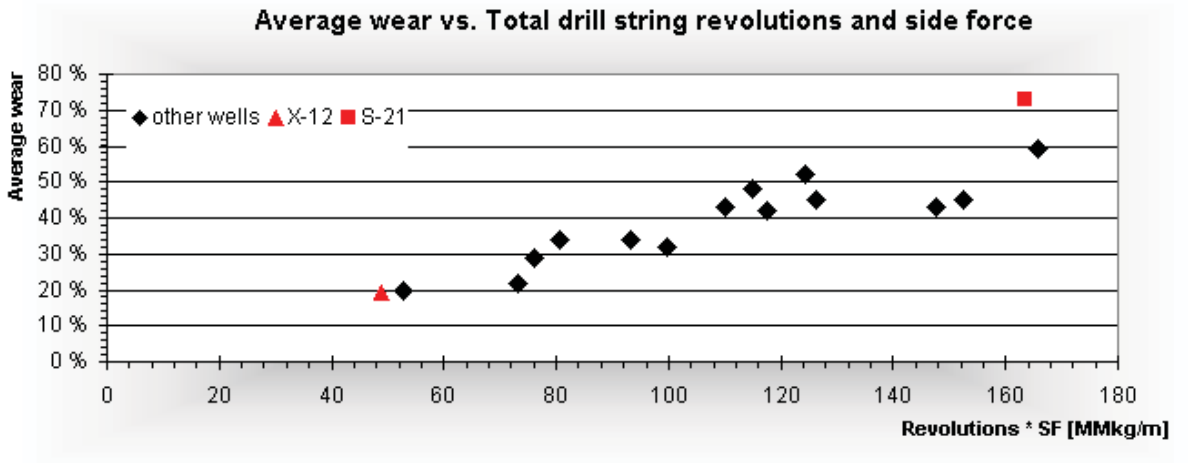

Fig. 94 Average wear vs. total revolutions multiplied with side force

10.3 Relative wear rates and study of other parameters

Having included side force and the total drill string revolutions the remaining deviation in wear rate is caused by all the other parameters influencing casing wear. The most important beneath all those parameters is most likely the hardbanding and shall be investigated after presenting the relative wear rates.

The colour code for different hardbandings:

Arnco XT300
OTW 12
Arnco XT100/XT200

The relative wear rates are normalized to well Q-14 so that comparison between differently defined relative wear rates is possible.

10.3.1 Relative wear rate in terms of drilling time

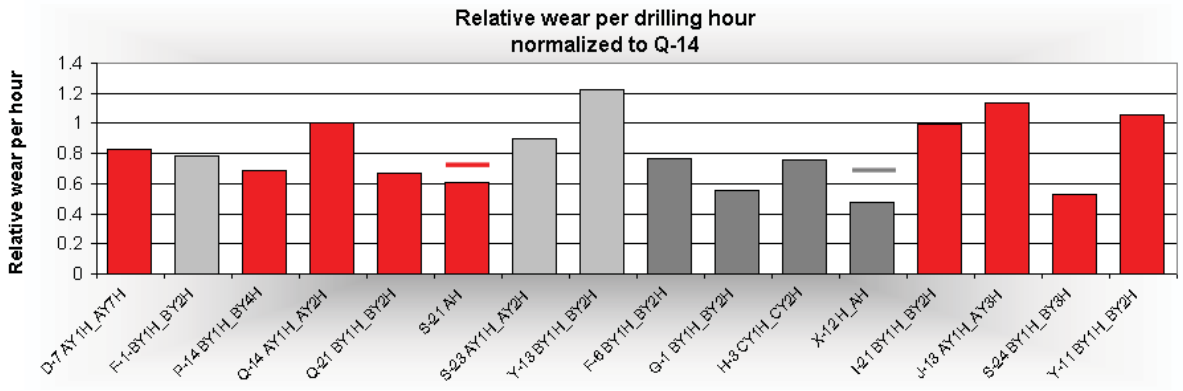

Fig. 95 Relative wear rate in terms of drilling time: For S-21 with 53% and 73% wear and for X-12 with 400 and 250 drilling hours

10.3.2 Relative wear rate in terms of revolutions

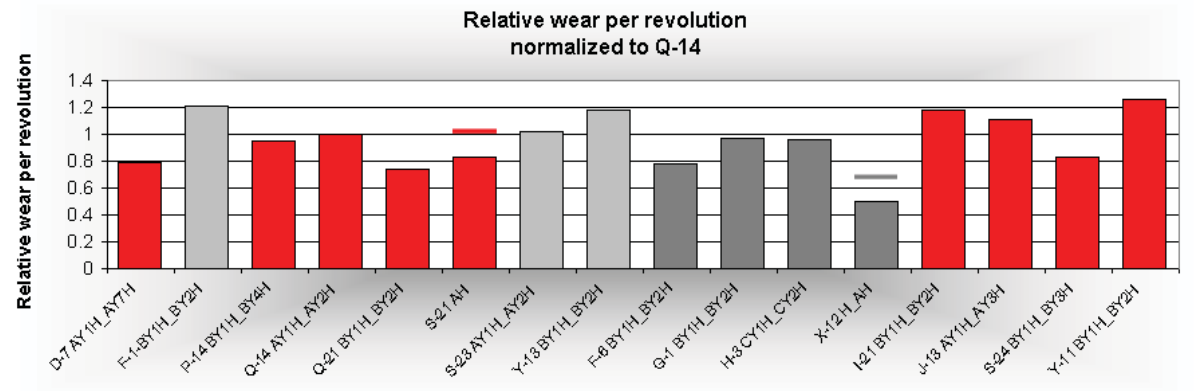

Fig. 96 Relative wear rate in terms of total drill string revolutions: For S-21 with 53% and 73% wear and for X-12 with 2.8 Mio and 1.8 Mio drill string revolutions

10.3.3 Relative wear rate in terms of revolutions and side force

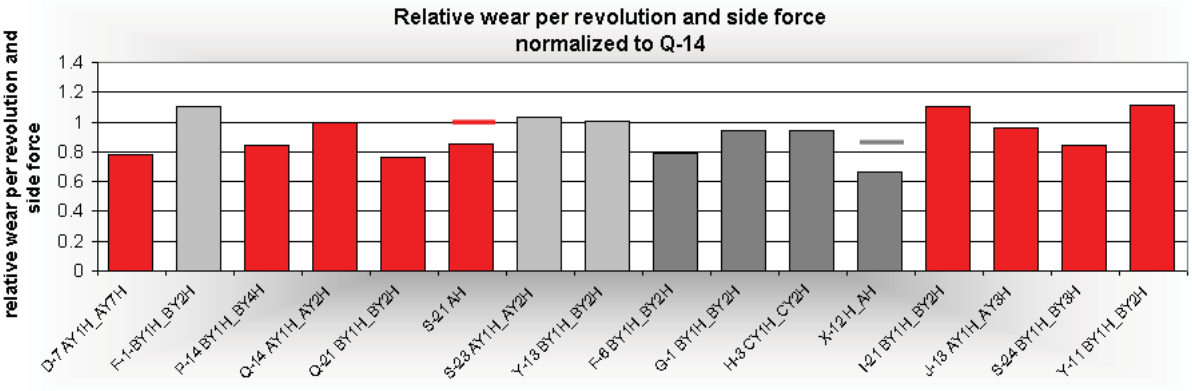

Fig. 97 Relative wear rate in terms of total drill string revolutions and side force: For S-21with 53% and 73% wear and for X-12 with 2.8 Mio and 1.8 Mio drill string revolutions

10.3.4 Study of the performance of different hardbandings

The relative wear rates in Fig. 97 shall now be compared to experimental tests for those hardbandings. Maurer wear factors are only available for Arnco XT100, XT200 and XT300. Experimental testing on behalf of Statoil for all hardbandings including OTW 12 hardbandings was performed by Trio OilTec Services. Trio OilTec is the manufacturer of OTW 12 (16.10). The tests were done on black steel casing and only allow a qualitative check.

	Arnco XT100/200	Arnco XT300	OTW 12
Test min. wear	2.5	2.8	3
Test max. wear	4.8	11.6	3

Tab. 5 Test results of hardbandings: Casing wear in g/hr

Comparing Fig. 95, Fig. 96 and Fig. 97 one can see that the tests are quite consistent with the wear observed in the field. Arnco XT300 was one of the best and the worst performer in the tests and in the field study. This hardbanding also obtained a very low wear factor in Maurer tests, but only if it remains crack free.

Arnco XT100/200 can perform slightly better than OTW-12; this was observed in the field study as well.

As the field results show a similar trend as the experimental results, one can concluded that the different hardbandings had an influence on the observed wear on Troll wells.

Higher adhesion wear for the chromium containing hardbanding could however not be found.

Thus a closer qualitative check should be done.

10.3.4.1 Assigning G-1 a wear factor of 3.7

The most consistent results are obtained for the Arnco XT100/XT200 hardbanded tool joints. Assuming G-1 had a wear factor approximately between the two tested wear factors for Arnco XT100/200, one can calculate the wear factors for the other wells.

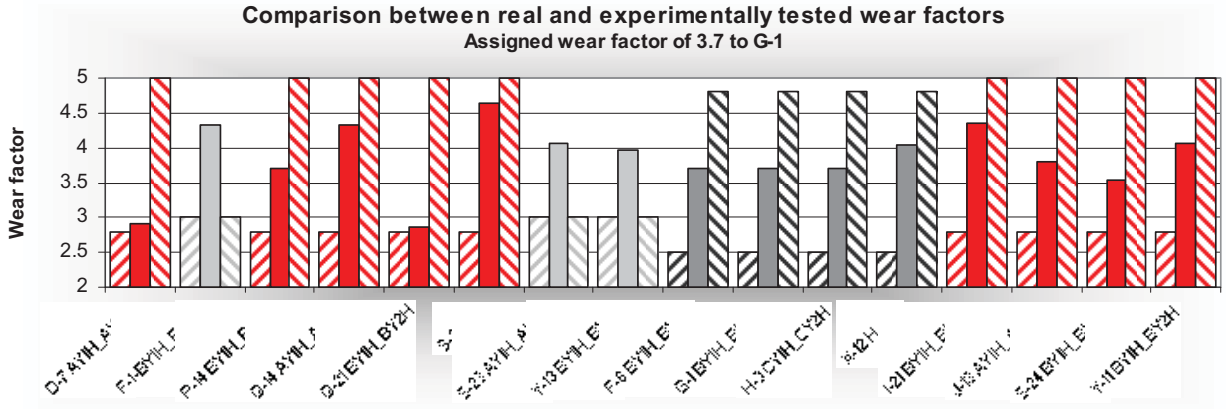

Fig. 98 Wear factor comparison: Field values and experimentally tested values

With such a "medium" range estimate for G-1 the wear rates for the Arnco XT300 wells are all within the experimentally tested range. OTW-12 would have a wear factor of rather 4.2 than 3. Only one test was run for this hardbanding and it should not be surprising if the wear factor in field is a bit different.

10.3.4.2 Assigning G-1 a wear factor of 2.7

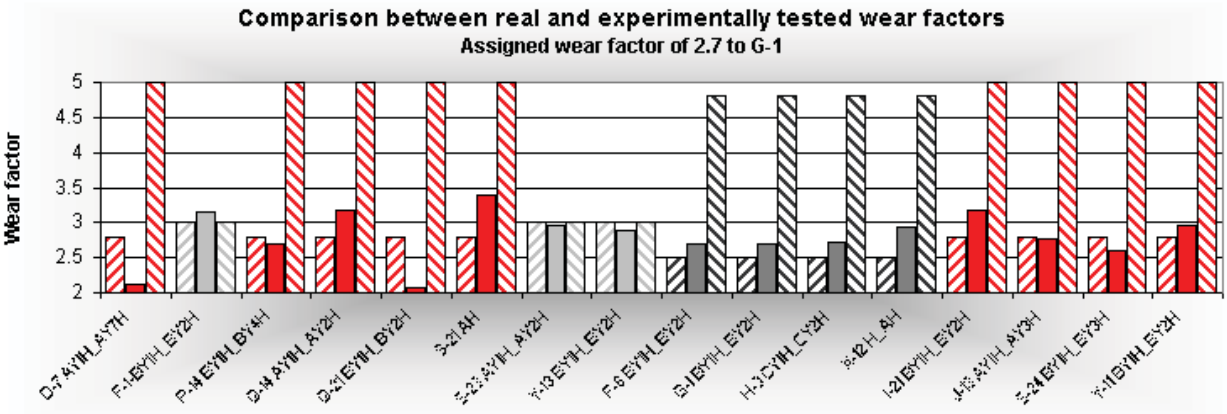

If we assign G-1 a wear factor on the lower end[xv] ,the conclusion is a bit different. The wear factors for D-7, Q-21, P-14 and S-24 would be a bit too low compared to test results. DEA-42 wear test results assign Arnco 200XT a lowest wear factor of 1.2 and Arnco 300XT a wear factor of 1.2, which is 20% less than Arnco 200XT.

The reported wear factor for OTW-12 would be according to experimental tests.

[xv] This well had a brand new hardbanding

11 Discussion of the analysis and results

11.1 Field data analysis

Casing wear analysis in the laboratory can confine the number of unknowns and keep a set of parameters constant to study the effect of single parameters. Running a set of tests aiming to reproduce the casing wear percentage with conditions that were present in the field can give the best interpretation of observed casing wear.

This analysis was a field analysis only and therefore the ultimate results of this study are limited to the available data quality and quantity.

11.1.1 Data quality

11.1.1.1 Baker Autotrak reports

In general the provided data are of good quality, only in two Autotrak reports small intervals are missing. If the missing interval is only some meters, then the error was assumed to be negligible, though it could influence the results.

11.1.1.2 USIT logs

The USIT logs were in general of good quality. High tool eccentricity could often be observed probably caused by the position of the shoulder of the tool in the groove. Eccentricity generally affects the internal radius measurement, whereas the thickness measurement is not affected. In two wells that both showed higher than expected wear (F-1 BY1H/BY2H and I-21 BY1H/BY2H) the logging quality was poor; for some wells only the logging report could be found in the data achieve.

An average wear value could be calculated for wells, where dlis files were at hand. Picking an average leaves always some room for interpretation.

11.1.1.3 Information on hardbanding

One of the most important parameters is the type, geometry and application of the hardbanding. The information of the recent type of hardbanding in use could be given for all wells.

In case of Songa Trym the hardbanding changed end of 2008, but this change was a gradual one. If the old hardbanding wasn't in good condition any longer, then the new OTW-12 was welded onto the tooljoint.

On all rigs one never knows in which condition the hardbanding was when the pipe was run in hole – a new hardbanding will have a different wear characteristic compared to one that already has been in use for some time. Cracks in the hardbanding can lead to a dramatic increase in wear rate.

11.1.2 Multi-lateral casing wear analysis

One of the main problems that arose out of the analysis, was due to the fact that always more than one branch / side track was drilled. The casing was subject to two to eight "casing wear cycles", but the casing was logged only after drilling the last branch.

To investigate if certain parameters, e.g. the effect of adding lubricator to the mud or the use of a downhole motor, can reduce casing wear, one has to keep this parameter constant for all branches as the average value out of some values will not be representative in the end. Perhaps a more detailed analysis could be possible if the casing was logged after drilling each branch.

11.2 Severity of the problem

The final well report for S-21 states that a leakage in the casing was probably the result of casing wear. From the observed wear results in the other wells one can conclude that casing wear is a severe problem in Troll wells.

Casing wear literature is more or less exclusively dealing with wear on black steel.

Preliminary studies on high corrosion resistant alloys, in particular martensitic stainless steel, are dealing with tribo-corrosion occurring in sour environment and high chloride content in the mud.

On the Troll wells analysed H2S is not an issue. A study on the corrosiveness of the low solids KCl/polymer "Troll mud" was conducted internally and came to the conclusion that the mud is not corrosive.

Most obviously high wall thickness loss on the chrome joints is caused by severe galling wear. Apart from noble metals such as gold and platinum any other metal is always covered by an oxide film when present in unreacted form in an oxidizing atmosphere. The passivation (or other forms of suitable lubrication) can hinder severe adhesive wear unless deliberately removed beyond a certain threshold load.

Most likely cold-welding occurred between tool joint and casing contact points under lateral load. The micro welds broke up during the movement and small fragments were torn out of the casing leading to a gradual loss of wall thickness. Metal at the sheared junctions became work hardened and abrasive transfer particles were formed. Those transfer particles contributed to the formation of a severe groove on the low side. This theory can be supported by a discussion with Dr. Steinar Wasa Tvervild (material expert, research centre Bergen, Statoil). The wear particles were most likely a composition of casing material and passivation layer.

Abrasive wear will also be promoted using L80Cr13 due to the relatively lower hardness of chrome steel compared to black steel P110. Additionally, the hardness contrast between chrome and tooljoint material is high. The hardness criteria to avoid abrasive wear - a minimum ratio of 0.8 between hard and soft metal – is not met with black steel as well, but is lower for the chrome casing.

More adhesive wear can occur with a combination of chrome based hardbandings (e.g. Armacor M, Arnco 200XT) on chrome casing. Arnco 300XT and OTW-12 are chromium free hardbandings. This observation, however, cannot be supported by the results of this analysis as excessive wear occurred with all hardbandings.

Given that only the chrome casing joints are worn in all wells and the black steel is in more or less perfect condition, it can be concluded that the parameters causing wear on Troll are ultimately not severe – at least not for non-stainless steels.

11.3 Possible reasons for trend deviations

Given the many unknowns in the analysis and the simplified analysis approach it should not be surprising to find wells, where the actual wear is up to 10 % higher or lower than the estimated one.

Comparing the relative wear rates in Fig. 95, Fig. 96 and Fig. 97 one can see that relative wear rates in terms of drilling time deviate a lot, whereas less deviation occurs if relative wear is calculated in terms of drill string revolutions and side force. Current Statoil prediction of casing wear is based on drilling time and a single wear value in the chrome section, the maximum wear. This approach can give a very wrong impression of how severe wear truly was. Firstly, drilling time is not sufficiently accurate to establish a trend. Secondly, extremely high maximum wear can be caused by on-spot wear in high local doglegs in one well, whereas in another well doglegs might be less severe and on-spot wear did not occur so often.

Remaining deviations in the relative wear rates in terms of revolutions and side force are most likely also caused by the underestimation of the influence of DLS and on-spot wear.

11.3.1 On-spot wear

The presence of calcite stringers, specifically of ultra hard stringers, will become manifest not only in the total number of drill string revolutions, but also in what is called on-spot wear. On-spot wear is created if a tool joint is rotating on the same position in the casing for a very long time due to low ROP. Extremely low ROP values are encountered in calcite stingers and less frequent pyrite nodules and other hard formation.

In the first step in the analysis a uniform revolution profile along the chrome section was assumed. This means every point of the liner has seen the same number of revolutions, which are the same fraction of total number of on and off bottom drill string revolutions in case of a constant ROP during drilling. The proportionality factor is determined by the fraction of tool joint length to total drill string length and is the same for all wells. It must be highlighted here that no point in the casing will see the total number of drill string revolutions.

In reality points in the casing will be subjected to different fractions of total drill string revolutions due to different ROP during drilling. In a theoretical case where there was a half meter thick stringer and between the stringers ten meters of easy drillable sand, the tool joints would rotate a lot on the relative same positions within the casing all the time. This is illustrated in Fig. 99 and Fig. 100.

Fig. 99 Position of the tool joint during encounter of first stringer: on-spot wear is created for the first time

Fig. 100 Position of the tool joint during encounter of the second stringer: on-spot wear is created at the same relative positions

To investigate on-spot wear is possible on a well by well basis as the current positions of the tool joints within the casing are known by current drilling depth, BHA length and drill string configuration. The attempt was made to remodel a wear profile for a single branch but the calculation effort exceeds the capacity of the standard office software.

However a basic qualitative statement on the likelihood of occurrence and severity of on-spot wear can be made by remodelling the revolution per meter profile for each branch during drilling. Additionally, the ROP profile was plotted to allow a verdict of the presence of hard stringers.

This was done for the wells with highest (F-1, I-21) and lowest relative wear rates (D-7, Q-21) to investigate whether the wells I-21 and F-1 had the potential to accumulate on-spot wear a several times during drilling ahead and D-7 and Q-21 did not.

The corresponding figures are plotted below.

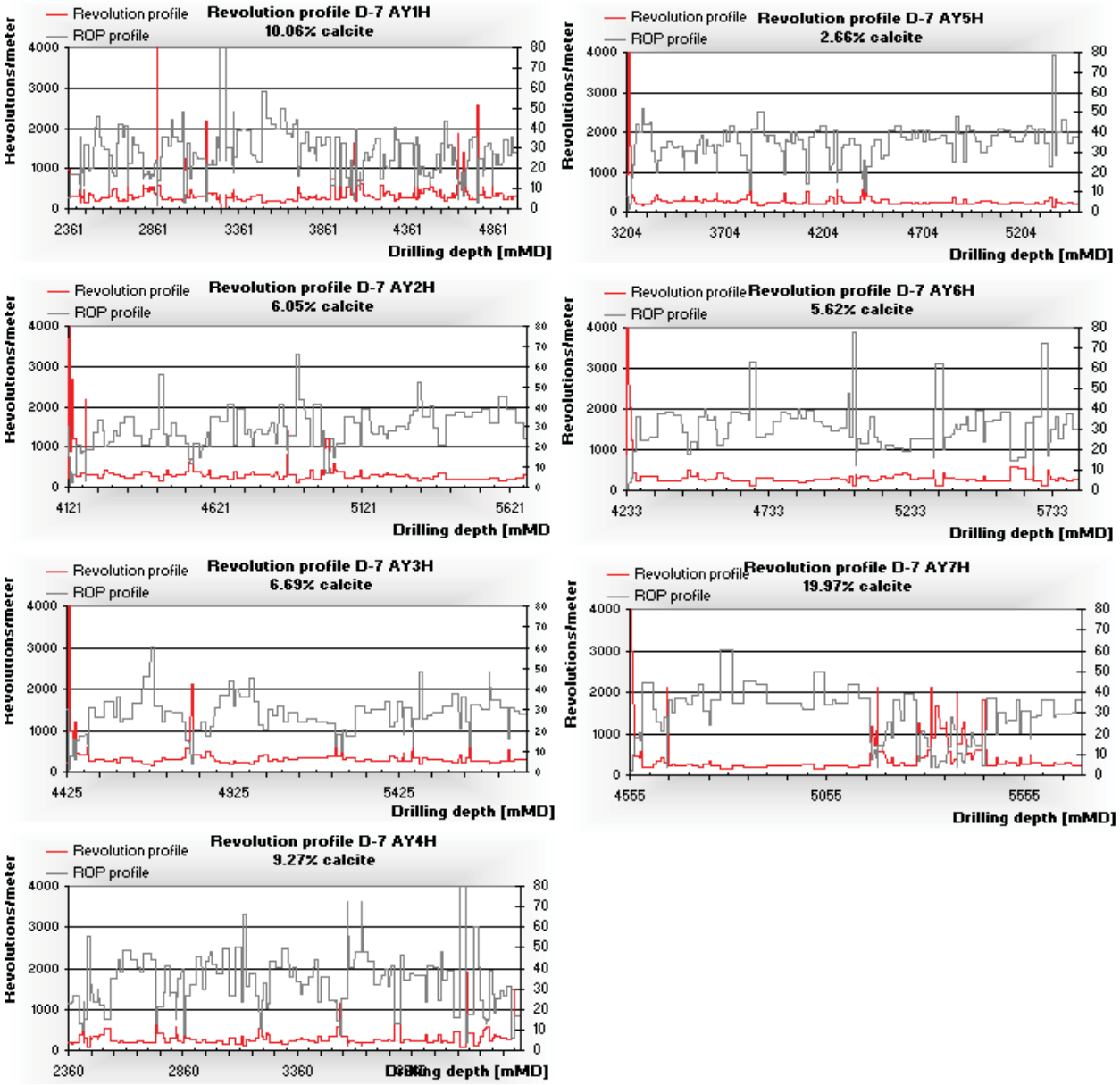

Fig. 101 Revolution per meter and ROP profile for all branches of well D-7

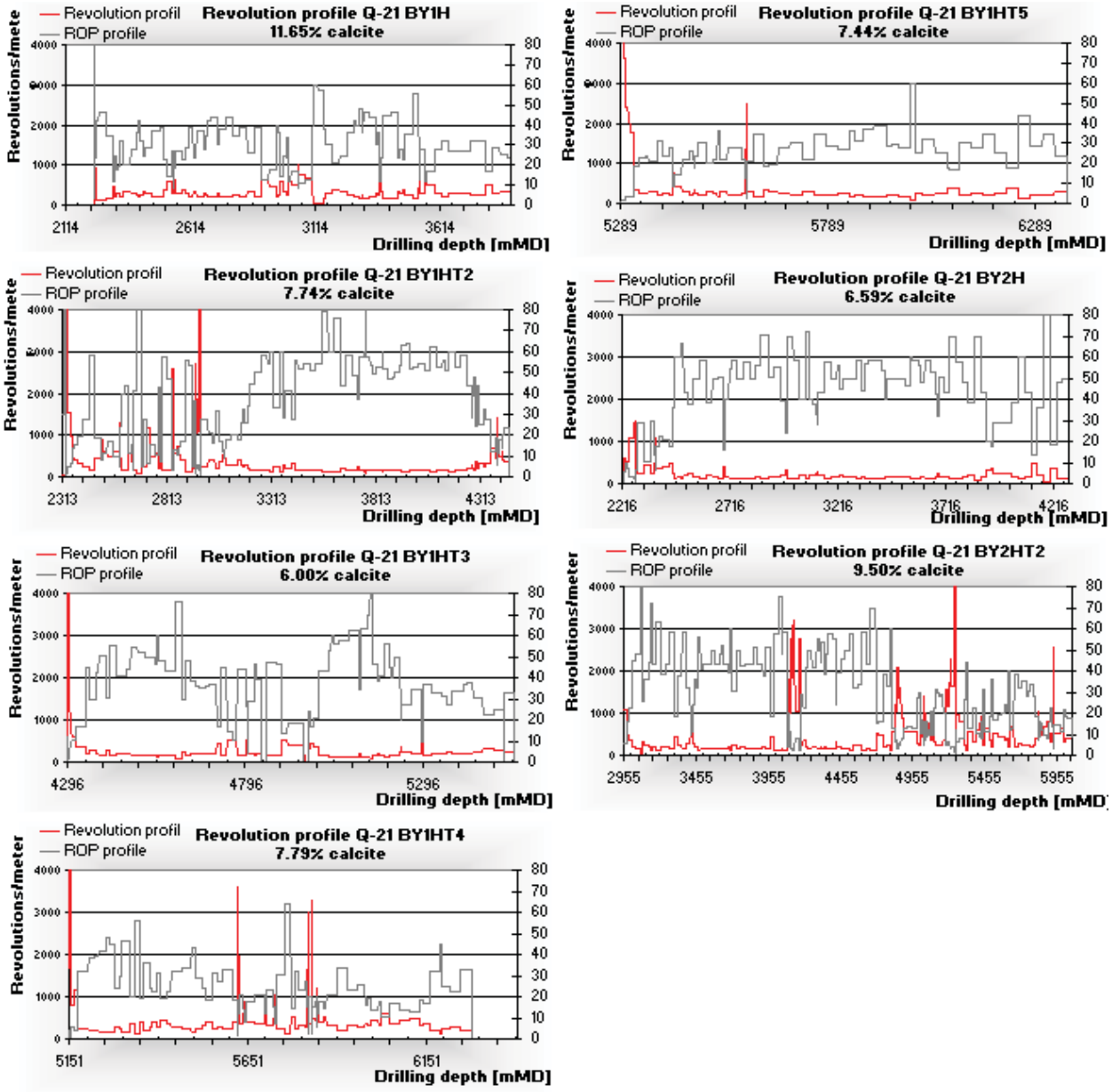

Fig. 102 Revolution per meter and ROP profile for all branches of well Q-21

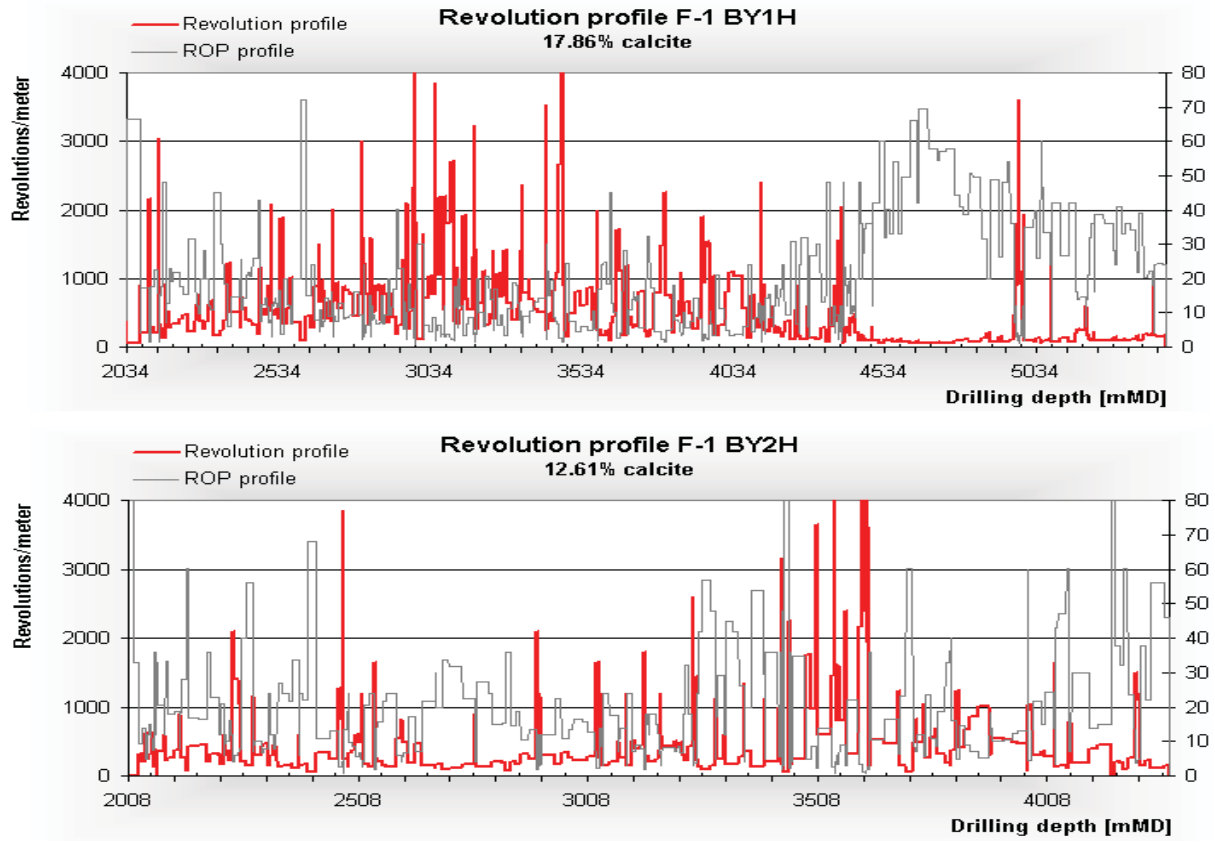

Fig. 103 Revolution per meter and ROP profile for well F-1

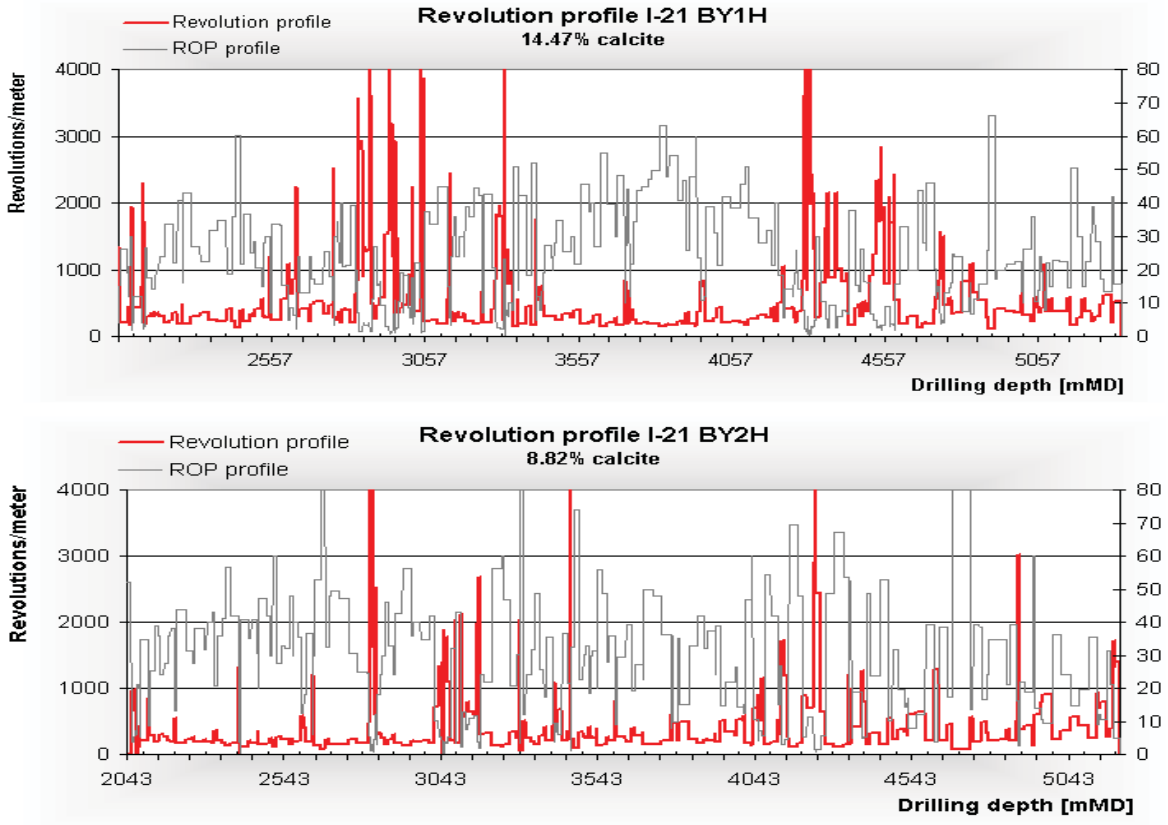

Fig. 104 Revolution per meter and ROP profile for well I-21

The figures show very clearly that the potential for creating on-spot wear was present in the wells I-21 and F-1, but less in wells Q-21 and D-7.

The only branch where D-7 rotated during drilling with slow ROP (<10 m/hr) was D-7 AY7H with a calcite content of nearly 20 %. This interval is approximately 300 meters long and here some on-spot wear was created.

Though some branches of D-7 had significant calcite content, the ROP did not drop to below 10 m/hr most of the time indicating that seldom ultra hard stringers were encountered.

Well F-1 drilled with low ROP and required a lot of revolutions to drill ahead in quite a few points. It is very likely that frequent on-spot wear accumulated in some points and gives very extreme wear in those points. The same is true for well I-21.

Ultimately, fewer revolutions were required to drill I-21 and F-1, but the revolutions profiles indicate that in those two wells the accumulation of on-spot wear created a revolution profile where in points the fraction of total revolutions exceeded the fraction of total revolutions well D-7 has seen.

Additionally, the relative wear rate could be promoted by on-spot wear: as the hardbanding is wearing the casing in one point for an extended period of time, hard-working of sheared off casing material could occur, which promotes ploughing and cutting wear.[xvi]

Well	Drilling hours with high revolutions / meter				Calcite content [%]
	> 2000		> 1500		
	Relative [%]	Absolute [hrs]	Relative [%]	Absolute [hrs]	
D-7	8	44	2	9	8
F-1	13	78	7	43	16
P-14	25	190	3	26	11
Q-14	7	13	3	5	1
Q-21	8	51	4	23	8
S-21	11	98	3	22	8
S-23	7	34	6	30	15
Y-13	8	18	4	9	8
F-6	5	15	4	10	6
G-1	25	205	14	112	25
H-3	15	70	8	43	9
X-12	31	123	5	22	6
I-21	20	107	7	39	12
J-13	13	38	2	5	6
S-24	2	9	2	10	3
Y-11	9	28	3	10	8

Tab. 6 Relative and absolute drilling time with high RPM and low ROP

Tab. 6 reflects the tendency of the investigated wells to accumulate on-spot wear. The wells with the highest tendency[xvii] are those where also calcite content was generally high. The relative drilling time, where more than 2000 revolutions were required to drill one meter is also reflected in the calcite content in the formation in most of the wells. Deviations occur

[xvi] Experimental testing necessary to verify the statement

due to different number of branches (on-spot wear is also created during mill out operations) and very likely due to the type of calcite, hard or ultra hard.

On-spot wear will be dominated by the anisotropy of the formation and thus hard to control and predict. A way to avoid bad surprises due to neglecting on-spot wear could be monitoring of on-spot wear during drilling.

11.3.2 Side force and dog leg severity

The side force for all wells is calculated with the soft string model assuming the string is on branch TD. In the soft string model the branch revolution weighted average weight on bit was used. As the wear rate is not linearly proportional to the side force the ultimately determined side force is not fully representative for the accumulated wear.

Sensitivity analysis showed that section length, drill pipe geometry, BHA and well trajectory had no significant influence on side force.

11.3.3 Dog leg severity

The influence of dog leg severity was neglected using the soft string model to calculate side forces. The effect of increased bending in dog legs can be investigated only by using the stiff string model to calculate side forces.

Maximum and average dogleg severity and absolute tortuosity values for the wells can be extracted from Fig. 105.

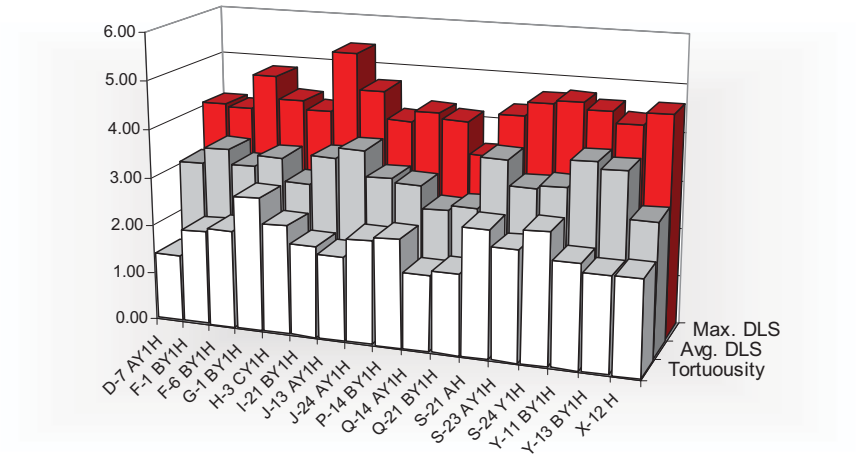

Fig. 105 Average and maximum dogleg severity [deg/30m] and absolute tortuosity [deg/30m]

To verify the statement that dog leg severity really caused higher side force and severely influenced the wear profile, the side force using stiff string model was simulated in WellPlan for dedicated wells.

[xvii] X-12 was drilling with roller cone and might not be representative

The wear curve of well H-3 (Fig. 106) closely follows the dog leg severity trends. In general high wear is observed at high dog leg severities and vice versa. Deviations from the trend are most likely caused by occasional on-spot wear, the uncertainty in real dog leg severity and difference in original casing wall thickness.

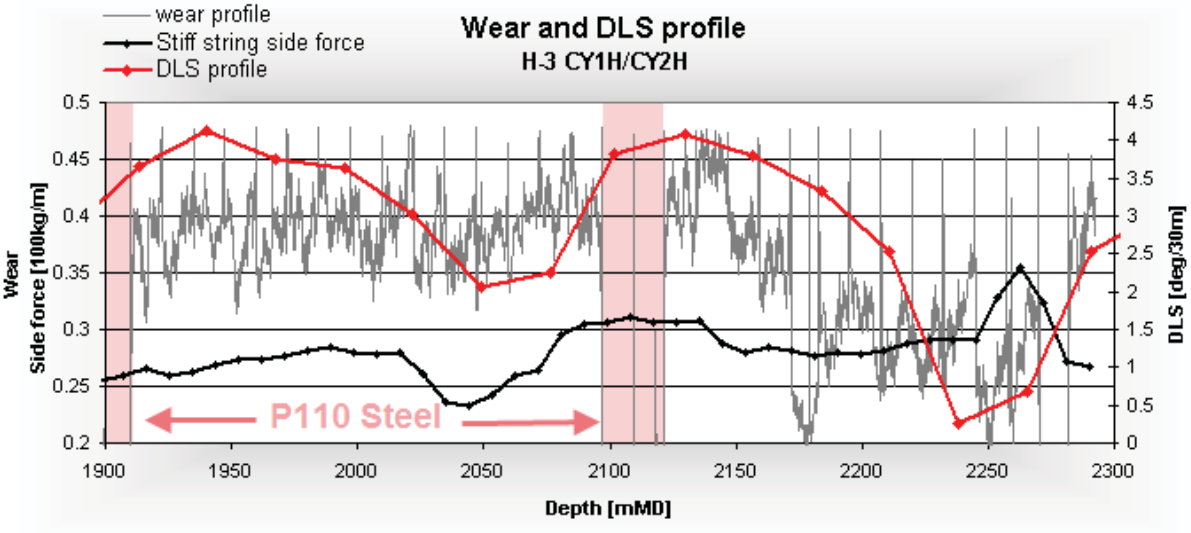

Fig. 106 Wear, DLS and stiff string side force for well H-3

In well I-21 the maximum wear occurred at approximately 1850m, where the dog leg severity was more than 4.5 degrees. I-21 was the well with the highest apparent dog leg severity of all wells (Fig. 106).

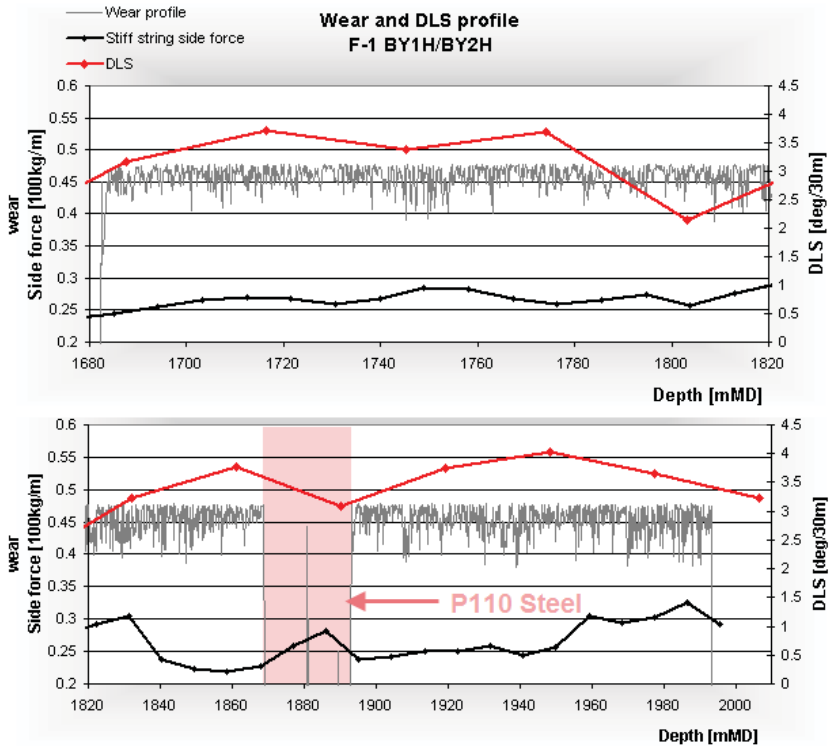

Fig. 107 Wear, DLS and side force profile for F-1

The same plot as for H-3 was generated for F-1. Unfortunately it is hard to interpret this plot as the required data (wear profile for different thickness search windows) could not be provided and the wear curve is cut off.[xviii] The maximum wear in this well was estimated to be at the last two chrome joints 1975-1995, where the stiff string side force was highest. Dog leg severity is in general higher in well F-1 compared to H-3. Additionally it is very likely that well F-1 experienced severe on-spot wear (Fig. 107). The points, where most severe on-spot wear occurred must not necessarily coincide with highest dogleg severities.

Furthermore another well (Y-11[xix]) with high relative wear was investigated. The revolution profile plotted against drilling depth (Fig. 108) indicates that in at least two points on-spot wear was created, but generally the wear profile was quite uniform and one should find the highest wear occurring in more severe doglegs.

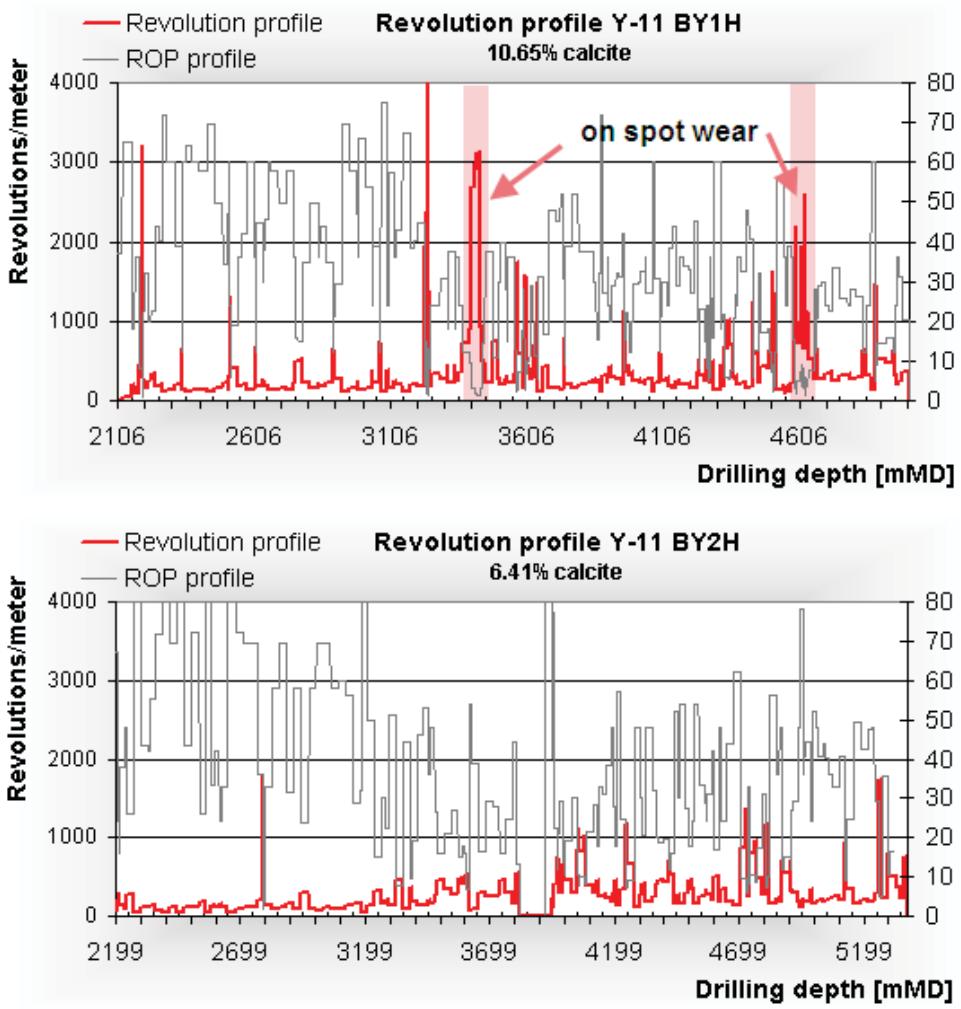

Fig. 108 Revolutions per meter and ROP profile for well Y-11

[xviii] Also the required files (.dlis type files) for wells of particular interest such as D-7, Q-21, S-21, P-14 and I-21 could not be provided

[xix] All relevant data available in good quality

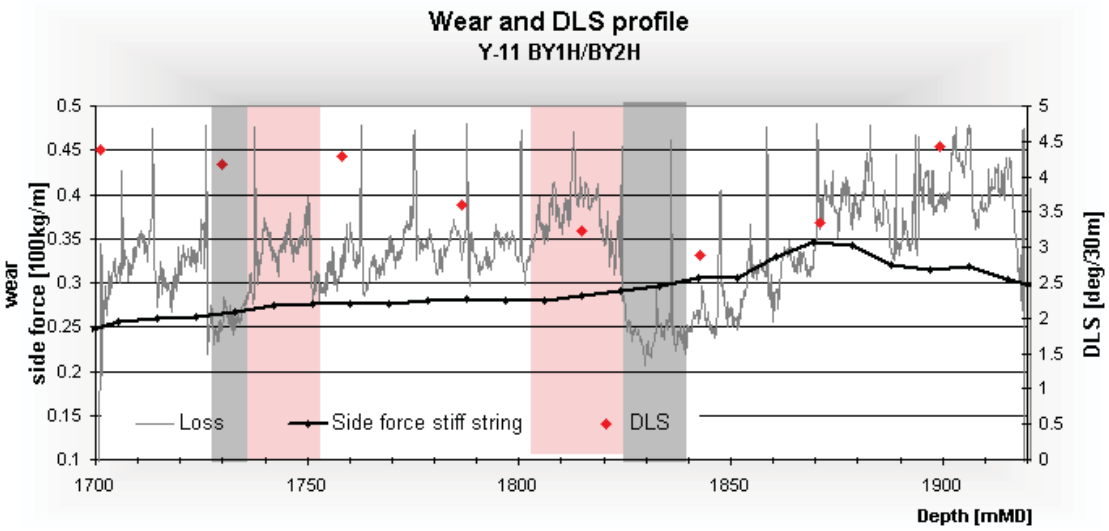

Fig. 109 Wear, DLS and side force profile indicating areas where dog leg was generated along the trajectory (red) and where real DLS was lower than apparent DLS

In general the wear profile for Y-11 follows the dog leg severity and side force trend (Fig. 109). The deviation occurring in two points is most likely to be caused by the real dog leg severities being greater or less than apparent calculated dog leg severities and a higher original casing wall thickness on those two joints.

One can also find an oscillating wear pattern probably caused by on-spot wear.

The highest relative wear rates were present in wells with higher dog leg severities in the chrome section (Tab. 7). This is terms means that the hardbanding performance in those wells must not have been worse than in other wells.

As a conclusion one can draw that dog leg severity definitely had a large influence on casing wear in the Troll wells.

Rel. wear per rev. and SF	Avg. DLS in chrome
I-21	Y-11
Y-11	S-21
F-1	Y-13
S-21	J-13
S-23	I-21
Y-13	F-1
Q-14	G-1
J-13	S-24
H-3	S-23
G-1	F-6
X-12	D-7
P-14	P14
S-24	H-3
F-6	X-12
D-7	Q-21
Q-21	Q-14

Tab. 7 Comparison of high relative wear rates and high DLS in chrome

11.3.4 Hardbanding

Concerning hardbanding the big unknown is the condition of the hardbanding when run in hole. I-21 reported severely worn hardbanding when pulling out of hole. As a consequence a huge amount of pipe had to be re-hardbanded. The same problem occurred in F-1, whereas less drill pipe was laid aside in the well H-3. As reported by drilling engineers general spot tests on the condition of the hardbanding are done. However, it can then not be excluded that some worn pipe was run in hole. However one should trust the drilling crew that they know how to do their job.

The reason for worn pipe is most likely extremely hard pyrite nodules[xx] and other hard minerals. Calcite is hard to drill, but calcite itself has a significantly lower hardness than the tool joint. Also the well with the highest calcite content, G-1 BY1H/BY2H, had no problems with worn drill pipe.

In general it is more likely that the higher relative wear rates are caused by higher dog leg severities. This statement can be supported by the fact that worn drill pipe did not rotate in the casing. Daily drilling reports give information at which depth the worn tool joints rotated during specific runs. Worn tool joints are always immediately above the BHA and the length of worn drill pipe never exceeds the recently drilled new formation.

11.3.5 Drilling with motor

Theoretically drilling with motor should decrease casing wear as less drill string revolutions are required to drill with the same number of bit revolutions. Fig. 110 was presented already earlier and shows the relationship between section length, drill string revolutions and calcite content. Only six wells in the analysis occasionally used motor, which makes it hard to see whether those wells really required less drill string revolutions and thus observed lower wear.

Well S-21 (8% calcite) seems to have required less drill string revolutions than the trend indicates for wells with similar calcite content.

Also F-1 (16%) plots a bit lower given the calcite content of the other four wells marked in red (9%, 11%, 12% and 15% calcite respectively). In case of G-1 (25%) the spread between the wells in red and this well seems to be too small for a minimum difference of 10% calcite.

Of course those are just indications as the drillability and also the relative time the motor was in use influences this trend.

[xx] Baker mud logger reported high amount of pyrite nodules in I-21

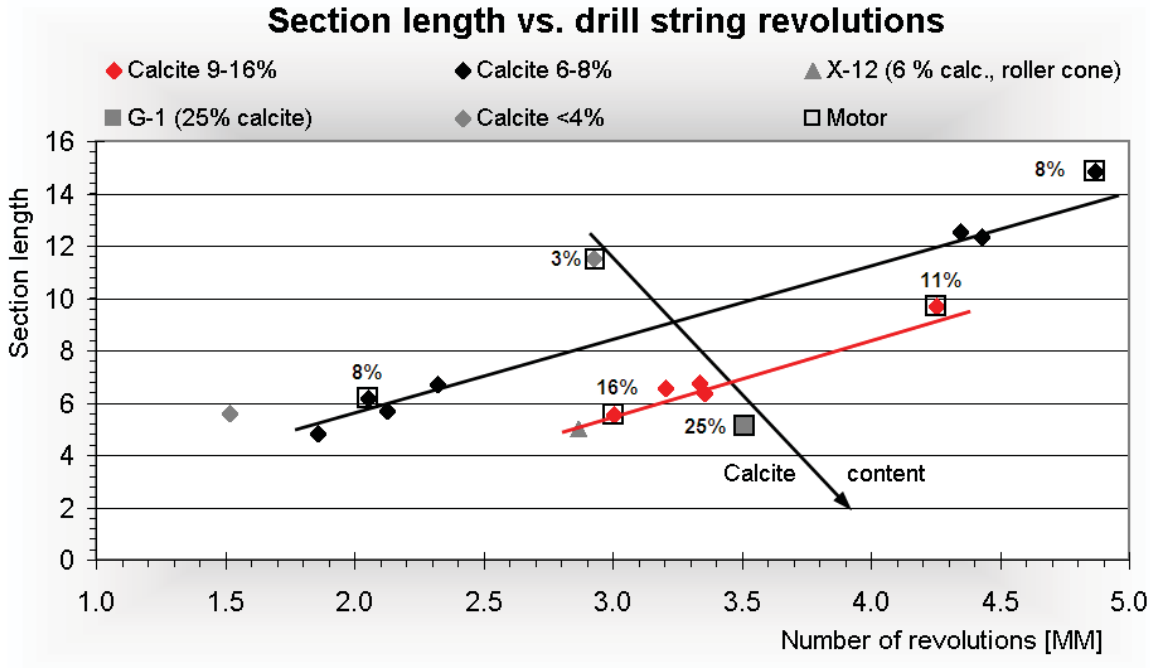

Fig. 110 Influence of use of a downhole motor

11.3.6 Influence of the water based drilling mud

The mud system in the 8-1/2" section was the same on all wells and one can assume that slightly different mud properties did not influence casing wear a lot.

Adding lubricator to the low solids WBM mud can decrease casing wear. The effect of lubricants strongly depends on the actual surface conditions of the casing and tooljoint at the time of addition and on the type and amount of solids in the mud [29].

In full scale testing equipment and field testing no significant influence of lubricants on weighted WBM could be observed. With an increasing amount of solids in the mud, these solids will penetrate the lubricant film and make it inefficient. Overtreatment with lubricant (normally occurring at 2-5%) can decrease wear rate/ friction.

Stainless steels are very prone to adhesive wear and the lubricator used on Troll is very likely just as ineffective as the many other lubricators and greases in prohibiting galling wear. Solid lubricators or lubricants containing substantial amounts of molybdenum disulfide, graphite, mica or talc are recommended to reduce galling wear.

On Troll wells the maximum lubricant concentration was 3% and only in five wells the average concentration exceeded 2% (App. 16.5). As the wear curve was not measured continuously on Troll wells, it is not possible to say whether lubricator could successfully decrease adhesive wear whenever 3% lubrication concentration was achieved. Experiments could give an answer to this.

Comparing the obtained relative wear rate to average lubricator does not show any connection between higher wear rate and low lubricator concentration and vice versa (Tab. 8).

Troll mud has a high salt concentration and chloride content between 25,000 – 40,000 mg Cl^-/ litre. The question of pitting corrosion in 13Cr materials at the Troll wells when O_2 is introduced in the WBM is then raised. Exposure of O_2 in salt mud gives the 13Cr casing substantial less corrosion resistance to pitting corrosion than carbon steel casing. The wear resulting from corrosion and abrasive/adhesive wear at the same time is much more severe than simply the sum of the thickness losses due to corrosion and wear.

USIT logs indicate only minor signs of corrosion in the wear groove in some wells and a study on the corrosiveness of drilling mud used on Troll came to the conclusion that the mud is not corrosive. Higher wear on Troll field is caused most likely due to the high adhesive wear occurring in WBM. However; minor tribo-corrosion could additionally promote high wear on Troll compared to other fields, e.g. Grane field, where an inhibitive OBM system is used.

Several studies and field observations indicate that oil based mud systems have a higher slipping effect between the tool joints and the casing, thus providing better lubrication, decreased friction and less adhesive wear.

Rel. wear per rev. and SF	Avg. Lube con.
I-21	1.82
Y-11	1.45
F-1	2.61
S-21	2.02
S-23	1.63
Y-13	1.22
Q-14	0.00
J-13	0.97
H-3	2.50
G-1	2.63
X-12	0.70
P-14	1.20
S-24	1.16
F-6	2.81
D-7	1.56
Q-21	1.54

Tab. 8 Comparison of high relative wear rate and average lubricator content

However the conclusion that e.g. wells in Grane field experienced less wear[46] is based on a comparison of section length or drilling time, which in this study was found to be not accurate enough to describe casing wear.

11.3.7 Other, minor factors

11.3.7.1 Number of side branches

Compared to wells D-7 (seven branches) and Q-21 (eight branches or sidetracks) and P-14 (four branches), the wells F-1 and I-21 only had two branches. The position of the drill string could be slightly shifted to the left or right when drilling a new branch. This could result in a more even wear and a less pronounced ultimate wear groove.

11.3.7.2 Initial wear rate

Experimental testing shows that casing wear is not a linear function. The initial wear rate is generally high and then decreasing to a more or less constant wear rate. Giving an estimate of the initial wear rate for a certain drilling environment is again only possible with experimental testing.

The initial wear rate for a well is controlled by the lateral load on the casing during drilling out of the 10-3/4" casing. During side tracking operations the casing will experience the highest loading. In the analysis it was assumed that BHA selection has no influence on the side force – this assumption is certainly not valid for the initial wear rate.

11.4 Recommendations

As the results of this thesis clearly reveal that the field observed wear percentages are mainly caused by long sections and hard calcite stringers and the resulting wear profile severely controlled by on the spot wear and dog leg severity, it would be very useful to develop and algorithm to allow continuous casing wear monitoring during drilling.

11.4.1 Continuous casing wear monitoring during drilling

Continuous casing wear monitoring during drilling could give a fairly good estimate of casing wear percentage and thus facilitate decision making on drilling ahead or drilling an additional branch.

As already outlined an accurate cumulative revolution profile can be determined by the known information of RPM, ROP and position of the tool joints (via drilling depth, length of the BHA and an average distance between the tool joints). This means that run by run the length of the BHA has to be specified and the accumulated revolutions of all previous runs along the chrome section added to the new run.

11.4.1.1 Example for run x

The chrome section here is assumed to be 50 m long and the string is lowered to drilling depth. At time 0 (Fig. 111) the first tool joint (pink) is about to enter the chrome section. Four other tool joints are already in the chrome section and will start to wear the casing as soon as rotation starts.

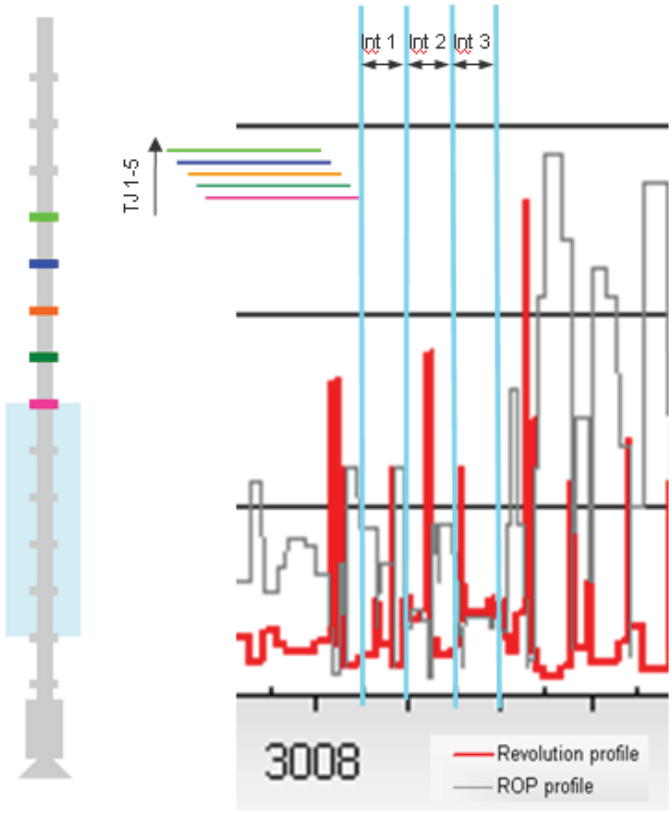

Fig. 111 Drill string at position t=0

After drilling 50 meters the following revolutions within the chrome section occurred (Fig. 112):

1. TJ 1 (pink) passed the chrome section completely: The revolutions it contributed along the 50 m of chrome correspond to the drilling revolution profile in Interval 1.
2. TJ 5 (light green) entered the chrome section last and only moved 10 metres. Along the first 10 metres of chrome it added the revolutions corresponding to the last 10 m of revolution profile in Interval 1. Along the remaining 40m of chrome one of the previous tool joint (grey) in this position added revolutions.
3. TJ 2-4 also added fractions of the (late) revolution profile in Interval 1 in the upper part of the chrome section. Additionally the tool joints (grey) that already have been lying in the chrome section before added revolutions to the lower chrome section, but according to the early revolution profile.

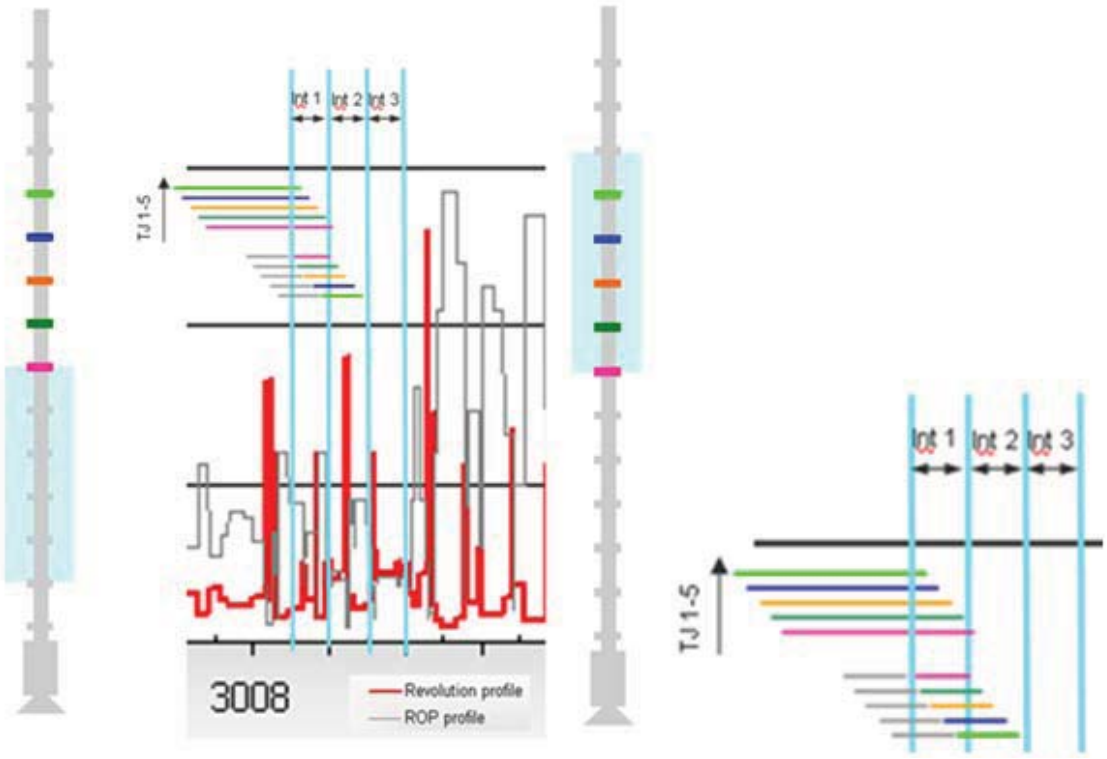

Fig. 112 Drill string after 50m drilling progress

After drilling the next 50 metres the process will repeat again (Fig. 113): 5 overlapping and party shifted 50 m long revolution profiles will occur. The old green tool joint will create wear along the last 40m of chrome (first 40m of revolution profile). The new green tool joint will wear the casing along the first 10m of chrome (last 10 m of revolution profile). The same is true for all other tool joint.

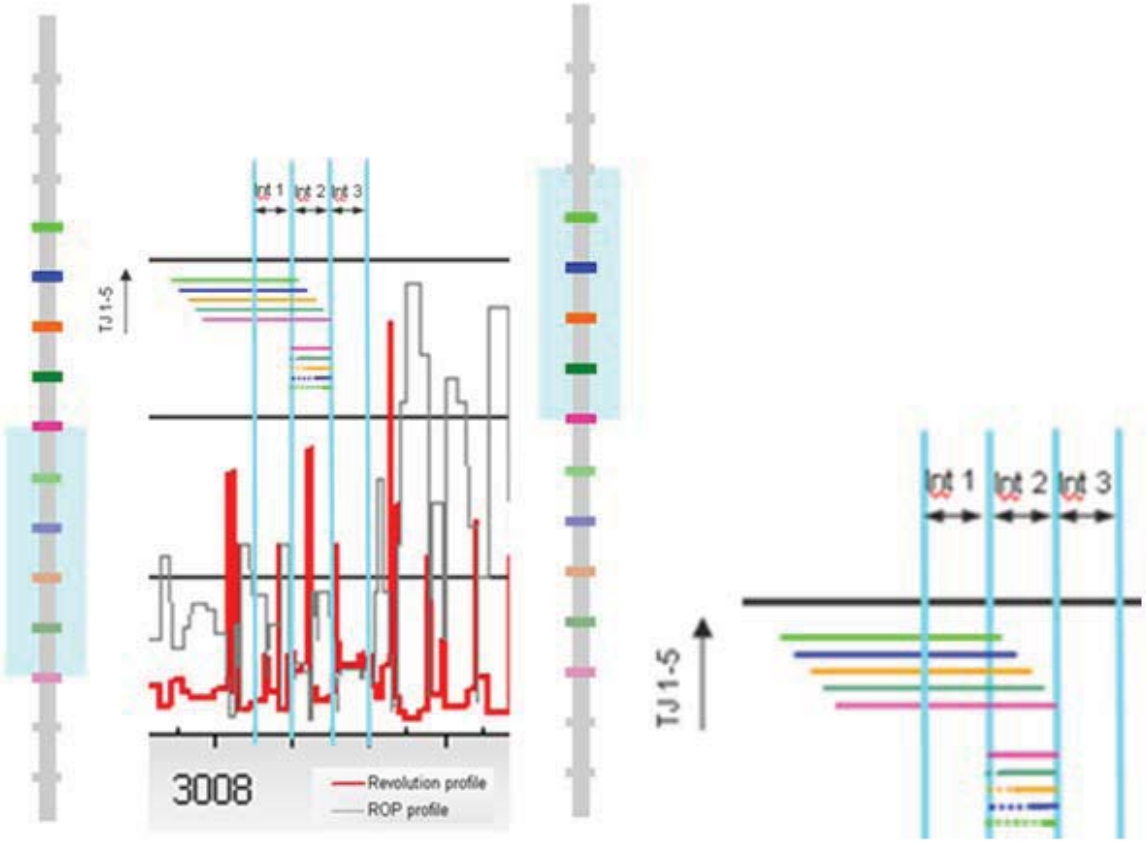

Fig. 113 Drill string after 100m drilling progress

It should be possible to define the number of tool joints fitting in a casing section of interest. Each tool joint repeats the revolution profile from a different starting point and end point. Here 5 nodes were sufficient, so 5 shifted revolution profiles will ever add up to the revolutions in the investigated section.

The corresponding side force can only be calculated in survey points. A software that can simulate casing wear should be able to realize when a new side force value must be used to calculate the revolution side force product.

11.4.1.2 Value of continuous casing wear monitoring

Though casing wear is a long time known problem in drilling wells, not a lot of research was done in this field. The main parameters causing casing wear are known and wear factors can be determined in the laboratory.

CWEAR uses the experimental results to predict casing wear, but has a several weak points:

- The prediction quality is often poor: Only a very limited number of different ROP, RPM, and WOB can be specified to simulate casing wear. It is therefore not suitable to predict casing wear on Troll, where on-spot wear frequently occurs.
- The software uses the soft string model to calculate lateral loads.

A software capable to monitor casing wear (based on the idea of CWEAR) should have the following additional features:

- Automatic upload of changed drilling parameters: Use them to calculate accumulated revolutions
- Automatic upload of survey data: Calculate stiff string side force
- Especially for chrome casing: More experimental testing on hardbanding/chrome wear factors in different drilling environments (WBM, OBM)

The value of such a programme would not only be limited to monitor casing wear on Troll, but also on other fields and wells. Multi-lateral drilling and extended reach drilling is becoming increasingly important and once such a programme is developed it could help in decision making of drilling ahead or an additional branch without running a USIT log each time.

11.5 Conclusive statements on the analysis

The high wear on the chrome casing is caused by the poor tribological properties of CRA steel in the drilling environment. If black steel would be used instead, casing wear would not be a problem on Troll.

The required number of drill string revolutions is the most critical factor contributing to wear. A close relationship between required drill string revolutions and calcite content of the formation and cumulative section length exists.

Average well side force calculated with soft string model is mainly influenced by drilling WOB. Side force simulated with stiff string model accounts for increased bending in dog legs. Doglegs have a high influence on the casing wear rate in Troll. Drilling with different BHA and short intervals where 5-1/2" drill pipe rotated in the chrome section had negligible influence. Different section length had no influence on side force as well.

Repeated on-spot wear, where side force was high, can explain excessive casing wear in some points in some wells (e.g. F-1 and I-21).

Different hardbanding performance seems to have influenced the observed wear and could be qualitatively cross checked with wear rate test results for black steel. A recommendation for a specific hardbanding cannot be given as further experimental testing should be conducted.

The water based mud system most likely promoted adhesive wear; the lubricator used could not suppress adhesive wear.

The still occurring deviations are low and it can be concluded that other factors, such as solids content of the mud, original casing wall thickness and the initial casing wear rate had a low influence on Troll casing wear.

Determining interaction and influence of those factors requires an in depth casing wear study including a lot of laboratory testing; it is not possible to control all of those factors.

Factors that definitely cannot be controlled or optimized are section length, number of branches and calcite content. Using a downhole motor can decrease the number of required drill string revolutions. The dog leg severity in the section where chrome joints are run should be as low as possible.

Optimizing some of these factors can possibly improve problems related to casing wear in wells with very low calcite content and short wells with moderate calcite content. Controlling these factors will very likely not decrease casing wear sufficiently to ensure well integrity in terms of the planned drilling activities.

12 Discussion of possible solutions

Statoil's planned drilling activities foresee more multi-lateral operations with deep side tracking out of the existing 10-3/4" liner. As a consequence of reusing the 10-3/4" inch liner it will be subjected to a higher number of total drill string revolutions and the casing wear problem become more severe than today. Under this outlook well integrity concerns will increase.

Improvements shall be discussed only to the extent relevant for Statoil's planned operational procedures and feasible in Troll wells.

To improve the situation a change in completion design or material selection are two possible solutions. Operational improvements could include the use of non rotating drill pipe protectors.

12.1 Non rotating drill pipe protectors

The main task of non-rotating drill pipe protectors (NRDPP) is to avoid contact between the tool joint and the casing wall. NRDPPs are mounted about two feet from the pin end of the tool joint and have a larger outer diameter than the tool joint. Thus, they come in contact with the casing before the tool joint contacts the casing (Fig. 114).

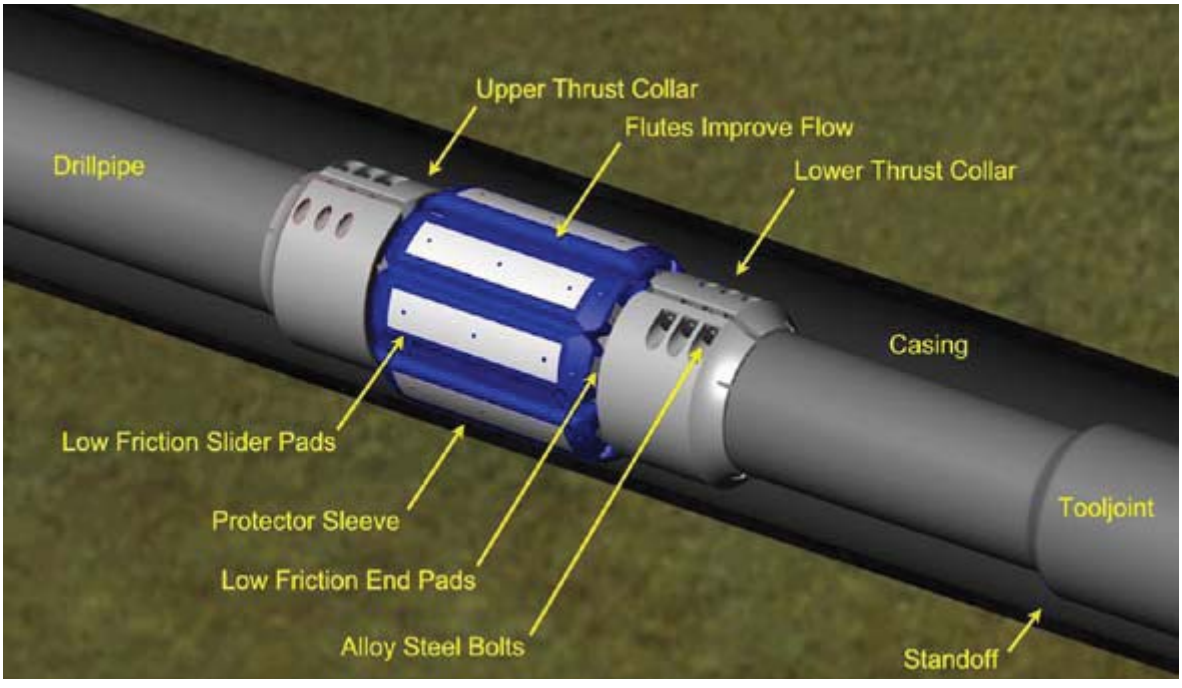

Fig. 114 Non rotating drill pipe protector

The drill string rotates in the protector limiting rotation against the casing wall. This reduces both casing and tool joint wear. When the NRDPP is in contact with the casing, the drill pipe rotates freely in the protector sleeve. Additionally, large reduction of drill string torque and drag is observed. Low drag NRDPP can reduce drill string torque up to 50% and drag up to 25%.[47]

Installation of a NRDPP involves opening a sleeve, placing it over the drill pipe between the collars and closing it with a retaining pin. The total installation time is 1-2 min.

Properly installed, NRDPP assemblies are quite robust and normally not susceptible to removal by rotational force. Only high axial force can damage them. Experiments have shown that properly installed collars can withstand loads up to 27,000 lbs without slippage on the drill pipe.

Installing of the drill pipe protectors can be trained to rig personal and done without additional service personal to save bed space offshore.

Operational limitations of NRDPPs in prolonged use are temperatures less than 350 ºF and normal side loading less than 2000 pounds. Both criteria are met in Troll.

A disadvantage of NRDPPs is the risk of slippage of the protector on the drill pipe when run in open hole. However some protection can be achieved by using protectors before the expected end of a bit run or BHA change.

Up to date NRDPPs have never been used in Troll wells. Drill pipe protectors are expected to decrease casing wear substantially in the chrome section, as not the tool joint, but the stationary protector will contact the casing wall. Whether slippage will occur can only be seen in field trials.

12.2 Change in material selection

As casing wear on Troll is primarily due to the poor tribological properties of the stainless steel used, the question arises whether a change in material selection can improve the situation.

Flow loop and bottle corrosion tests of 13Cr and 3Cr steel coupons have been performed as well with the conclusion that 3Cr steel cannot be used instead of 13Cr steel[48]. The tests have been performed using simulated condensed and produced waters saturated with CO_2. The data on the coupon samples show that 3Cr steel corrodes significantly in both condensed water and produced water conditions. Steady-state corrosion rates of more than 1.5 mm/y were found in both fluids. 13Cr sample corrode little in condensed water and less in produced water.

As using a less corrosion resistant material is not a solution, the remaining alternative is to use a material with similar corrosion resistance as stainless steel and better anti-galling

characteristics. One alloy composition that incorporates these features is Nitronic 60 (alloy 218), which is an alloy of Cr 17, Mn 8, Ni 8.5, Si 4, N 0.13, C 0.10 and Fe.

By adding silicon and manganese the matrix inhibits wear, galling, and fretting even in the annealed condition[49]. Higher strengths are attainable through cold or hot working the material. This working does not enhance the anti-galling but increases strength and hardness. Chromium and nickel additions give it better corrosion resistance than 304 and 316 stainless steels and improved chloride pitting resistance while having approximately twice the yield strength.

The high mechanical strength in annealed parts permits use of reduced cross sections for weight. Steel supply companies (e.g. Speciality Steel Supply, High performance alloys) offer Nitronic 60 stainless steel as seamless pipe (AMS 5848).

Nitronic 60 is often used in aerospace and nuclear industry. It is used in the oil industry in hydraulic lines in riser joints.

As this is definitely no standard casing material and has never been used as such before, it can be assumed that the material costs are way higher than for "conventional" stainless steel. [xxi]

12.3 Changing the completion design

One of the very early conclusions of the study was that high casing wear on Troll is due to a trade off in material wear resistance made against CO_2 corrosion resistance.

One possible way to overcome the problem is to change the completion design, such that no contact between flowing hydrocarbons and black steel exists.

Approximately two years ago the completion design has been changed already and the chrome section in the 9-5/8" liner below the swell packer could be replaced as corrosion rates in stagnant hydrocarbon environment are sufficiently low. Before that the two flow valves were in the 10-3/4" liner and chrome steel used all the way down to the screen hanger packers.

As outlined in Chapter 9 black steel can also be used between the gas lift perforations and the isolation packer. Statoil completion engineers have already found a solution to avoid exposure of the black steel above the gas lift perforations.

If the planned changes in completion design are incorporated, casing wear on Troll will no longer be a problem as the used of chrome steel is omitted. Reusing the liner will be possible and a huge amount of costs can be saved on all wells where the new completion is installed.

[xxi] No information on costs by the manufacturing company was given on demand

12.4 Expandable casing patch

A possible solution for wells, where already worn chrome casing is in the hole, would be to run an expandable casing patch out of carbon steel prior to sidetracking. By this one can avoid additional wall thickness loss in the chrome casing. CO_2 corrosion on the carbon steel would not affect well integrity, as the already existing chrome casing would still serve as a protection in case the carbon steel would corrode away within the lifetime of a typical Troll well (now about five years).

12.4.1 Expandable tubular technology

Expandable casing patches are used primarily to:

- Isolate production perforations
- Repair worn or weakened casing
- Repair corroded or eroded production casing

The basic concept underlying expandable-tubular technology is simple. A mechanical expansion device (expansion cone or mandrel) is propagated through downhole tubulars utilizing hydraulic pressure. The differential pressure is applied by pumping through a work string connected to the cone and the mechanical force is applied by either raising or lowering the work string. The progress of the cone expands the tubulars to the desired internal and external diameters in a plastic deformation process, which is also known as cold drawing (Fig. 115). The steel is deformed past its elastic yield limit into its plastic deformation region (Fig. 54), but not its ultimate yield strength. Expansions of over 25 percent have been accomplished.

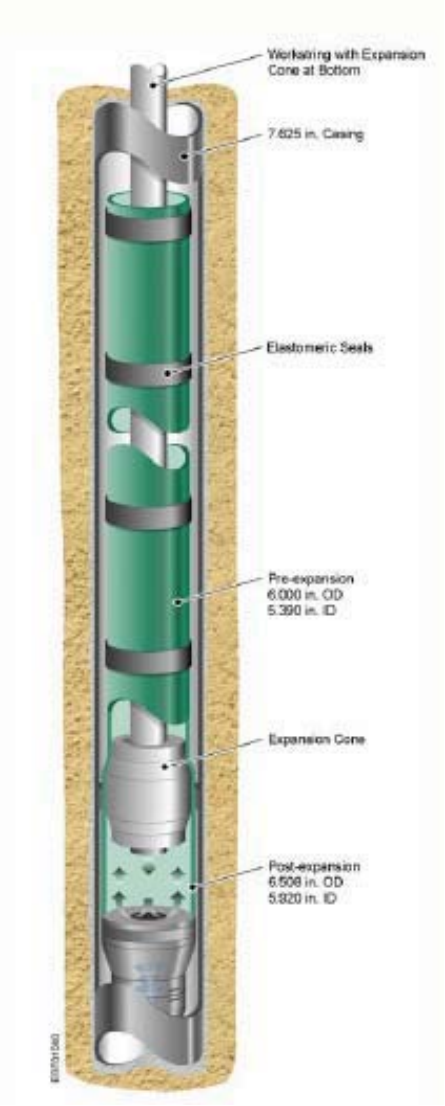

Fig. 115 Expansion process

There are two different kinds of expandable repair systems. One is to utilize solid expandable tubular and to expand every joint of the whole liner or casing and the other uses expandable elements at top and bottom of the patch and non-expanded joints in between.

The advantages of the full solid expandable liner include:

- Sufficient clearance after setting the solid expandable liner / casing
- Simple running and expansion tools and less operational problems
- Bigger production tubing for better production

- Full bore ID clearance post expansion facilitates future remedial work

12.4.2 Advantages, disadvantages and risks

Side tracking out of a deeper set casing or liner comprises enormous cost saving potential. Additional costs for the expandable liner section are roughly four times more than standard set casing. On the other side drilling time and costs can be saved, as the whole 17-1/2" and 12-3/4" x 13-1/2" section are omitted. Costs for the 13-1/4" casing and 10-3/4" liner also fall away.

The chance that the casing has to be renewed after the lifetime of the well is realistic due to the high predicted corrosion rates in flowing hydrocarbon environment

Initially there will be a very small decrease in clearance: Liner ID will decrease from 9.660" to 8.850" (Enventure Set® Expandable Technology 10-3/4", 60.7 lb/ft).

The risk of galvanic corrosion between the chrome casing and the carbon steel casing should be investigated for this suggestion.

13 Conclusions

Wear of the internal casing surface is a complex mechanism that long time has not been considered as a real problem in drilling wells.

Since easy oil is found, the drilling industry has changed dramatically: deeper, super extended reach, and designer wells are drilled to access new reserves. In offshore drilling and so in Troll field, subsea templates with limited well slots require a lot of multi lateral drilling to develop offshore fields economically. This can under some circumstances cause severe casing wear during drilling.

The aim of the thesis was to give a general overview on casing wear mechanisms, models, influencing parameters, logging tools and problems related to casing wear. The focus of the field study was to identify the main parameters that cause casing wear in Troll field and to give possible solutions for future Troll wells.

In Troll field excessive casing wear is primarily caused by a trade off in casing material wear resistance against corrosion resistance due to CO_2 in the production fluids. Corrosion resistant 13% chrome steel has very poor tribological properties promoting both adhesive and abrasive wear. The amount of wear in the investigated Troll wells depends primarily on the section length and calcite content in the formation. Higher side force contributed to casing wear. The higher the drilling WOB, the higher the side force in the chrome section was. Side force was especially high in dog legs, where increased casing wear can be observed on the ultrasonic logs. Excessive wear on some points is most likely caused by on-spot wear when the tool joints are rotating very long on the relative same position during drilling ultra-hard calcite stingers and other hard formation. Wear is furthermore promoted by the water based mud system and no evidence could be found that lubrication effectively suppressed adhesive wear. The performance of the different hardbandings in use could qualitatively be verified by crosschecking with hardbanding performance test results. A definite answer on whether one hardbanding caused more wear than another can only be given by running experimental casing wear tests.

Possible solutions for future Troll wells under the consideration of reusing the 10-3/4” liner could be the installation of non rotating drill pipe protectors or changing the completion design. Statoil completion engineers have found a completion solution avoiding any contact with flowing production fluids. Thus black steel can be used for the whole liner and casing wear will no longer be a problem on Troll.

For wells where the chrome liner is already in place a possible solution is to set an expandable casing patch prior to drilling a new lateral branches.

To avoid high casing wear during drilling, the following should be considered in general:

- Casing material selection: The casing steel should have a high wear resistance. Severe adhesive wear can occur with casing grades for the application in corrosive environment. Stainless steels are softer and more prone to wear.
- Type, composition and application of the hardbanding: Casing friendly hardbandings with low casing wear factors and low wear factors in open hole should be used. Chrome containing hardbandings on 13Cr casings can cause severe adhesive wear. The hardbanding should be applied in a raised condition and have a smooth surface.
- Drilling mud composition: In oil based mud systems casing wear is generally low. In water based mud systems weighting materials, especially barite, and high lubricator concentrations can promote the formation of a protective layer and lower casing wear.
- Well trajectory and hole geometry: Careful trajectory planning can prevent high wear. Doglegs should be avoided, especially in shallow parts of the well. The smoother the wellbore profile, the lower the side load will be. Casing buckling should be prevented since this creates abrupt doglegs and accelerates casing. High-angle wells should be designed such that the frictional drag is minimised.
- Drilling strategy: More sliding and less rotating can lower casing wear. Using a downhole motor decreases the total number of drill string revolutions.

Investigation of parameters causing casing wear on Troll furthermore showed that casing wear in this field and most likely also on other fields is predictable. As casing wear for a long time was not considered a real problem in the drilling industry, no software solution capable for accurately monitoring casing wear during drilling is on the market today. Due to the change in drilling programs more and more operators are facing casing wear problems today and the development of such software would definitely bridge a gap in the drilling market.

14 References

[1] **"Facts about the Troll area"**, Statoil homepage: www.statoil.com (http://www.statoil.com/en/ouroperations/explorationprod/ncs/troll/pages/default.aspx)

[2] **"Success Factors in Troll Geosteering"**, S.Leiknes and I.Osvoll, Norsk Hydro ASA

[3] **"Real-Time BHA Bending Information Reduces Risk when Drilling Hard Interbedded Formations"**, J.Hood, SPE, BakerHughes INTEQ, J.Hovden, Norsk Hydro, G.Heisig, SPE, K.D.Ernesti, SPE, BakerHughes INTEQ, and A.Knipper, SPE, BakerHughes OASIS

[4] **Norwegian Petroleum Directorate**, http://www.npd.no/engelsk/cwi/pbl/en/su/all/151.htm

[5] **"The Tribology Handbook"**, M.J. Neale, Second Edition

[6] **"Engineering Tribology"**, Gwidon W. Stachowiak and Andrew W. Batchelor, Department of Mechanical and Materials Engineering, University of Western Australia,

[7] **"A Classification of Three-Body Abrasive Wear and Design of a New Tester",** A. Misra and I. Finnie, ASTM Int. Conf. on Wear of Materials, 1979 Dearborn, Michigan, USA, editors: K.C. Ludema, W.A. Glaeser and S.K. Rhee, pp. 313-318.

[8] **"Advanced Engineering Design"**, Beck

[9] **"Special procedure of Sumitimo's high allow material with VAM connection"**, S. Nagasaku, Sumitomo Metal Industries Ltd., May 2006

[10] **"Casing wear booklet"**, Western Well Tool

[11] **"Recent Advances in Casing Wear Technology"**, R.W. Hall, Jr., Ali Garsaki, Greg Deskins, and John Vozniak; Maurer Engineering Incorporated; 1994

[12] **"Contact Pressure Threshold: An Important New Aspect of Casing Wear"**, Russel W. Hall, Jr., SPE, and Kenneth P. Malloy Sr., SPE, Mohr Engineering Division – Stress Engineering Services, 2005

[13] **"Casing Wear – The effect of contact pressure"**, J. Steve Williamson, SPE, Sii Drillco

[14] **"Directional Drilling Textbook"**, T.A. Inglis, 1988

[15] **"Tortuosity versus Micro-Tortuosity – Why Little Things Mean a Lot"**, by Tom M. Gaynor, David C-K Chen, Darren Stuart and Blaine Comeaux, Sperry-Sun Drilling Services, Halliburton; 2001

[16] **"Straight-Hole Drilling in Crooked-Hole Country"**, MacDonald, G.C., and Lubinski, A; Drilling and Production Practice, API 1951

[17] **"Quantifying Tortuosities by Friction Factors in Torque and Drag Model"**, Tom Gaynor, Doug Hamer, David C-K Chen, Sperry-Sun, Halliburton, and Darren Stuart, The Peak Group, 2002

[18] **"Point the bit to penetrate hard streaks"**, Blaine Comeaux; 2006; E&P Magazin (www.epmag.com/archives/features/4303.htm),

[19] **"The Use of the Industry's First 3-D Mechanical Caliper Image While Drilling Leads to Optimized Rotary-Steerable Assemblies in Push- and Point-the-Bit Configurations"**, Junichi Sugiura, SPE and Steve Jones, SPE, PathFinder Energy Services, 2008

[20] **"The prediction and control of casing wear"**, William B. Bradley, SPE-AIME, Shell Development Co.; Bradley B. Fontenot, SPE-AIME, Shell Oil Co.

[21] **"Evolution if Drilling Programs and Complex Well Profiles Drive Development of Fourth-Generation Hardband Technology"**, Alvaro Chan, SPE, Dan Hannahs, SPE, Michael J. Jellison, SPE, Grant Prideco; Michael Breitsameter, Daniel J. Branagan, The Nano Steel Company; Harvey Stone, Noble Drilling (Canada) Ltd.; and Greg Jeffers, Nabors Drilling USA LP, 2008

[22] **"Casing wear – some causes, effects and control measures"** by Lewis, R. W. and Wrigth Jr., T. R.; World Oil (Oct. 1974), 99-103

[23] http://www.arncotech.com

[24] **"Trio Hardbanding Presentation at Statoil in Stjørdal 17.12.2008"** by Bengt Larsson, Trio OilTec Services

[25] **"Hardbanding and It's Role in Directional/Horizontal Drilling**", John G. Moblez, Arnco Technology Ltd., 1999

[26] **"The facts and myths of hardbanding",** John G. Mobley, Arnco Technology Trust, Ltd. 2000

[27] **"Drill string design, drilling techniques impact wear**", Roy L Dudman and Rock A Dudman, PinTec Services Inc

[28] **"Torque reduction techniques in ERD wells"** by J.H. Schamp and B.L. Estes, ExxonMobill Development Co., and S.R. Keller, SPE, ExxonMobil Upstream Research Co.

[29] **"Effect of Mud Composition on Wear and Friction of Casing and Tool Joint**", G.M. Bol, Shell E&P Laboratorium

[30] **"Casing Wear: Laboratory Measurements and Field Prediction"**, Jerry P. White, SPE, Exxon Production Research Co., Rapier Dawson, SPE, Exxon Production Research co., 1987

[31] **"Directional And Horizontal Drilling Manual"** by Richard S. Carden & Robert D. Grace, PetroSkills 2007

[32] "**Cement Evaluation Course 09 Notes**", Kevin Constable, Statoil internal

[33] **"Developments in the Visualisation of Well Tubular Condition",** D.Oliver, Sondex Wireline Ltd.

[34] **"Casing Burst Strength After Casing Wear",** J. Wu, Chevron Texaco and M.G. Zhang, LGMZ Inc.

[35] **"Bulletin on Formulas and Calculations for Casing, Tubing, Drill Pipe and Line Pipe Properties"**, API Bulleting 5C3, Sixth Edition, American Petroleum Institute, Washington D.C., Oct. 1994

[36] **"Burst Pressure Prediction of Thin Walled, Ductile Tubulars Subjected to Axial Load"**, P.R. Parsley, Tschechaid Corp., E.P. Cernocky, Shell Oil. Co., and R. Wink,, Stress Engineering Services Inc.

[37] "**Effect of Wear and Bending on Casing Collapse Strength"**, Yukihisa Kurliyama, Yasushi Tsukano and Toshitaro Mimaki, Nippon Steel Corp., and Tetsua Yonezawa, Japan National Oil Corp., 1992

[38] **Santa Clara University Design Centre**: www.scudc.scu.edu http://www.scudc.scu.edu/cmdoc/dg_doc/images/material/property/mechanic/str_str/strain.gif

[39] "**Internal corrosion and corrosion protection of carbon steel in hydrocarbon service",** Tore R. Andersen, Hydro Oil and Energy, Porsgrunn Research Center, Statoil internal

[40] **"Corrosion Management of Wet Gas Pipelines",** S. D. Kapusta et al, Corrosion'99, paper no. 45

[41] "**Improvements on de Waard-Milliams Corrosion Prediction and Applications to Corrosion Management",** B. F. M. Pots et al, Corrosion'2002, paper no. 02235

[42] "**Troll Olje Oil and Gas Provinces. Evaluation of Corrosion in C-steel PUP Joints**", Anne Marie K. Halvorsen, Research Centre Porsgrunn, Statoil internal

[43] **"Ultrasonic report tubing hanger, pupjoint F-1",** Atle Hjellvik, Mongstadbase testhall 1

[44] **"Galvanic corrosion in oil and gas environments",** T. Hara et al, NACE Corrosion'96, Paper no. 63

[45] **"Casing Wear During Drilling: Simulation, Prediction, and Control",** J.M. Schoenmakers, SPE, Koninklijke/Shell E&P Laboratorium

[46] **"Analysis of casing wear",** Master thesis by Therese Sønstabø. Bergen June 2008

[47] **"Reduction of Drill String Torque and Casing Wear in Extended Reach Wells Using Non-Rotating Drill Pipe Protectors",** N.B. Moore, P.W. Mock, R.E. Krueger, Western Well Tool, 1996

[48] **"Flow Loop and Bottle Testing of 3Cr and 13Cr Steel Coupons",** IFE/KR/F – 2008/173

[49] **"Technical data sheet Nitronic 60",** http://www.specialtysteelsupply.com/brochure/nitronic-60-technical-data.pdf

15 List of figures

16 Appendix

16.1 Galling wear test results for stainless steel

From: Armco Nitronic 60 Stainless Steel Manual

http://www.hpalloy.com/alloys/brochures/Nitronic60book.pdf

Couple — (Brinell Hardness)			Threshold Galling Stress ksi (MPa) (Stress at which galling began)
Waukesha 88 (141)	vs.	Type 303 (180)	50+ (345)
Waukesha 88 (141)	vs.	Type 201 (202)	50+ (345)
Waukesha 88 (141)	vs.	Type 316 (200)	50+ (345)
Waukesha 88 (141)	vs.	17-4 PH (405)	50+ (345)
Waukesha 88 (141)	vs.	20 Cr-80 Ni (180)	50+ (345)
Waukesha 88 (141)	vs.	Type 304 (207)	50+ (345)
Silicon Bronze (200)	vs.	Silicon Bronze (200)	4 (28)
A-286 (270)	vs.	A-286 (270)	3 (21)
NITRONIC 60 (205)	vs.	A-286 (270)	49+ (338)
NITRONIC 60 (205)	vs.	20 Cr-80 Ni (180)	36 (248)
NITRONIC 60 (205)	vs.	Ti-6Al-4V (332)	50+ (345)
AISI 4337 (484)	vs.	AISI 4337 (415)	2 (14)
AISI 1034 (415)	vs.	AISI 1034 (415)	2 (14)
NITRONIC 60 (205)	vs.	AISI 4337 (448)	50+ (345)
NITRONIC 60 (205)	vs.	Stellite 6B (415)	50+ (345)
NITRONIC 32 (234)	vs.	AISI 1034 (205)	2 (14)
NITRONIC 32 (231)	vs.	Type 201 (202)	50+ (345)
NITRONIC 60 (205)	vs.	17-4 PH (322)	50+ (345)
NITRONIC 60 (205)	vs.	NITRONIC 50 (205)	50+ (345)
NITRONIC 60 (205)	vs.	PH 13-8 Mo (297)	50+ (345)
NITRONIC 60 (205)	vs.	PH 13-8 Mo (437)	50+ (345)
NITRONIC 60 (205)	vs.	15-5 PH (393)	50+ (345)
NITRONIC 60 (205)	vs.	15-5 PH (283)	50+ (345)
NITRONIC 60 (205)	vs.	17-7 PH (404)	50+ (345)
NITRONIC 60 (205)	vs.	NITRONIC 40 (185)	50+ (345)
NITRONIC 60 (205)	vs.	Type 410 (240)	36 (248)
NITRONIC 60 (205)	vs.	Type 420 (472)	50+ (345)
NITRONIC 60 (210)	vs.	Type 201 (202)	46+ (317)
NITRONIC 60 (210)	vs.	AISI 4130 (234)	34 (234)
NITRONIC 60 (205)	vs.	Type 301 (169)	50+ (345)
Type 440C (600)	vs.	Type 420 (472)	3 (21)
Type 201 (202)	vs.	Type 201 (202)	20 (137)
NITRONIC 60 (205)	vs.	Cr plated Type 304	50+ (345)
NITRONIC 60 (205)	vs.	Cr plated 15-5PH (H 1150)	50+ (345)
NITRONIC 60 (205)	vs.	Inconel 718 (306)	50+ (345)

Type 201 (202)	vs.	Type 304 (140)	2	(14)
Type 201 (202)	vs.	17-4 PH (382)	2	(14)
Type 410 (322)	vs.	Type 420 (472)	3	(21)
Type 304 (140)	vs.	AISI 1034 (205)	2	(14)
Type 304 (337)	vs.	Type 304 (337)	2	(14)
Type 304 (207)	vs.	Type 304 (337)	2	(14)
Duplex 2205 (235)	vs.	Type 303 (153)	2	(14)
Duplex 2205 (235)	vs.	Type 304 (270)	2	(14)
Duplex 2250 (235)	vs.	Type 316 (150)	2	(14)
Duplex 2205 (235)	vs.	Type 416 (342)	2	(14)
Duplex 2205 (235)	vs.	17-4 PH (415)	2	(14)
Duplex 2205 (235)	vs.	NITRONIC 60 (210)	30	(207)
IN 625 (215)	vs.	Type 303 (153)	2	(14)
IN 625 (215)	vs.	Type 304 (270)	2	(14)
IN 625 (215)	vs.	Type 316 (161)	2	(14)
IN 625 (215)	vs.	17-4 PH (415)	2	(14)
IN 625 (215)	vs.	NITRONIC 60 (210)	33	(227)
Stellite 21 (270)	vs.	Type 316 (161)	2	(14)
Stellite 21 (270)	vs.	NITRONIC 50 (210)	2	(14)
Stellite 21 (270)	vs.	NITRONIC 60 (210)	43+	(297)
K-500 Monel (321)	vs.	Type 304 (270)	2	(14)
K-500 Monel (321)	vs.	Type 316 (161)	2	(14)
K-500 Monel (321)	vs.	17-4 PH (415)	2	(14)
K-500 Monel (321)	vs.	NITRONIC 50 (245)	2	(14)
K-500 Monel (321)	vs.	NITRONIC 60 (210)	17	(117)
NITRONIC 60 (210)	vs.	Tribaloy 700 (437)	45+	(310)
Stellite 6B (450)	vs.	Type 316 (61)	8	(55)
Stellite 6B (450)	vs.	Type 304 (150)	47+	(324)
Stellite 6B (450)	vs.	NITRONIC 60 (210)	50+	(345)
Type 410 (210)	vs.	Type 410 (210)	2	(14)
Type 410 (363)	vs.	Type 410 (363)	2	(14)
Type 410 (210)	vs.	Type 410 (363)	2	(14)
17-4 PH (H 1150 + H 1150) (313)	vs.	17-4 PH (H 1150 + H 1150) (313)	2	(14)
Type 410 (210)	vs.	17-4 PH (H 1150 + H 1150) (313)	2	(14)
NITRONIC 60 (210)	vs.	17-4 PH (H 1150 + H 1150) (313)	21	(145)
NITRONIC 60 (210)	vs.	Type 410 (210)	24	(165)

+ Did not gall

16.2 Chrome casing properties

From: Steel Products Manual for Stainless Steels, Iron and Steel Society, ISBN:1-886362-34-3, p.168,169

UNS S42000—Type 420

Martensitic

Type 420 is a martensitic chromium stainless steel capable of being heat treated to a maximum hardness of approximately Rockwell C50.

It has better corrosion resistance, in general, in the hardened and tempered condition than in the annealed condition.

See also the Section on Typical Applications.

UNS S42000

Chemical Composition Limits
Cast or Heat Analysis, Percent

C	Mn	P	S	Si	Cr
0.15	1.00	0.040	0.030	1.00	12.0
Min	Max	Max	Max	Max	14.0

Physical Properties in the Annealed Condition

Modulus of Elasticity in Tension

psi	MPa
29.0×10^6	200,000

Modulus of Elasticity in Torsion

psi	MPa
11.7×10^6	81,000

Density

lb/in^3	kg/m^3
0.28	7,750

Electrical Resistivity

Microhm — mm 68°F (20°C)
550

Specific Heat

Btu/lb °F	kJ/kg·K
32-212°F	0-100°C
0.11	0.46

Thermal Conductivity

Btu/ft/h/°F	W/m·K
212°F	100°C
14.4	24.9

Mean Coefficient of Expansion

in/in/°F		cm/cm/°C	
32-212°F	5.7×10^{-6}	0-100° C	10.3×10^{-6}
32-600°F	6.0×10^{-6}	0-315° C	10.8×10^{-6}
32-1000°F	6.5×10^{-6}	0-538° C	11.7×10^{-6}
32-1200°F	6.8×10^{-6}	0-649° C	12.2×10^{-6}

Melting Range

°F	°C
2650-2750	1454-1510

Thermal Treatment

Initial Forging

°F	°C
2000-2200	1093-1204

Slow cool and anneal from these temperature

Full Annealing

°F	°C
1550-1650	842-898

Cool slowly from these temperatures.

Process Annealing

°F	°C
1300-1450	734-787

Hardening

°F	°C
1800-1900	981-1036

Cool rapidly from these temperatures.

Tempering

°F	°C
300-700	149-371

MECHANICAL PROPERTIES

Form and Condition	*ASTM Specification*	*Tensile Strength ksi(MPa), Min*	*Yield Strength ksi(MPa), Min*	*Elongation %, Min*	*Reduction in Area %, Min*	*Hardness HB, Max*	*HR, Max*
Plate, Sheet & Strip							
Annealed	A176	100(690)Max	—	15	—	217	B96
Bar							
Annealed	A276	95(655)[a]	50(345)[a]	25[a]	55[a]	241[b]	—
Forgings							
Annealed	A473	—	—	—	—	223	—

[a]Typical value.
[b]For cold finished material, the maximum hardness shall be 255.

16.3 Presentation of USIT logging results and results of reduced burst pressure rating for dedicated wells

16.3.1 Well 31/2 – F – 1 BY1H / BY2H

The 10 ¾ in. liner was logged with a USIT in the interval from 2,003 – 1,445 m.

Diameter in	Casing/ Liner	Grade	Coupling	Weight [lbs/ft]	Setting depth from MD[m]	Setting depth to MD[m]	Setting depth to TVD[m]	RKB hanger MD[m]	Float collar MD[m]	R/A marker MD[m]	No of joints
13 3/8"	Casing	P-110	Vam TOP	72,000	354,7	1 628,0	1 473,0	354,7	1 585,0		107
10 3/4"	Casing	P-110	Vam TOP	60,700	1 554,6	1 634,3	1 474,1				5
10 3/4"	Casing	P-110	Vam TOP	60,700	1 634,1	1 682,4	1 501,4				4
10 3/4"	Casing	13 Cr-80	Vam TOP	60,700	1 682,4	1 868,1	1 578,1				15
10 3/4"	Casing	P-110	Vam TOP	60,700	1 868,1	1 892,2	1 584,0				2
10 3/4"	Casing	13 Cr-80	Vam TOP	60,700	1 892,2	1 991,8	1 595,6				8
10 3/4"	Casing	P-110	Vam TOP	60,700	1 991,8	2 003,9	1 595,9				1

16.3.1.1 Data quality

Centralisation is poor, especially in the L80Cr13 intervals due to the wear groove. Tool eccentricity of up to 0.5 inch often exceeds the tolerance limit of 0.215in (2% of the casing outer diameter). The FPM value is more or less constant and gives a fluid velocity of 177 µs.

The wear groove is so severe that the wear base cannot be read from the log. Loop processing allows investigating down to a limit of 0.25 in remaining wall thickness before the data get too noisy.

16.3.1.2 Logging results

Section	Depth	Grade	Wear	Max. wear
1	1554 - 1682	P110	No wear	0%
2	1682 – 1868	L80 Cr13	Continuous wear groove on the left side	53%
3	1868 – 1892	P110	No wear	0%
4	1892 – 1992	L80 Cr13	Continuous wear groove on the left side	53%

5	1992 - 2003	P110	Shallow wear groove	Within API spec. (6%)

In section 2 and 4 wear exceeds the logging resolution of 53% in short intervals. The ultimate depth of the wear groove cannot be determined, but the max. remaining wall thickness is 0.25 in.

Especially at beginning and end of section 4 excessive wear occurred in short intervals occasionally. Those intervals coincide with high tool eccentricity. Possibly tool eccentricity is caused by severe local doglegs in this sections. Indication for this is given by both the drilling daily reports (drilled through hard calcite both at the beginning and end of section 4) and the directional survey. It seems to be likely that the real doglegs in this section are much more severe than the apparent ones. Eccentricity in the other parts of the L80Cr13 is probably due to the position of the tool in the groove.

The position of the wear groove is unknown, as the rotate image mode was set on off. Due to drill string mechanics it should be on the low side, as the string was in compression during drilling the horizontal 8 ½ section.

16.3.1.3 Burst rating (API approach)

Grade	OD [in]	t [in]	σ yield [psi]	Factor [-]	Burst strength [bar]	SF	DF burst	Safety
L80 Cr13	10.75	0.545	80000	0.875	489	2.06[xxii]	1.1	1.87
	10.75	0.545	80000	1	559	2.35	1.1	2.14
	10.75	0.25	80000	0.875	224	0.94	1.1	0.86
	10.75	0.25	80000	0.98[xxiii]	251	1.08	1.1	0.96

If one uses the API approach and accounts for a wall thickness loss of 0.875 the remaining burst strength gives a SF lower than one. Neglecting the API design factor, the remaining strength gives 256 bar, in this case the safety factor exceeds one, but the safety is still lower than one.

As the API approach is quite conservative, one can assume that the casing burst strength will be higher than the tabulated values. However, one should also consider that the wall thickness may be thinner than 0.25in.

16.3.2 Well 31/5 – I – 21 BY1H / BY2H

The 10 ¾ in. liner was logged with a USIT in the interval from 1,954.4 – 1,649.1mMD.

Note: The liner is a combination L80Cr13 and P110 joints in the interval 1,649.1 – 1,744mMD.

[xxii] Safety factor = actual design factor from well plan
[xxiii] The factor of 0.98 derives from a max. allowable tool eccentricity of 2 %

Diameter in	Casing/ Liner	Grade	Coupling	Weight [lbs/ft]	Setting depth from MD[m]	Setting depth to MD[m]	Setting depth to TVD[m]	RKB hanger MD[m]	Float collar MD[m]	R/A marker MD[m]	No of joints
13 3/8"	Casing	L-80	Vam TOP	72,000	337,1	1 577,2	1 436,4	337,1	1 533,3		103
9 5/8"	Casing	P-110	Vam TOP	53,500	1 515,2	2 134,8	1 581,3	1 521,6	2 103,9		19

16.3.2.1 Data quality

Centralisation is good and always within the tolerance limit. The FPM value is zoned and gives fluid velocities of 176.83µs and 176.82µs. There is some loss of signal on the USI log in the L-80 casing. These areas appear right on the side of the groove and are of a significant size. The elongated features are not fully repeating and are probably not real features. They are probably caused by the position of the tool related to the shoulder of the groove.

16.3.2.2 Logging results

Section	Depth	Grade	Wear	wear
1	1649 - 1744	P110	No wear	0%
2	1682 – 1868	L80 Cr13	Continuous wear groove on the left side	53% (Possibly > 60%)
3	1868 – 1892	P110	No wear	0%
4	1892 – 1992	L80 Cr13	Continuous wear groove on the left side	53% (Possibly > 60%)
5	1992 - 2003	P110	Shallow wear groove	Within API spec. (6%)

16.3.2.3 Burst rating (API approach)

Grade	OD [in]	t [in]	σ yield [psi]	Factor [-]	Burst strength [bar]	SF	DF burst	Safety
L80 Cr13	10.75	0.545	80000	0.875	489	2.57	1.1	2.34
	10.75	0.545	80000	1	559	2.94	1.1	2.67
	10.75	0.25	80000	0.875	224	1.18	1.1	1.07
	10.75	0.25	80000	0.98	251	1.32	1.1	1.20
	10.75	0.218	80000	0.98	219	1.15	1.1	1.05

If one uses the API approach and accounts for a wall thickness loss of 0.875 the remaining burst strength gives a SF lower than one. Neglecting the API design factor, the remaining strength gives 251 bar, in this case the safety factor and the safety exceed one. For a possible wall thickness loss of 60% the safety goes down to closely 1.

As the API approach is quite conservative, one can assume that the casing burst strength will be higher than the tabulated values. However, one should also consider that the wall thickness may be thinner than 0.25in.

16.3.3 Well 31/5 – H – 3 CY1H/CY2H

The 10 ¾ in. liner was logged with a USIT in the interval from 1,786 – 2,290mMD.

Diameter in	Casing/ Liner	Grade	Coupling	Weight [lbs/ft]	Setting depth from MD[m]	Setting depth to MD[m]	Setting depth to TVD[m]	RKB hanger MD[m]	Float collar MD[m]	R/A marker MD[m]	No of joints
13 3/8"	Casing	P-110	Vam TOP	72,000	350,0	1 834,3	1 497,4	350,0	1 813,0		
10 3/4"	Casing	P-110	Vam TOP	45,500	351,5	1 781,5	1 472,5	351,5			
10 3/4"	Casing	L-80	Vam TOP SC80	60,700	1 776,9	2 412,8	1 594,9		2 381,0		

16.3.3.1 Data quality

Centralisation is often close and sometimes slightly outside the tolerance limit – especially in the interval 1,910 – 2,150mMD. The FPM value is zoned and gives fluid velocities of 176.83µs and 176.82µs. There is some loss of signal on the USI log in the L-80 casing. These areas appear right on the side of the groove and are of a significant size. The elongated features are not fully repeating and are probably not real features. They are probably caused by the position of the tool related to the shoulder of the groove.

16.3.3.2 Logging results

Section	Depth [mMD]	Grade	Wear	wear
1	1790 - 1911	P110	Slightly ovalized on some joints; minor to no groove on liner	~0-6%
2	1911 – 2097	L80 Cr13	Continuous wear groove on the right side; ovalization	~36% - 45% (hard to estimate due to ovalization + eccentr.)
3	2097 – 2122	P110	No significant groove; still some ovalization in the upper joint	~6%
4	2122 – 2270	L80 Cr13	Continuous wear groove; ovalization	~36 - 45% (hard to estimate due to ovalization + eccentr.)
5	2270 - 2281	P110	Minor wear groove	~6%
6	2281 – 2290	L80 Cr13	Continuous wear groove; ovalization	~36 - 45% (hard to estimate due to ovalization + eccentr.)

Eccentricity and ovalization

The wear groove is on the right, low side of the casing, due to steering to the right in the near horizontal section. Eccentricity of the tool is varying and probably caused by the tool in the wear groove and high doglegs.

P110 casing shows nearly no wear compared to L80 Cr13 casing. As expected tool centralisation in better in P110.

16.3.3.3 Burst rating (API approach)

Grade	OD [in]	t [in]	σ yield [psi]	Factor [-]	Burst strength [bar]	SF	DF burst	Safety
L80 Cr13	10.75	0.545	80000	0.875	489	8.21	1.1	7.46
	10.75	0.545	80000	1	559	9.38	1.1	8.53
	10.75	0.3	80000	0.875	269	4.52	1.1	4.11
	10.75	0.3	80000	0.98	302	5.06	1.1	4.60

The obtained safeties exceed one for this well. Wear was significantly lower compared to the other two wells. Also the maximum expected burst load will be lower for this well.

16.4 Baker AutoTrak report

Operator: StatoilHydro | Field: | Troll | Start Time/Date: 03:05 30/Jan/2009 | Rig:
Well: 31/5 J-13 AY 1H | Wellbore: 31/5 J-13 AY 1H | End Time/Date: 21:35 3/Feb/2009 | Songa Dee
BHA Run #: 7 | Bit #: 4 | Hole Size: 8 1/2 in | Page No.: 1

Time / Depth Data

Drilling Parameters Data

Time From	Time To	Drill Time (hours)	Circ. Time (hours)	Total Time (hours)	MD From (m)	MD To (m)	Dist (m)	Avg ROP (m/hr)	M	Bit/S Force %	Vect Dir deg	Walk Force %	Targ Inc deg	Surf RPM	TQ On (kN.m)	TQ Off (kN.m)	WOB (tonne)	P/U Hkld (tonne)	S/O Hkld (tonne)	Rot Hkld (tonne)	Flow l /min	Press bar	Mud Wt sg	Comments
30/Jan/2009																								
03:05	03:55		0.83	0.83	2007.00	2008.00	1.00	1.20	DC	0.00	0.00	0.00	0.00	60	18.0	0.0	3	90	70	83	1600	91	1.25	Tag & drill out DrBlm SFD.Pick off bottom 6x.Break through.Stuck at bit.
03:55	06:15		2.33	3.17	2008.00				C	0.00	0.00	0.00	0.00	0	0.0	0.0	0				1600	88	1.25	Work pipe.Jar vs low impact.Pull free 110t OP.Clean DAB area
06:15	06:40		0.42	3.58	2008.00	2025.00	17.00	40.80	DC	0.00	0.00	0.00	0.00	60	17.0	0.0	2				1600	85	1.25	Wash / ream to float
07:05	07:25		0.33	3.92	2025.00	2058.00	33.00	99.00	DC	0.00	0.00	0.00	0.00	60	17.0	0.0	2				1600	85	1.25	Tag float@2058m.Vary rpm for SS.No reduction in SS
07:25	07:40		0.25	4.17	2058.00	2059.00	1.00	4.00	DC	0.00	0.00	0.00	0.00	60	17.0	0.0	2				1600	85	1.25	
07:50	08:10		0.33	4.50	2059.00	2064.00	5.00	15.00	DC	0.00	0.00	0.00	0.00	60	19.0	0.0	6				1600	85	1.25	
08:10	08:30		0.33	4.83	2064.00	2080.00	16.00	48.00	DC	0.00	0.00	0.00	0.00	60	19.0	0.0	5				2170	146	1.25	DL RO.Clean surface lines.Pressure for displacement
09:50	10:10		0.33	5.17	2080.00	2085.00	5.00	15.00	DC	0.00	0.00	0.00	0.00	60	19.0	0.0	5				2170	146	1.12	
10:10	11:15	1.08		6.25	2085.00	2087.00	2.00	1.85	RO	0.00	0.00	0.00	0.00	80	20.0	18.0	2				2170	122	1.12	Drill out shoe.While displacing mud.Pack off below shoe.Work clear
11:35	12:25	0.83		7.08	2087.00	2115.00	28.00	33.60	H	42.00	0.00	48.00	90.00	80	24.0	18.0	6				2170	122	1.12	SS - 6
12:55	14:00	1.08		8.17	2115.00	2146.00	31.00	28.62	H	42.00	0.00	48.00	90.00	140	24.0	18.0	10				2170	122	1.12	
14:00	14:45	0.75		8.92	2146.00	2174.00	28.00	37.33	H	42.00	0.00	48.00	90.00	140	24.0	18.0	12				2170	122	1.12	NBI varying +/- 0.3deg
15:10	15:25	0.25		9.17	2174.00	2182.00	8.00	32.00	H	42.00	0.00	48.00	90.00	150	24.0	18.0	8				2170	122	1.12	High SS.Hold back to check NBI
15:25	16:00	0.58		9.75	2182.00	2203.00	21.00	36.00	H	42.00	0.00	29.00	90.00	150	24.0	18.0	5				2170	122	1.12	Little improvement in SS
16:25	16:50	0.42		10.17	2203.00	2231.00	28.00	67.20	H	42.00	0.00	29.00	90.50	150	24.0	18.0	10				2170	122	1.12	Take SCR's
17:15	17:30	0.25		10.42	2231.00	2246.00	15.00	60.00	H	42.00	0.00	29.00	90.50	150	24.0	18.0	12				2170	119	1.12	
17:30	17:45	0.25		10.67	2246.00	2264.00	18.00	72.00	H	42.00	0.00	-58.00	90.50	150	24.0	18.0	10				2170	120	1.12	
18:00	18:30	0.50		11.17	2264.00	2293.00	29.00	58.00	H	42.00	0.00	-58.00	90.50	150	24.0	18.0	12				2170	119	1.12	Grease washpipe.
18:55	19:00	0.08		11.25	2293.00	2300.00	7.00	84.00	H	42.00	0.00	-58.00	90.50	150	24.0	18.0	12				2170	119	1.12	
19:00	19:15	0.25		11.50	2300.00	2313.00	13.00	52.00	H	42.00	0.00	-32.00	90.50	150	24.0	18.0	12				2160	117	1.12	
19:15	19:30	0.25		11.75	2313.00	2322.00	9.00	36.00	H	42.00	0.00	-32.00	91.00	150	24.0	18.0	12				2160	117	1.12	
19:45	20:15	0.50		12.25	2322.00	2342.00	20.00	40.00	H	42.00	0.00	-32.00	91.00	150	24.0	18.0	12				2160	117	1.12	
20:15	20:40	0.42		12.67	2342.00	2351.00	9.00	21.60	H	42.00	0.00	-45.20	91.50	150	24.0	18.0	12				2160	117	1.12	Ream HLD at 2345m.
21:00	21:50	0.83		13.50	2351.00	2376.00	25.00	30.00	H	71.00	0.00	-45.20	91.00	150	22.0	18.0	12				2160	117	1.12	

Legend: M- Mode, BR - Back Ream, C - Circulate off Bottom, DC - Drilling Cement, DL - Down Link Off Bottom, H - Hold, RO - Ribs Open, S - Steer, WR - Wash and/or Ream

16.5 Lube concentrations

Well	Branch	Lube conc. [%]		Branch Revolutions	Well lube conc. [%]	Well	Branch	Lube conc. [%]		Branch Revoluti	Well lube conc.
		Start	End					Start	End		
D-7	AY1H	1	2	960545	1.56	Q-21	BY1H	0	0	631200	1.54
	AY2H	2	2	559980			BY1H T2	0.4	2	758665	
	AY3H	2	2	473080			BY1H T3	2	3	369370	
	AY4H	1.75	0.9	632844			BY1H T4	3	3	438640	
	AY5H	1	1.5	712533			BY1H T5	3	3	491380	
	AY6H	1.1	1.5	533240			BY2H	1	0	420025	
	AY7H	1.5	2	475865			BY2H T2	0	3	1317650	
F-1	BY1H	2	3	1898242	2.61	S-21	AH	0	0	354545	2.18
	BY2H	3	2.6	1108212			AH T2	0	3	1190244	
F-6	BY1H	2	3	788350	2.81		AH T3	3	2.5	480560	
	BY2H	3	3	1340195			BY1H	3	2.5	1051665	
G-1	BY1H	1.5	3	1725229	2.63		BY2H	3	3	211000	
	BY2H	3	3	1784735			BY2H T2	3	3	833565	
H-3	CY1H	2	3	1982590	2.50		BY3H	2	2	359510	
	CY2H	2	3	1351635			BY3H T2	2	2	388490	
I-21	BY1H	0	3	1948623	1.82	S-23	AY1H	0	2.5	1835022	1.63
	BY2H	2	2.5	1412713			AY2H	1.8	2.5	1368305	
J-13	AY1H	0	0	676110	0.97	S--24	Y1H	0	2	774817	1.16
	AY2H	2	2	610690			Y1H T2	2	2	241030	
	AY3H	0	2	1034365			Y2H	0	2.5	959090	
P-14	BY1H	0	2	970429	1.20		Y3H	0	2	949470	
	BY2H	1.5	1.5	997730		X-12	H	0	0	1250920	0.70
	BY3H	1.5	2	1060913			AH	0	2.5	1616305	
	BY4H	1	0.3	1225897		Y-11	BY1H	0	2	1134675	1.45
Q-14	AY1H	0	0	725440	0.00		BY2H	2	2	921145	
	AY2H	0	0	792990		Y-13	BY1H	0	2	1041369	1.22
							BY2H	1	2	817550	

16.6 Side force calculation for soft string model

If you are using the soft string model, the side force or normal force is calculated using the following equation.

$$F_N = \sqrt{(F_T\ \Delta\alpha\ Sin(\Phi))^2 + (F_T\ \Delta\Theta + WL\ Sin(\Phi))^2}$$

Where:

F_N = Normal or side force

F_T = Axial force at bottom of section calculated using Buoyancy method

$\Delta\alpha$ = Change in azimuth over section length

Φ = Average inclination over the section

$\Delta\Theta$ = Change in inclination over section length

L = Section length

W = Buoyed weight of the section

16.7 BHA set up

16.7.1 Autotrak G3, LithoTrak and OnPilot

String Parameters									
#	Component	Mfr	S/N	Gauge OD in	OD in	ID in	Fishing Neck in	Length m	Total Length m
20	Drill pipe	RIG			5	4.276		1.00	128.58
19	HWDP	RIG			5	3		36.60	127.58
18	Sub - other	Weatherford - pup joint			5	3	6 9/16	3.23	90.98
17	Accelerator	Weatherford	MA6500-016		6 3/4	2 1/2	6 9/16	10.75	87.75
16	HWDP	RIG			5	3		18.47	77.00
15	Sub - other	Weatherford - pup joint			5	3	6 9/16	3.23	58.53
14	Jar	Weatherford	HJ6500-108		6 3/4	2 1/2	6 1/2	9.57	55.30
13	HWDP	RIG			5	3		18.95	45.73
12	Sub - float	INTEQ	10463853		6 5/8	2	6 1/2	1.09	26.78
11	NMSub - stop	INTEQ	10601962		7	2 1/4	7	0.78	25.69
10	CCN	INTEQ	10326522	8	6 11/16	2 1/4	6 3/4	2.76	24.91
9	ORD	INTEQ	10157032	8 3/8	6 7/8	2 1/4	6 7/8	2.83	22.15
8	NMSub - other	INTEQ - Flex Sub	10170052		7	2 1/4	7	2.11	19.32
7	BCPM	INTEQ	10419652		7	2 1/4	7	4.89	17.21
6	MWD - stab - mod	INTEQ	10390396	8 3/8	7	2 1/4	7	1.29	12.32
5	OnTrak - MWD	INTEQ	10135413		7	2 1/4	7	5.00	11.03
4	CoPilot	INTEQ	10471966		7	2	7	2.26	6.03
3	MWD - stab - mod	INTEQ	10560200	8 3/8	7	2 1/4	7	1.26	3.77
2	ATK Steerable Stab	INTEQ	10185783	8 1/2	7 11/16	2 1/4	7	2.20	2.51
1	Bit - PDC - fixed cutter	HC	7500712	8 1/2				0.31	0.31

16.7.2 XTreme, LithoTrak, TestTrak and Copilot

String Parameters									
#	Component	Mfr	S/N	Gauge OD in	OD in	ID in	Fishing Neck in	Length m	Total Length m
22	Drill pipe	RIG			5 1/2	4.778		1.00	3225.41
21	Drill pipe	RIG	TALLY		5	4.276		3093.00	3224.41
20	HWDP	RIG	TALLY		5	3		64.28	131.41
19	Drill pipe	IPE Handeling Pup	PJ134		5	4.276		2.63	67.13
18	Jar	IPE	HJ6500-244		6 3/4	2 1/2	6 3/4	9.65	64.50
17	HWDP	RIG	TALLY		5	3		9.19	54.85
16	Sub - float	INTEQ (Solid Float)	10463850		6 3/4	2 7/8	6 1/2	1.11	45.66
15	Stab - string	INTEQ	SSBN3635	8 3/8	6 3/4	2 7/8	6 3/4	1.56	44.55
14	NMSub - stop	INTEQ	10201021		7	2 1/4	6 1/2	0.74	42.99
13	TesTrak	INTEQ	10241375		7	2 1/4	7	7.43	42.25
12	NMSub - other	INTEQ (Flex Sub)	10481358		5	2 1/4	7	2.11	34.82
11	CCN	INTEQ	10654749	8 1/4	6 3/4	2 1/4	6 3/4	2.77	32.71
10	ORD	INTEQ	10373412	8 3/8	6 7/8	2 1/4	6 7/8	3.02	29.94
9	NMSub - other	INTEQ (Flex Sub)	10144663		7	2 1/4	7	2.10	26.92
8	BCPM	INTEQ	10367019		7	2 1/4	7	4.91	24.82
7	MWD - stab - mod	INTEQ	10481616	8 3/8	7	2 1/4	7	1.30	19.91
6	OnTrak - MWD	INTEQ	10305072	8 3/8	7	2 1/4	7	5.05	18.61
5	MWD - stab - mod	INTEQ	10373423	8 3/8	7	2 1/4	7	1.29	13.56
4	Modular Motor	INTEQ	10149015	8 3/8	7	2	7	7.66	12.27
3	CoPilot	INTEQ	10082444		7	2 1/4	7	2.13	4.61
2	ATK Steerable Stab	INTEQ	10270993	7 3/4	7	2 1/4	7	2.17	2.48
1	Bit - PDC - fixed cutter	Hughes Christensen	7500673	8 1/2				0.31	0.31

16.8 S-21 Casing wear back calculation

Grade	OD [in]	t [in]	σ yield [psi]	Factor [-]	Burst strength [bar]	SF	DF burst	Safety
L80 Cr13	10.75	0.545	80000	0.875	489	**1.75**	1.1	1.59
	10.75	0.14	80000	1	**144**	0.51	1.1	0.47
	Remaining thickness:		0.14			Casing wear:		**74 %**

16.9 Average branch side force rotating off bottom

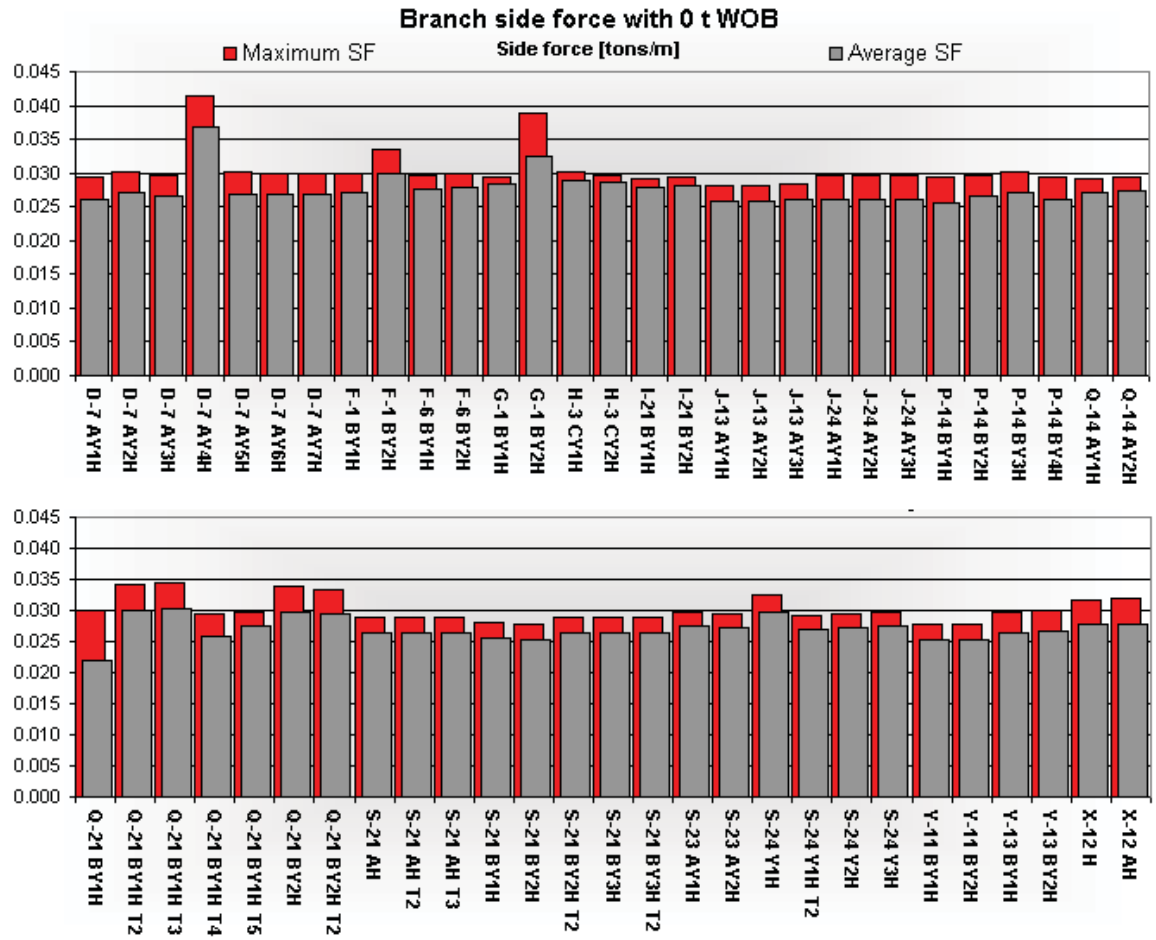

16.10 Trio OilTec Services wear test results

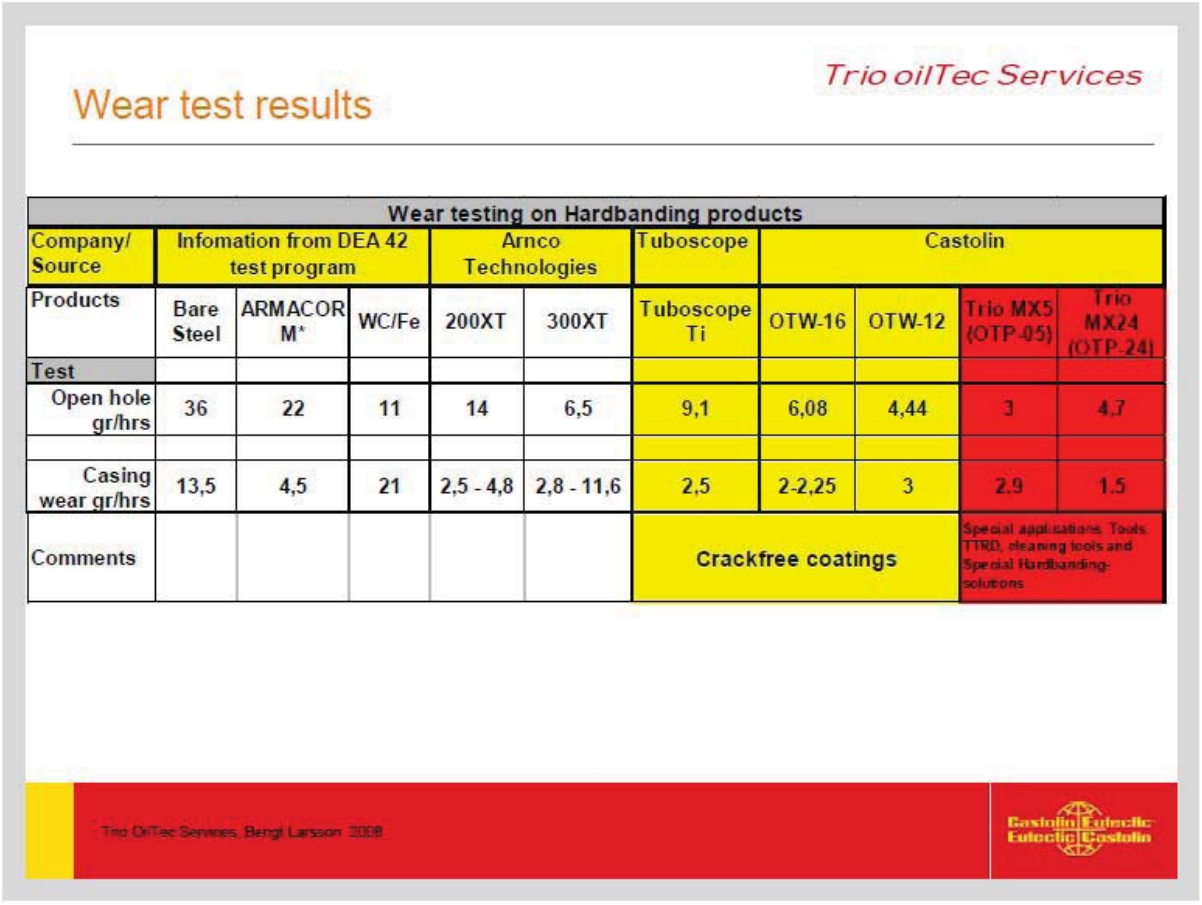

Trio oilTec Services

Wear test results

Wear testing on Hardbanding products										
Company/ Source	Infomation from DEA 42 test program			Arnco Technologies		Tuboscope	Castolin			
Products	Bare Steel	ARMACOR M*	WC/Fe	200XT	300XT	Tuboscope Ti	OTW-16	OTW-12	Trio MX5 (OTP-05)	Trio MX24 (OTP-24)
Test										
Open hole gr/hrs	36	22	11	14	6,5	9,1	6,08	4,44	3	4,7
Casing wear gr/hrs	13,5	4,5	21	2,5 - 4,8	2,8 - 11,6	2,5	2-2,25	3	2,9	1,5
Comments						Crackfree coatings			Special applications, Tools, TTRD, cleaning tools and Special Hardbanding-solutions	